UNIVERSITA' DEGLI STUDI DI PAVIA

FACOLTA' DI INGEGNERIA
DIPARTIMENTO DI INGEGNERIA INDUSTRIALE E DELL'INFORMAZIONE

DOTTORATO DI RICERCA IN BIOINGEGNERIA E BIOINFORMATICA
XXIX CICLO - 2016

USE OF PHYSIOLOGY-BASED ELEMENTS TO PREDICT THE PHARMACOKINETICS OF NEW DRUGS

PhD Thesis by
ITALO POGGESI

Advisor:
Prof. Paolo Magni

PhD Program Chair:
Prof. Riccardo Bellazzi

Abstract (Italiano)

Le attivita' di ricerca riportate in questa Tesi sono state condotte nei laboratori del Dipartimento di Ingegneria Industriale e dell'Informazione dell'Universita' di Pavia e nel laboratorio del gruppo di farmacologia clinica di Janssen R&D.

La valutazione della farmacocinetica (PK, che e'cio' che il corpo fa ad un farmaco: lo assorbe, lo distribuisce ai differenti distretti tissutali, lo elimina attraverso i processi di metabolismo e escrezione renale o biliare) e' di fondamentale importanza nello sviluppo di nuovi farmaci. Diverse metodologie possono essere utilizzate allo scopo. Si possono applicare analisi farmacocinetiche non-compartimentali (NCA), che stimano i parametri farmacocinetici primari (biodisponibilita' clearance, volume di distribuzione) sulla base del calcolo delle aree sotto la curva delle concentrazioni plasmatiche-tempo, dei loro momenti e pendenze. Si possono usare modelli empirici compartimentali (in genere modelli mammillari in cui l'eliminazione del farmaco avviene dal compartimento centrale). In questo caso le curve concentrazioni plasmatiche-tempo sono descritte da modelli che assumono che il farmaco diffonda in un piccolo numero di compartimenti e che venga eliminato da uno di questi. Tali compartimenti non hanno alcuna corrispondenza con tessuti o organi reali. Anche in questo caso lo scopo dell'analisi e' di descrivere il piu' accuratamente possibile le concentrazioni plasmatiche in modo da poter calcolare i parametri farmacocinetici primari. I modelli di farmacocinetica fisiologica (PBPK) sono quelli che piu' di tutti forniscono una descrizione anatomicamente e fisiologicamente accurata. Essi sono modelli compartimentali, in cui i compartimenti rappresentano tessuti od organi reali e che prendono in considerazione la loro reale interconnessione attraverso i vasi sanguigni arteriosi e venosi, i loro volumi, perfusione, struttura e composizione e le basi fisiologiche della distribuzione e dell'eliminazione (clearance) dei farmaci da tali compartimenti. Comunque, in tutti gli approcci, inclusi i piu' empirici, i parametri farmacocinetici primari possono essere interpretati alla luce di considerazioni fisiologiche, cosi' che possano fornire approcci per predire le farmacocinetiche in differenti sistemi (preclinici e clinici, nelle diverse popolazioni di pazienti o volontari sani) o per anticipare le differenze farmacocinetiche dovute a fattori intrinseci (eta', gestazione, insufficienza renale od epatica) o estrinseci (somministrazione del farmaco con cibo o con altri farmaci).

Lo scopo di questa Tesi e' di mostrare che approcci fisiologiche possono essere implementati in tutte le fasi dello sviluppo di un farmaco, dalla fase di sviluppo preclinico alla caratterizzazione clinica ed oltre, quando il farmaco e' in uso sul mercato. Inoltre, si vuole sottolineare che ci sono aspetti per cui la caratterizzazione fisiologica dei modelli PBPK non e' ancora del tutto matura per avere predizioni sufficientemente accurate. Si vuole percio' mostrare che anche approcci empirici (NCA o modelli compartimentali) possono fornire interessanti elementi per identificare le limitazioni degli aspetti di disegno sperimentale degli studi farmacocinetici o di conoscenza scientifica che limitano lo sviluppo dei modelli PBPK e la loro applicazione in campo predittivo.

Dopo una sezione introduttiva, in cui alcune delle limitazioni dei modelli PBPK sono descritte, alcune di queste sono affrontate nei successivi capitoli. La insufficiente predittivita' dei modelli PBPK per la predizione delle farmacocinetiche nell'uomo e' affrontata nel Capitolo 3, in cui si descrive l'uso di un approccio di stima Bayesiana dei parametri di un modello PBPK basato sui dati ottenuti negli esperimenti di farmacocinetica preclinica. I capitoli 4 e 5 mostrano alcune limitazioni dei dati ottenuti negli studi di farmacocinetica in pazienti con insufficienza epatica e renale: queste valutazioni si basano su un vasto database di dati concernenti farmaci che sono sul mercato. Queste limitazioni possono impedire la comprensione fisiologica delle modificazioni farmacocinetiche relative a queste indicazioni ed il conseguente sviluppo di modelli PBPK predittivi. Negli stessi capitoli sono proposte alcune tecniche di analisi multivariata per chiarire alcuni degli aspetti ancora incerti della caratterizzazione delle farmacocinetiche in queste condizioni, la cui risoluzione potrebbe consentire di affrontare il problema usando approcci PBPK. Nel Capitolo 6 sono stati utilizzati concetti fisiologici applicati all'analisi compartimentale (non linear mixed-effects model) di bedaquilina (un composto per il trattamento della tubercolosi) per predire l'effetto della somministrazione contemporanea di altri farmaci che possano avere effetti inibitori od induttori del metabolismo. Questa valutazione supporta il concetto che l'uso di elementi fisiologici in modelli empirici puo' dare buone predizioni anche in assenza di un vero e proprio modello PBPK, che al momento sono molto popolari per predire le interazioni tra farmaci.

Gli esempi riportati in questa Tesi sono funzionali a dimostrare che l'integrazione (di informazioni, ma anche di tecniche modellistiche diverse) e' di fondamentale importanza per affrontare le complessita' farmacocinetiche e l'incompleta comprensione dei fenomeni e per superare le limitazioni derivanti dalle imperfezioni dei disegni sperimentali.

.

Abstract (English)

The research activities reported in this Thesis have been conducted in the laboratories of the Dipartimento di Ingegneria Industriale e dell'Informazione and the Global Clinical Pharmacology group of Janssen R&D.

The assessment of the pharmacokinetics (PK: what the body does to a drug: absorption, distribution, metabolism and excretion) is part of the development of new drugs. Different methodologies can be used for this purpose. There is the so-called "model-independent" non-compartmental analysis (NCA), which estimates the primary pharmacokinetic parameters (absolute bioavailability, clearance, volume of distribution, etc.) based on the area under the plasma concentration-time curve, its first moment and the slopes. For the same purpose, empirical compartmental models (mammillary, in which, typically, the drug is eliminated from a central compartment) can be used: the plasma concentration-time curve is described by a model which assumes that drugs are diffusing into a small number of compartments and eliminated from one of these compartment. These compartments have no correspondence with anatomical tissues or organs. Again, the aim of this PK analysis is to provide an accurate description of the plasma concentration-time curve to calculate the primary pharmacokinetic parameters. The pharmacokinetic description that is mostly grounded to anatomical and physiological concepts is represented by the physiology-based pharmacokinetic (PBPK) modeling. PBPK models are compartmental models, in which compartments represents real tissues or organs and that take into consideration the interconnection of tissues and organs via the vasculature, the information on volumes and blood perfusions, tissues composition and structure, and the physiological basis of the drug distribution and clearance in the different tissues. However, in all the previously mentioned pharmacokinetic representations, included the most empirical ones, the primary pharmacokinetics parameters can be interpreted in the light of physiological concepts, so that they can be used for predicting the outcome in different systems (preclinical or clinical, different subject populations, etc.) or the PK differences due to intrinsic (pediatric, pregnancy, hepatic-renal impairment) or extrinsic factors (meal drug-drug interactions).

The aim of this Thesis is to show that full PBPK models are currently used in different phases of drug research and development, from the preclinical to the clinical development and post-marketing experience. In addition, for those aspects in which the science is not as mature as yet to trust the *in silico* predictions of PBPK models, the physiology-based elements present in the empirical approaches (NCA or compartmental models) can provide a useful

background for understanding the considerations to establish the limitations of the current PBPK models and what are the missing information to have a full and trustable representation of the PK complexities.

After an introductory section, in which the limitations of the full PBPK approaches are described, some of these limitations are addressed in the subsequent chapters. The unsatisfactory predictive capabilities of PBPK models is addressed in Chapter 3, in which a Bayesian estimation approach is proposed based on the data emerging from the preclinical PK studies, in a whole body PBPK context. Chapter 4 and 5 describe some of the limitation of the data obtained in the PK studies aiming to define the PK differences in subjects with hepatic and renal impairment, respectively. These limitations may prevent the full PK understanding and, in turn, the application of a full PBPK model. In the same chapters, some multivariate analyses approaches are proposed on the outcome of the simple NCA assessments to shed additional light on physiology and study design aspects that require a better scientific understanding that currently prevent the reliable use of PBPK models. In Chapter 6, physiological concepts on the outcome of the compartmental non-linear mixed-effects model analysis of an anti-tuberculosis drug (bedaquiline) were used to predict the effect of the simultaneous administration of comedication known to alter the metabolism of drugs. This assessment was undertaken to show the concept that physiological elements can be considered in empirical approaches, that may provide good predictions even in absence of a full PBPK model (that are currently widely used for predicting drug-drug interactions).

The examples reported in the following chapters of this thesis demonstrate how integration (of different information sources and of different mathematical and modeling techniques and approaches) is of paramount importance to efficiently handle problems, address limitations of the studies and increasing the scientific understanding of the phenomena at the basis of the PK processes.

Contents

Chapter 1

Introduction and Thesis Overview

1.1. Background

Drug development is a very long, complex, expensive, and risky process. From the first identification of the new molecular entity (NME) - by chemical synthesis or separation from a natural mixture - to its commercialization, this process takes as long as 10 years, divided into different phases, including preclinical phase (of unpredictable duration, followed by the formal preclinical characterization required to give the compound to human for the first time, typically lasting 6-12 months), clinical pharmacology phase (phase 1, lasting several months), therapeutic exploratory studies (phase 2, lasting from several months to approximately 2 years) and therapeutic confirmatory studies (phase 3, lasting 1-4 years) [http://www.fda.gov/ForPatients/Approvals/Drugs/ucm405622.htm, accessed August 1, 2016]. In each of these phases, there is a substantial risk that the candidate drug is not characterized by acceptable features (unsatisfactory therapeutic effect, excessive toxicity, production and formulation difficulties, inadequate pharmacokinetics), so that its development must be interrupted, which is called attrition. The available statistics indicate that attrition is responsible for the interruption of the development of approximately 90% of the NMEs entering the first-time in human studies [Kola & Landis, 2004]. The total cost for drug development – including the capitalization costs – are reported to be in excess of 800 million dollars [Paul et al, 2012].

The aim of drug development in the pharmaceutical industry is in essence to characterize the safety and efficacy of a new drug. In particular, it is considered of paramount importance to establish its risk-benefit ratio, *i.e.*, the balance of the benefits derived from the cure or the suppression of the symptoms of a certain disease and the risks that may be due to the safety and tolerability issues (i.e., adverse events) that may arise due to the use of drugs, which are characterized by high intrinsic biological activities [http://www.fda.gov/downloads/ForIndustry/UserFees/PrescriptionDrugUserFee/UCM329758.pdf, accessed Aug 1, 2016].

The risk-benefit ratio can be more easily and quantitatively handled when it can be related to the exposure to the drug. In Fig. 1.1, an example of the risk-benefit concept is summarized via the so-called "utility curve" [Khan et al, 2009]: in the plot, the x-axis represents the exposure to the drug (e.g., plasma concentration achieved at different dose levels or therapeutic regimens), the y-axis represents the weighted effect (positive for efficacy and negative for safety). The green and the orange curves represent the efficacy (green curve) and safety (orange curve) -exposure relationships, represented here as bands to account for uncertainty. The algebraic sum of the weighted effects is called (combined) utility curve (blue curve) and identifies the region (in terms of exposure or dose), in which the benefit-risk for this drug is maximal.

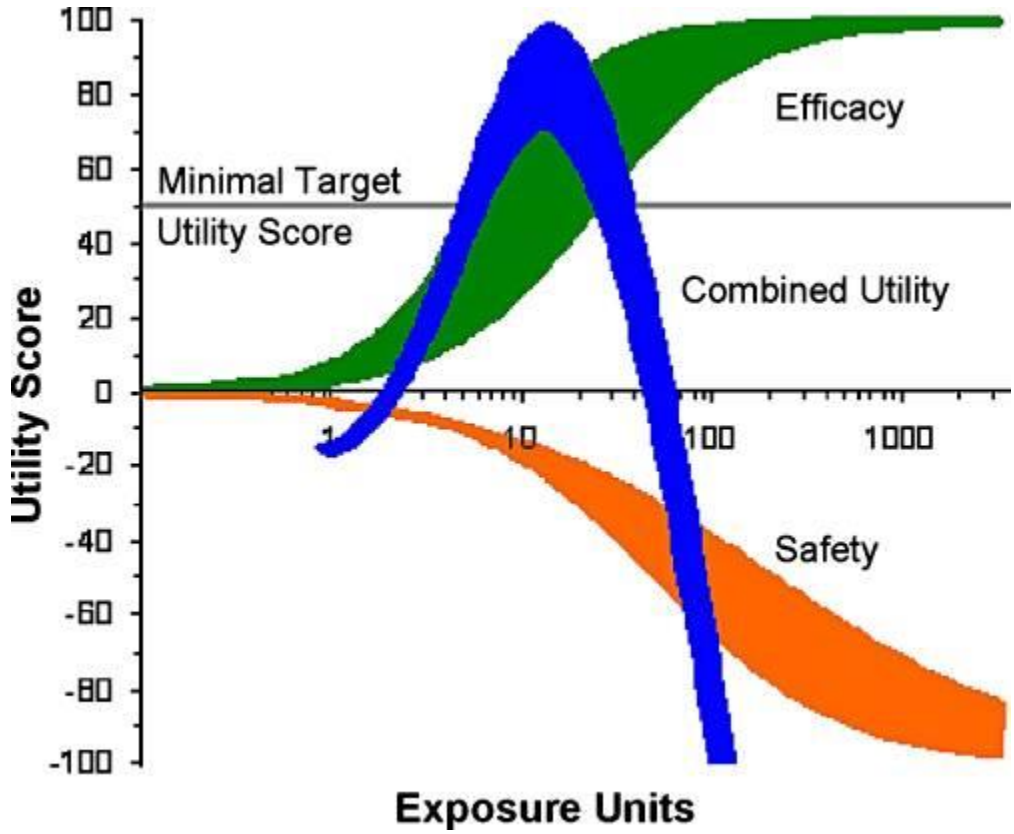

Figure 1.1. Schematic of a utility curve with uncertainty derived from the combined consideration of efficacy and safety [from Khan et al, 2009].

Exposure can be described by the dose level of the drug or by drug concentrations in the systemic circulation (plasma, serum, etc.) or summary metrics of the systemic exposure (maximal concentration, area under the plasma concentration-time curve, etc.). The systemic exposure is dependent on how and how quickly the body is able to handle the xenobiotics, and, therefore, to the pharmacokinetics (PK) of the drug at large. Establishing compelling relationships between PK and pharmacological, clinical efficacy and clinical safety effects (all this is generically referred to as pharmacodynamics [PD]) is therefore an aspect of paramount importance in

the drug development process. These relationships are also called exposure-effect relationships or pharmacokinetic-pharmacodynamic (PK-PD) relationships.

In the recent past, the business model of drug development was criticized as not sustainable on the long term. The large increase of the research costs of the pharmaceutical industry was not mirrored by an increase of the number of new molecular entity achieving the market (Fig 1.2).

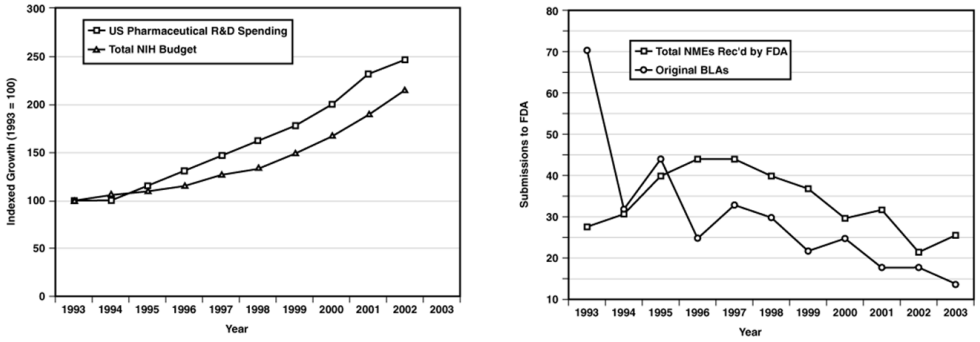

Figure 1.2. Left: 10-year trends in biomedical research spending; right: 10-year trends in major drug and biological product submissions to FDA (Innovation or Stagnation: Challenge and Opportunity on the Critical Path to New Medical Products, U.S. Department of Health and Human Services, FDA, March 2004; http://www.fda.gov/ScienceResearch/SpecialTopics/CriticalPathInitiative/CriticalPathOpportunitiesReports/ucm077262.htm#execsummary , accessed August 1, 2016).

Among many other measures proposed for improving the probability of success of the drug development process, a smarter – and possibly a more sophisticated - use of modeling approach has been advocated [http://www.fda.gov/downloads/ScienceResearch/SpecialTopics/CriticalPathInitiative/CriticalPathOpportunitiesReports/UCM113411.pdf, accessed Jan 6, 2017]. The use of pharmacometrics, defined as the "development and application of pharmaco-statistical models of drug efficacy and safety from preclinical and clinical data to improve drug development knowledge management and decision-making", was exploited in the drug development processes. Also regulatory authorities, such as the US Food and Drug Administration (FDA) or the European Medicines Agency (EMEA), increased the number of pharmacometrician reviewers to be able to cope with the more sophisticated modeling approaches that pharmaceutical industries are applying to support the submission of new drugs [http://www.fda.gov/AboutFDA/CentersOffices/OfficeofMedicalProductsandTobacco/CDER/ucm167032.htm].

PK and PK-PD models, especially when mechanistic elements are considered, grounds can provide strength to this approach. Whilst there are many approaches for describing the PK of new drugs (non-compartmental PK analysis, compartmental PK analysis), physiology-based pharmacokinetic models (PBPK) is the PK approach that, most of all, relies

on anatomical, morphological and physiological grounds. PBPK models are compartmental pharmacokinetic models, in which the biochemical bases of the absorption and disposition of compounds are considered at the tissue level, taking into due consideration the interconnection of tissues and organs via the vasculature, the information on tissues compositions, volumes and blood perfusions and the physiological basis of the drug clearance in the different tissues (a schematic of a basic PBPK model is shown in Fig.1.3). A brief background on PK concepts is reported in the section 1.2. Additional details on the structure and the equation of whole body PBPK models are reported in Chapter 3.

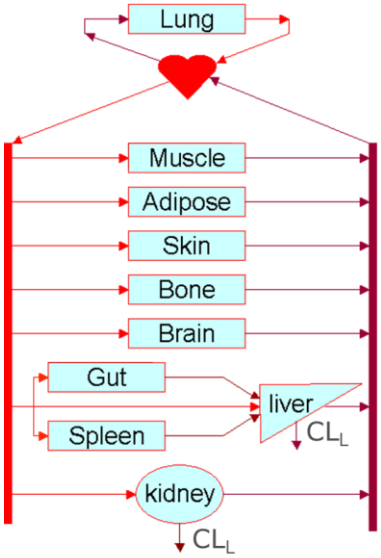

$$\frac{dC_T}{dt} = \frac{1}{V_T} \cdot \left\{ Q_T \cdot C_{input} - \frac{Q_T \cdot C_T}{\frac{P_{T:P}}{P_{B:P}}} - CL_T \cdot C_{input} \right\}$$

C_T Drug concentration for tissue T
C_{input} Drug concentration in input
Q_T Blood flow
V_T Tissue volume
$P_{t:p}$ Tissue-plasma partition coefficient
B:P Blood to plasma ratio
CL_T Tissue clearance ($CL_T = 0$ in non-eliminating tissues)

Figure 1.3. Schematics and typical mass balance equation of a basic PBPK model.

PBPK are part of the system pharmacology models, in which system-specific and compound-specific features can be identified, potentially allowing to translate the PK features in different systems (e.g., to predict the PK in human subjects from preclinical data, the PK in elderly or diseased subjects from clinical data in young healthy subjects, the effect of a comedication based on the PK of the compound given alone). Approximately in the last fifteen years, numerous papers have illustrated the increasing role of PBPK in drug research and development.

In this thesis, the application of physiology-based concepts (not necessarily aiming to the development of full blown PBPK models) in early (e.g., preclinical to clinical interface) or late clinical development (prediction of drug-drug interaction and characterization of PK in special population) will be described (Fig. 1.4), trying to address some of the gaps that still are present.

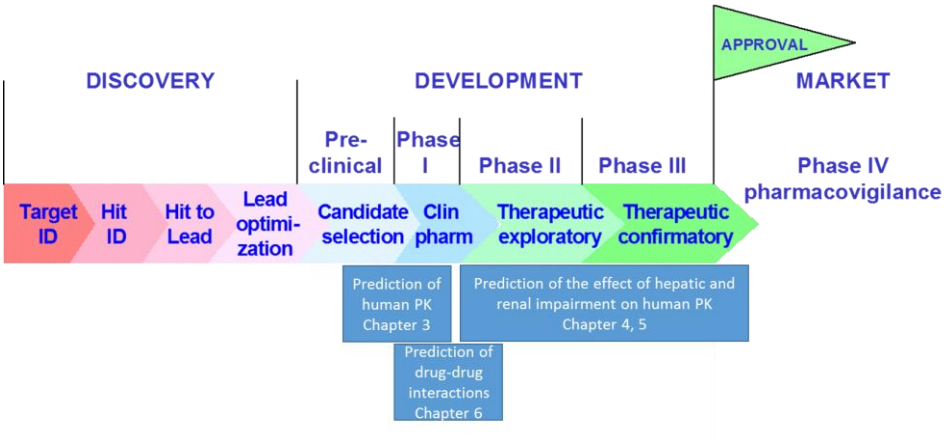

Figure 1.4. Allocation of the physiology-based applications described in this thesis in the drug development phases.

1.2. **Brief Background on Pharmacokinetics**

Pharmacokinetics is the study of the processes by which the body handles drugs and the rates at which these processes occur. For a more extensive description, the reader is recommended to refer to basic manuals on the topic, the best examples of which are the book or Rowland and Tozer [Rowland and Tozer, 2011] and Gibaldi and Perrier [Gibaldi and Perrier, 1982]. Briefly, the body absorbs the drug from the site of absorption (e.g., the gut, the muscle or the epidermis for oral, intramuscular and subcute drugs, respectively) and transfer it to the systemic circulation (for drugs given intravenously, therefore, the absorption is considered immediate and instantaneous), by which the drug is distributed to various tissue districts. In particular, the drug is delivered to the biophase where it can exert its therapeutic effect. In addition, the compound is delivered to organs such as the liver and the kidney that are responsible of the metabolism (i.e., the irreversible elimination of the compound *via* the formation of other chemical entities, the drug metabolites) and the excretion (i.e., the irreversible elimination of the unchanged drug via the renal or biliary excretion). All these processes are characterized by extent and rates and they can be evaluated measuring how the drug concentrations and amounts are changing with time in body fluids, such as blood, plasma, tissue samples and excreta. These data can be described using metrics of exposure (for instance, the maximal concentration in plasma or the area under the plasma concentrations-time curve). In this context, the pharmacokinetics is the knowledge that allows to translate a dosing regimen into the corresponding summary metrics of systemic exposure. Under defined assumptions, the pharmacokinetic theories allow to estimate from the drug concentrations-time curves measured in a suitable reference fluid (for instance, the plasma) the primary pharmacokinetic parameters that are able to characterize this translation. Examples of these primary parameters are the volume of

distribution (V, the proportionality constant that relates the amount of drug in the body with the concentrations), the clearance (CL, the proportionality constant that relates the rate of elimination to the concentrations) and the absolute bioavailability (F, the fraction of the dose that is absorbed in the systemic circulation when the drug is given extravascularly).

The assessment of pharmacokinetics is an essential portion of the development of new drugs. Different methodologies can be used for this purpose. There is the so-called "model-independent" non-compartmental analysis (NCA), which estimates the primary pharmacokinetic parameters based on the area under the plasma concentration-time curve, its first moment and the slopes. For the same purpose, empirical compartmental models (mammillary, in which, typically, the drug is eliminated from a central compartment) can be used: the plasma concentration-time curve is described by a model which assumes that drugs are diffusing into a small number of compartments and eliminated from one of these compartment. These compartments have no correspondence with anatomical tissues or organs. Again, the aim of this PK analysis is to provide an accurate description of the plasma concentration-time curve to calculate the primary pharmacokinetic parameters.

In both the previous approaches, the principal pharmacokinetic parameters can be defined based on their definition. For instance, for the clearance:

$$\frac{dAmt}{dt} = CL \cdot C,$$

where dAmt/dt is the rate of elimination and C is the concentration. The expression can be integrated, and, assuming that CL is invariant,

$$Amt = CL \cdot AUC,$$

where Amt is the amount eliminated (corresponding to the administered dose, in case of intravascular administration) and AUC is the area under the curve of the plasma (or any other reference fluid) concentration-time curve. The absolute bioavailability of extravascular dosing can be obtained (again in case of invariant CL, a condition that is described as linear pharmacokinetics) based on the comparison of the extravascular (EV, for instance, oral) and intravascular (IV) AUC referred to the same dose level:

$$Amt_{EV} \cdot F_{EV} = CL \cdot AUC_{EV}$$

$$Amt_{IV} = CL \cdot AUC_{IV}$$

Resolving for CL:

$$F_{EV} = \frac{AUC_{EV}/Dose_{EV}}{AUC_{IV}/Dose_{IV}}$$

The volume of distribution is a parameter that can be time-dependent; one of the relevant volume terms in the pharmacokinetic theory is the volume of the terminal phase (V_z), which assumes the presence of a log-linear terminal portion of the plasma concentration-time curve, characterized by a terminal half-life $t_{1/2,z}$. V_z is the proportionality constant between the amount of the compound present in the body and the concentrations on the terminal phase. Based on the clearance concept and the related equations, it can be easily demonstrated that:

$$V_z = CL \cdot \frac{t_{1/2,z}}{\ln(2)}$$

As mentioned above, the pharmacokinetic description that is mostly grounded to anatomical and physiological concepts is represented by the physiology-based pharmacokinetic (PBPK) modeling. PBPK models are compartmental models, in which compartments represents real tissues or organs and that take into consideration the interconnection of tissues and organs via the vasculature, the information on volumes and blood perfusions, tissues composition and structure, and the physiological basis of the drug distribution and clearance in the different tissues.

In the recent years PBPK applications boosted in the scientific literature and numerous papers (Jones et al., 2006, Jones et al., 2012a, Jones et al., 2012b) illustrated how different companies implemented PBPK approaches in their programs from the early to the late phases of development, contributing to the decrease of the costs of drug development. A typical example of this is the drug-drug interaction (DDI) plan for new drugs, formerly including dozens of different clinical pharmacology studies associating the new drug with all the potentially coadministered medications. Now the DDI plan is strongly streamlined, being based on a few studies, by which a relevant PBPK can be developed and validated: based on this, the extent of the DDI with the other medications can be accurately predicted and it is not rare now to find labels of drugs in which the potential effect of coadministered drugs are described via PBPK-based simulations (see for instance, https://www.janssenmd.com/pdf/imbruvica/PI-Imbruvica.pdf, accessed August 1, 2016).

However, in all the previously mentioned pharmacokinetic representations, including the most empirical ones, the primary pharmacokinetics parameters can be interpreted in the light of physiological concepts, so that they can be used for predicting the outcome in different systems (preclinical or clinical, different subject populations, etc.) or the PK differences due to intrinsic (pediatric, pregnancy, hepatic-renal impairment) or extrinsic factors (meal drug-drug interactions).

1.3. **Thesis overview**

The thesis is organized in six chapters, that are briefly described below.

1.3.1. Chapter 1 – Introduction and thesis overview

In this chapter a brief introduction is included on the role of physiology-based pharmacokinetic modeling in the drug development and on the pharmacokinetic theory. The structure of the thesis is also described.

1.3.2. Chapter 2 - The successes and failures of PBPK modeling: there is room for improvement

In this chapter, a brief overview of the outstanding advancements achieved in the last 20 years by PBPK modeling approaches is given. Whilst, in the early years, PBPK applications were confined to environmental toxicology and toxicants, now the vast majority of the papers relate to drugs and drug development. It is likely that newly developed computational approaches (such as the in silico tissue-composition models able to estimate tissue to plasma coefficients of partition), the newly gained knowledge-base (such as the information available on the escalation the hepatic clearance based on in vitro tissue experiment in microsomes and hepatocytes), and the recent availability of commercial platforms for PBPK modeling (such as SIMCYP and Gastroplus) are responsible of the flourishing of these PBPK applications.

Among the successes of this last period, it is noteworthy the potential for a precise prediction of the magnitude of drug-drug interactions (DDI) using PBPK, without the need of conducting actual in vivo studies, which in many cases is reflected in the labels of the most recent New Drug Applications (NDAs) (see for instance the label of ibrutinib, where the effects of the co-administration of moderate cytochrome P-450 3A inhibitors and inducers on the PK of the drug were based on PBPK simulations, https://www.janssenmd.com/pdf/imbruvica/PI-Imbruvica.pdf, accessed August 1, 2016). Other applications show instead substantial limitations and gaps. An example of this is the prediction of the human PK, based on in vitro and in vivo data in animals, which is characterized by uncertainties similar to those characterizing the older, relatively empirical approaches, such as allometric scaling. Other examples of these limitations concern the prediction of the PK alterations in subjects with hepatic or liver impairment, the precision of which is still unsatisfactory.

This chapter is based on the editorial: Poggesi I, Snoeys J, Van Peer A. The successes and failures of physiological-based pharmacokinetic modeling: there is room for improvement, published in Expert Opin Drug Metab Toxicol 2014, 10:631-5.

1.3.3. Chapter 3 - Use of WB-PBPK models and preclinical data for predicting the pharmacokinetics in the first-time in human studies

As indicated in Chapter 1, the capability of PBPK approaches to predict the PK in humans based on non-clinical experiments is relatively limited and it is not improved with respect to more traditional empirical scale-up techniques, such as allometric scaling. However, it must be remembered that in the preclinical development of a new drug, numerous experiments are performed to assess the pharmacokinetics in the preclinically relevant

pharmacological and toxicological species, following the administration of the new molecular entity (NME). Therefore, it should be possible to update and refine the PK predictions in humans as soon as the knowledge-base is increased when new preclinical studies are available. In this chapter, the basic PBPK approached based on the use of in silico input parameters was complemented with the parameter refinement derived by the use of the data obtained in the in vivo study in animals, using a Bayesian approach as implemented in the SAAM software.

This chapter is essentially based on the manuscript: Bizzotto R, Nucci G, Zamuner S, Sadiq WM, Poggesi I. Use of WB-PBPK models and preclinical data for predicting the pharmacokinetics in the first-time in human studies, that is being submitted to the European Journal of Pharmaceutical Sciences.

1.3.4. Chapter 4 – Some physiological considerations on the predictions of pharmacokinetic alterations in subjects with liver disease

Despite the substantial improvement of the description of the physio-pathological changes linked to hepatic impairment that are being included in the commercially available PBPK platform (e.g., SIMCYP), the predictions of the PK in subjects with hepatic impairment are still far from satisfactory. In many instances, the effects of hepatic impairment on the PK of drugs is predicted to be larger than the observed one, especially for conditions characterized by mild and moderate impairment. This may be due to different aspects, such as the limitations in the description of the different kind of liver disease, the absence of comprehensive liver function test that can describe the liver disease, the limitations of the actual experiments related to the assessment of the effect of liver impairment on the pharmacokinetics of drugs. In this chapter, a database was collected from the available PK data in this special population reported in the public domain (drug labels and scientific literature). Multivariate analyses approaches were able to predict the ratio of the systemic exposure (area under the plasma concentration-time curve) in subjects with hepatic impairment relative to that observed in healthy subjects. From this assessment, it is apparent that more comprehensive study designs may be needed to deepen the scientific knowledge of the PK alterations in these conditions. The smart use of multivariate analysis can also provide a substantial stimulus for a more detailed mechanistic understanding of the absorption and disposition changes to be expected in liver disease.

This chapter is based on the paper: Gonzalez M, Goracci L, Cruciani G, Poggesi I. Some considerations on the predictions of pharmacokinetic alterations in subjects with liver disease, published in Expert Opin Drug Metab Toxicol 2014, 10: 1397-408.

1.3.5. Chapter 5 – Some physiological considerations on the predictions of pharmacokinetic alterations in subjects with renal disease

Considerations analogous to those outlined for Chapter 4 can be done for the predictions of the PK in subjects with renal impairment. Although this special population may be more easily handled considering the main role of the amount of drug eliminated by renal excretion and by the residual renal function available in the subjects with renal impairment, there are cases (e.g., the unexpected effect of renal function impairment on the PK of drugs that are not excreted *via* the kidnelys) that makes the situation complicated. In this chapter, a similar database as the one collected for Chapter 4 was collected from the available data reported in the public domain and multivariate analyses approaches were applied to predict the effect of renal impairment on the PK of drugs.

This chapter is essentially based on the manuscript: Borella E, Poggesi I. Magni P. Predictive assessments of pharmacokinetic alterations in subjects with renal disease, that is being submitted to Clinical Pharmacokinetics. Part of this material was made available as a poster communication: Borella E, Poggesi I, Magni P. Predictive assessments of pharmacokinetic alterations in subjects with renal disease. PAGE 24 (2015) Abstr 3442 [www.page-meeting.org/?abstract=3442].

1.3.6. Chapter 6 – Modeling potential drug-drug interaction risks using a PBPK approach

As already indicated in the Chapter 2, the predictions of DDIs can be considered one of the major successes in the application of the PBPK based modeling approaches. In this chapter, physiological pharmacokinetic elements (the estimation of the clearance of a drug when it is co-administered with an inhibitor of cytochrome P-450 3A - one of the major drug metabolizing enzymes) are combined with a population PK approach (non-linear mixed effect models) to predict the potential level of drug-drug interaction. The exercise was motivated by the objective difficulties in designing clinical trials able to describe the level of interaction at steady state, due to the long terminal half-life (6-9 months) of the victim drug, bedaquiline.

This chapter is essentially based on the poster communication: Rossenu S, Del Bene F, Vermeulen A, Poggesi I. Modelling potential drug-drug interaction risks with a combined top-down/bottom-up approach. PAGE 24 (2015) Abstr 3560 [www.page-meeting.org/?abstract=3560].

1.4. References

Bizzotto R, Nucci G, Zamuner S, Sadiq WM, Poggesi I. PBPK modelling: an integrated approach for predicting human pharmacokinetics. Being submitted to Eur J Pharm Sci.

Borella E, Poggesi I, Magni P. Predictive assessments of pharmacokinetic alterations in subjects with renal disease. Being submitted to Clin Pharmacokin.

Borella E, Poggesi I, Magni P. Predictive assessments of pharmacokinetic alterations in subjects with renal disease. PAGE 24 (2015) Abstr 3442 [www.page-meeting.org/?abstract=3442].

Gibaldi M, Perrier D. Pharmacokinetics. 2nd edition, 1982, Marcel Dekker, New York and Basel.

Gonzalez M, Goracci L, Cruciani G, Poggesi I. Some considerations on the predictions of pharmacokinetic alterations in subjects with liver disease, Expert Opin Drug Metab Toxicol 2014, 10: 1397-408.

Jones HM, Parrott N, Jorga K, Lavé T. A novel strategy for physiologically based predictions of human pharmacokinetics. Clinical pharmacokinetics. 2006, 45:511-42.

Jones, H.M., Chen, Y., Gibson, C., Heimbach, T., Parrott, N., Peters, S.A., Snoeys, J., Upreti, V.V., Zheng, M., Hall, S.D. Physiologically based pharmacokinetic modeling in drug discovery and development: a pharmaceutical industry perspective. Clin. Pharmacol. Ther. 2012a, 97: 247–262.

Jones, H.M., Dickins, M., Youdim, K., Gosset, J.R., Attkins, N.J., Hay, T.L., Gurrell, I.K., Logan, Y.R., Bungay, P.J., Jones, B.C., Gardner, I.B. Application of PBPK modelling in drug discovery and development at Pfizer. Xenobiotica 2012b, 42: 94–106.

Khan AA, Perlstein I, Krishna R. The Use of Clinical Utility Assessments in Early Clinical Development. AAPS J. 2009 Mar; 11(1): 33–38

Kola I, Landis J. Can the pharmaceutical industry reduce attrition rates? Nat Rev Drug Discov. 2004;3(8):711-6.

Paul SM, Mytelka DS, Dunwiddie CT, Persinger CC, Munos BH, Lindborg SR, Schacht AL. How to improve R&D productivity: the pharmaceutical industry's grand challenge. Nature Rev Drug Disc 2010, 9, 203-14.

Poggesi I, Snoeys J, Van Peer A. The successes and failures of physiological-based pharmacokinetic modeling: there is room for improvement, Expert Opin Drug Metab Toxicol 2014, 10:631-5.

Rowland M, Tozer TN. Clinical Pharmacokinetics and Pharmacodynamics. Concepts and Applications. 4rth edition, 2011, Lippincott, Williams and Wilkins, Baltimore and Philadelphia.

Rossenu S, Del Bene F, Vermeulen A, Poggesi I. Modelling potential drug-drug interaction risks with a combined top-down/bottom-up approach. PAGE 24 (2015) Abstr 3560 [www.page-meeting.org/?abstract=3560].

Chapter 2

The successes and failures of PBPK[1]

This section is a focused review of the most recent achievement of the PBPK modeling, illustrating the successes of the approach, but also some unaddressed limitations. Some of these limitations will be examined in more detail in the subsequent chapters of this Thesis.

2.1. Abstract

From the beginning of the years 2000s physiologically-based pharmacokinetic (PBPK) models in the field of drug research and development started increasing. This proliferation of applications was prompted by the availability of new data and computational approaches required for the parameterization of PBPK models and the availability of commercial software platforms. PBPK approaches have been used to predict the pharmacokinetics in humans based on non-clinical data, the potential for drug-drug interactions, and the expected changes in the pharmacokinetics in case of different physiopathological conditions. In this respect, PBPK is also assuming a more important role in regulatory submissions. Although PBPK methodologies are not perfect yet, their continuous and consistent application is providing a more profound understanding of the determinants of the drug absorption and disposition of new drugs and candidate drugs. We are confident that, with its increased use, PBPK methodologies will gradually improve in their predictive capabilities.

[1] This chapter is based on the editorial: Poggesi I, Snoeys J, Van Peer A. The successes and failures of physiological-based pharmacokinetic modeling: there is room for improvement, published in Expert Opin Drug Metab Toxicol 2014, 10:631-5. Please note that the conclusion section has been named 'Expert Opinion' following the journal requirements.

2.2. **Introduction**

Physiologically-based pharmacokinetic (PBPK) approaches consist of compartmental pharmacokinetic models, in which basic biological knowledge is considered (for instance, the organ interconnectivity via the vasculature, information on tissues and organs – such as compositions, volumes and blood flow perfusions – and the understanding of physicochemical, physiological and biochemical processes governing absorption and disposition of compounds) [Rowland et al, 2011]. At variance from empirical compartmental pharmacokinetic models, the compartments in PBPK models are describing real anatomical spaces (tissues or organs) [Jones at al., 2011]. In addition, instead of allowing the complexity of the model to increase based on the data under consideration (e.g., increasing the number of compartments in the PK model, an example of the so-called "top-down" approach), PBPK represents an example of "bottom-up approach", which integrates from the beginning the known relevant characteristics and the complexities of the system (e.g., including compartments for all tissues and organs that are considered biologically relevant). PBPK models share the characteristics of the system pharmacology models, in which it is possible to dissect system-specific and compound-specific parameters, which can exploit the potential for translating and predicting the effect of a compound in a different system compared to the one in which the model was originally developed (i.e., as in the case for predicting the pharmacokinetics in humans from preclinical data, the pharmacokinetics in a special population from the pharmacokinetics in healthy subjects, or the effect of a comedication based on the characteristics of the compounds given alone) [Jones et al., 2011]. From a mathematical standpoint, these models are built based on a collection of mass balance equations which describe the compound concentration-time profile in all (whole-body PBPK) or some of the relevant tissue compartments.

Approximately up to a decade ago, PBPK models were mostly used for environmental toxicants or pollutants, for which there were insurmountable ethical constraints to generate data in the human population, so that the only approach was to try and predict the outcome of the exposure to toxicants in humans based on preclinical assessments [Rowland et al., 2011]. Despite numerous groups were active on the development and utilization of PBPK models, the application of PBPK to drug development was relatively limited (see Rowland et al., 2011 for a comprehensive list of references). If we search the public domain, looking for papers including the term "PBPK" (Figure 2.1) it is possible to see that the scientific production is bending upwards after the years 2002-2005 (a similar trend, based on a different search, was reported by Rowland et al., 2011). It is interesting to notice that the increase in the number of published papers on this topic was essentially boosted by the papers related to PBPK models of drugs, whilst the number of papers related to non-drugs appear relatively steady.

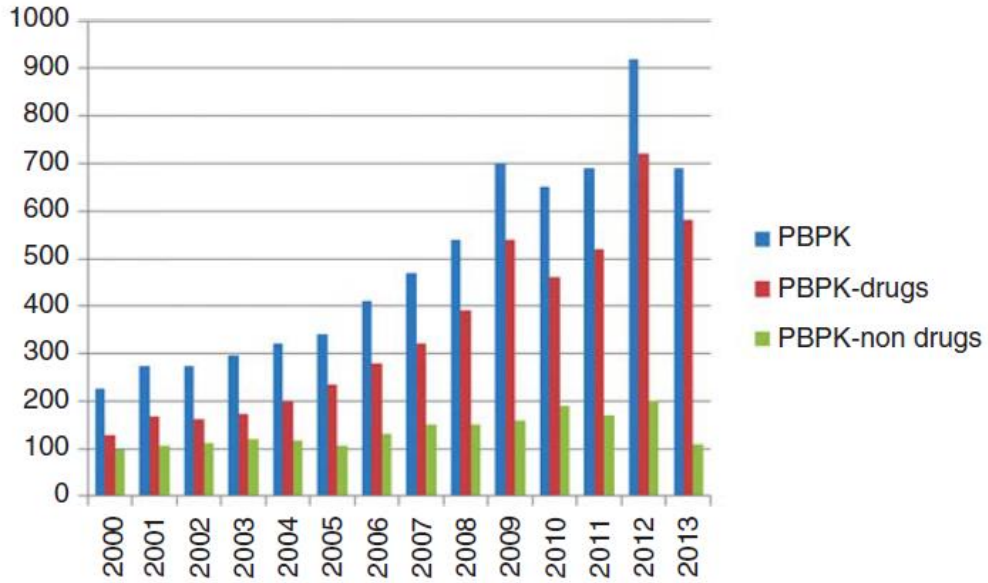

Figure 2.1. Number of papers mentioning the terms "PBPK"or "PBPK"AND "drugs"(google Scholar, accessed November 11, 2013).

Despite some uncertainties and difficulties, clearance concepts and the impact of hepatic extraction on bioavailability was well understood based on the seminal papers published in the seventies [Rowland et al., 1973; Wilkinson & Shand, 1975]. In the years preceding and around 2000, however, the in vitro intrinsic clearance measurements based on liver preparations and the use of informative human liver cytochrome P450 (P450) metabolic data (developed as part of the candidate drugs screening processes) started booming, providing an invaluable input to the development of PBPK models. Another improvement of paramount importance was the development of tissue composition models that appeared in the literature in that period [Pouline & Theil, 2002; Rodgers & Rowland 2005, Berezhkovskiy, 2004], which allowed to predict the tissue partition coefficients of compounds without measuring tissue concentrations. Another important cause of the increase in PBPK-related activities can be considered the organization, in 2002, of the workshop "Physiologically Based Pharmacokinetics (PBPK) in Drug Development and Regulatory Science" organized by the Center for Drug Development Science, Georgetown University, Washington [Poulin et al., 2011]. All this triggered the implementation and development of several platforms that were soon commercially available. Whilst, at the beginning, PBPK models were developed by users using generic or PK-related platforms (for instance ACSL, MATLAB, SAAM, or WINNONLIN), commercial programs, such as SIMCYP, Gastroplus, PK-SIM or Chloe-PK, made the PBPK approach available to a very large audience of scientists within the pharmaceutical industry. Overall, these software companies are currently dedicating such amount of resources, producing good science, and providing comprehensive tools that (unless very specific company-related issues need to be addressed)

it is now less of a need for pharma companies to dedicate scientists to the development and implementation of their own structural PBPK models; company scientists can reliably use the available commercial tools and focus instead their attention on the specific compound or company-related questions.

Overall, we are now dealing with a knowledge base that was essentially unthinkable at the beginning of the 2000.

Is it all a success story? No, it is not.

In a recent series of papers, the results of a study (inspired by PhRMA) on the accuracy of human pharmacokinetic predictions based on non-clinical data was described. In this study, anonymized data (in vitro and preclinical PK data) of drugs and candidate drugs were analysed with a battery of standardized approaches to provide the corresponding PK predictions in humans. The predictions were then compared with the actual outcomes of the clinical PK studies. The accuracy of PBPK approaches for predicting the PK profiles was relatively good when intravenous pharmacokinetics were considered, but it was far less satisfactory for compounds given orally (only a modest proportion of 23% of predicted plasma concentration-time profiles were characterized by medium to high degree of accuracy, based on prespecified criteria) [Poulin et al., 2011]. In addition, PBPK did not appear to be more accurate than other, more traditional methodologies (e.g., allometry) in predicting the PK behavior in humans [Rowland & Benet, 2011]. This indicates that still there are processes that are hiding their determinants and features, preventing to capture them in a mathematical description. For instance, considering that absorption models are lacking of the required accuracy, the physiological description of solubility and dissolution processes and their pharmaceutical formulation-based modulation must be still imperfect or, on the other hand, imperfect must be the experimental models or the input data used so far to characterize the processes. This is an area of intense investigations (in this regards, see, for instance, the papers emerging from the Oral Biopharmaceutical Tools [OrBiTo] project, for example Kostewicz et al., 2013).

Whilst the in vitro-in vivo extrapolation (IVIVE) of CYP-related hepatic metabolic clearance has already been matter of intense investigation, only recently the IVIVE application to extrahepatic or non-CYP related metabolism has been growing (see for instance Houston, 2013). Another area that requires improvements and it is subject of intense research is the involvement of transporters. Transporters have not often been included in PBPK models yet. Also in this case, the experimental models used for their characterization may not allow an easy scaling to the in vivo situation. Alternatively, additional modeling approaches should be used on the data obtained from in vitro experiments before they are actually used as input to PBPK models [Zamek-Gliszczynski et al., 2013].

A number of PBPK approaches have been reported concerning the prediction of PK in special populations. Very active are for instance the areas concerning the PBPK characterization in the pediatric population [Johnson & Rostami-Hodjegan, 2011] and in pregnant women [Vinks, 2013]. PBPK

models in subjects with hepatic impairment, with some notable exceptions [Johnson et al., 2010], seem instead less popular in the literature, despite the regulatory pressure on these themes and similar considerations can be done for subjects with renal impairment (likely due to the potential difficulties in establishing the role of endogenous metabolic and/or transporter inhibitors present in these conditions) [Sun et al., 2006] or subjects with other pathologies as, for instance, cancer (possibly due to the heterogeneity of this population) [Cheeti et al., 2013].

PBPK approaches have the benefit to provide – essentially as a byproduct – the concentration of the compounds in different tissue districts and biophases (sometime with outstanding precision, see Fig. 2.2). Unfortunately, this is not leading to the availability of a large number of corresponding pharmacokinetic-pharmacodynamic (PK-PD) models.

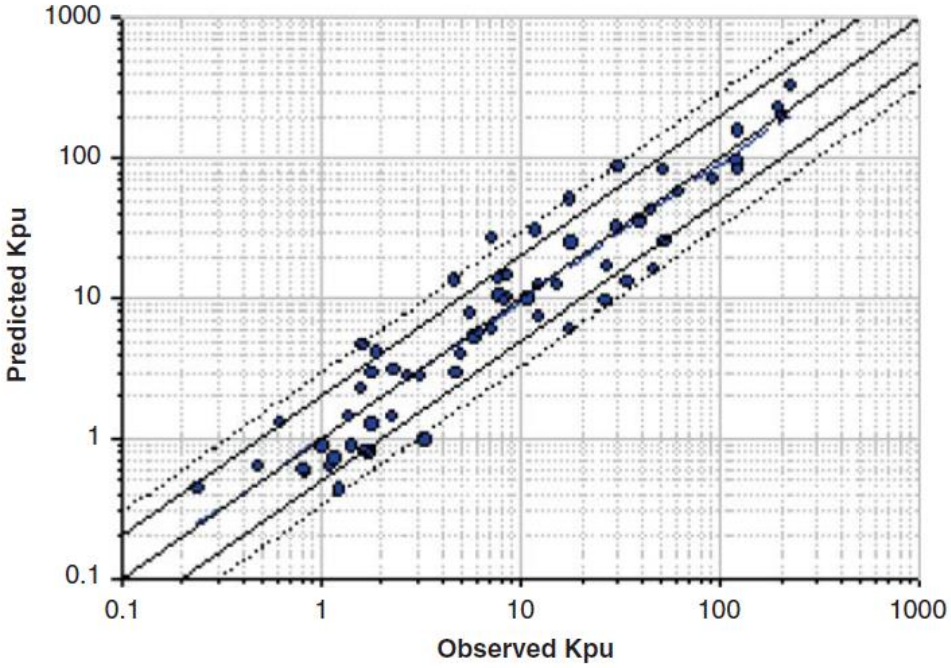

Figure 2.2. Relationship between observed values of unbound tissue partition coefficients in heart and predictions based on the tissue composition model. Plot prepared based on the data reported in the paper Rogers & Rowland, 2005.

2.3. **Expert opinion**

Despite PBPK approaches are well interlaced with the history of the development of the pharmacological science, only recently science, models, knowledge base of physiological data and computational tools acquired a substantial momentum. The numerical difficulties in solving systems of differential equations are not limiting anymore the application of PBPK approaches. The audience of PBPK modelers has substantially increased

with the adoption and use of the available commercial PBPK platforms and with the associated trainings and spread of knowledge (even if, in this respect, enough is never enough). The PBPK efforts reported in the recent scientific literature were almost unthinkable up to 10 years ago; an example for all, the flourishing literature addressing drug-drug interactions with PBPK exercises is absolutely exceptional. Initial PBPK modelling efforts are also starting for large molecules. Regulatory awareness and acceptance [Zhao et al., 2011; Huang et al., 2013] is fuelling the applications from the companies (if companies are not doing PBPK, agencies will do). Interesting attempts are also ongoing to provide a unified vision of the relationships between PBPK and standard compartmental PK [Pilari & Huisinga 2010].

On the other side, there are areas that require - definitely - the generation of new experimental data and – possibly - the development of new science. Surely we will always be dealing with an imperfect knowledge and with some "unknown unknowns"; however, the continuous and consistent application of these modelling approaches will improve the performance of PBPK models.

Do not go away, PBPK "is here to stay!" [Rostami-Hodjegan et al., 2012]

2.4. References

Berezhkovskiy LM. Determination of volume of distribution at steady state with complete consideration of the kinetics of protein and tissue binding in linear pharmacokinetics. J. Pharm. Sci. 2004; 93:364–74.

Cheeti S, Budha NR, Rajan S et al. A physiologically based pharmacokinetic (PBPK) approach to evaluate pharmacokinetics in patients with cancer. Biopharm Drug Disp. 2013; 34: 141–154.

Houston BJ. Prediction of human pharmacokinetics in 2013 and beyond. Drug Metab Dispos 2013, 41:1973-4.

Huang S-M, Abernethy DR, Wang Y, et al. The utility of modeling and simulation in drug development and regulatory review. J Pharm Sci 2013; 2912-23.

Johnson TN, Boussery K, Rowkland-Yeo K et al. A semi-mechanistic model to predict the effects of liver cirrhosis on drug clearance. Clin Pharmacokinet 2010; 49:189-206.

Johnson TN, Rostami-Hodjegan A. Resurgence in the use of physiologically based pharmacokinetic models in pediatric clinical pharmacology: parallel shift in incorporating the knowledge of biological elements and increased applicability to drug development and clinical practice. Pediatric Anesthesia 2011; 21:291–301.

Jones HM, Rowland-Yeo K. Basic concepts in Physiologically based pharmacokinetic modeling in drug discovery and development. CPT:Pharmacometrics and System Pharmacology 2013; 2:e63.

Kostewicz ES, Abrahamsson B, Brewster M, et al. In vitro models for the prediction of in vivo performance of oral dosage forms. Eur J Pharm Sci Published on line 27 August 2013, http://dx.doi.org/10.1016/j.ejps.2013.09.008.

Pilari S, Huisinga W. Lumping of physiologically-based pharmacokinetic models and a mechanistic derivation of classical compartmental models. Journal pharmacokin pharmacodyn 2010; 37:355-405.

Poulin P, Theil FP. Prediction of pharmacokinetics prior to In vitro studies. 1. Mechanism-based prediction of volume of distribution. J Pharm Sci 2002; 91:129-56.

Poulin P, Jones RDO, Jones HM et al. PHRMA CPCDC initiative on predictive models of human pharmacokinetics, Part 5: prediction of plasma concentration–time profiles in human by using the physiologically-based pharmacokinetic modeling approach. J Pharm Sci 2011; 100:4127-57.

Rodgers T, Rowland M. Physiologically based pharmacokinetic modeling 2: Predicting the tissue distribution of acids, very weak bases, neutrals and zwitterions. J. Pharm. Sci. 2005; 95:1238–57.

Rostami-Hodjegan A, Tamai I, Pang S. Physiologically based pharmacokinetic (PBPK) modeling: It is here to stay! Biopharm Drug Disp 2012; 33:47–50.

Rowland M, Benet LZ, Graham GG. Clearance concept in pharmacokinetics. J Pharmacokin Pharmacodyn 1973; 1:123-36.

Rowland M, Peck C, Tucker G. Physiologically-based pharmacokinetics in drug development and regulatory science. Annu Rev Pharmacol Toxicol 2011; 51:45-73.

Rowland M, Benet LZ. Lead PK commentary: predicting human pharmacokinetics. J Pharm Sci 2011; 100:4047-9.

Sun H, Frassetto L, Benet LZ. Effects of renal failure on drug transport and metabolism. Pharmacology & Therapeutics 2006; 109: 1 – 11.

Wilkinson GR, Shand DG. A physiological approach to hepatic drug clearance. Clin Pharmacol Ther 1975; 18:377-90.

Vinks AA. The future of physiologically based pharmacokinetic modeling to predict drug exposure in pregnant women. CPT: Pharmacometrics & Systems Pharmacology 2013; 2:e33.

Zamek-Gliszczynski MJ1, Lee CA, Poirier A, et al. ITC Recommendations for Transporter Kinetic Parameter Estimation and Translational Modeling of Transport-Mediated PK and DDIs in Humans. Clinical Pharmacology & Therapeutics 2013; 94:64–79.

Zhao P, Zhang L, Grillo JA et al. Applications of physiologically based pharmacokinetic (PBPK) modeling and simulation during regulatory review. Clin Pharmacol Ther 2011; 89:259–67.

Chapter 3

PBPK modelling for predicting human pharmacokinetics[2]

One of the limitations mentioned in the previous chapter is the unsatisfactory accuracy of the PBPK approaches, when applied in a blinded mode, to predict the PK in humans. However, during the development of a research program, numerous information is available and can be considered in the development of the PBPK model, which is the best suited approach for finding a synthesis of the diverse sources of information. In this Chapter, a basic PBPK model is complemented with information obtained in preclinical PK studies in rats. Based on this data, some of the parameters of the PBPK model can be modulated, using Bayesian estimation and the basic PBPK assumptions as priors. The new model can then be used to simulate the PK in humans with a substantial improvement of the predictions.

3.1. **Abstract**

The mechanistic structure of physiology-based pharmacokinetics (PBPK) models make them ideal tools for predicting systemic exposure in first-in-man studies, but their predictive performance is sometime disappointing and their accuracy is not better than other less mechanistic approaches, such as allometry. However, the capability of these models of integrating the information gathered during pre-clinical drug development has not been fully exploited as yet. In this work, the PK of 15 compounds from psychiatric

[2] This chapter is essentially based on the manuscript: Bizzotto R, Nucci G, Zamuner S, Sadiq WM, Poggesi I. Use of WB-PBPK models and preclinical data for predicting the pharmacokinetics in the first-time in human studies, that is being submitted to the European Journal of Pharmaceutical Sciences.

programs, in both rats and humans, was predicted with a basic PBPK model. The fold errors on the area-under-the-curve (AUC) predictions in man were within 2 and 3 in 20% and 33% of the cases. Multivariate analysis was applied to the rat outcomes to study the predictive performance of the PBPK model and the sensitivity of its outputs to its inputs. For each compound, lipophilicity, protein binding, hepatic clearance and tissue binding were identified by fitting the rat PK data and using the experimental/standard values as priors. The refined parameter values were then used to predict again the PK in man. The percentage of fold errors on AUC predictions within 2 and 3 increased to 27% and 60%, respectively. In conclusion, this work shows that the knowledge obtained from preclinical experiments should be integrated in the PBPK model, in order to account for the uncertainty in some of the parameters values and for the potential for some of the PBPK model assumptions not to hold. This integration would allow to increase the accuracy of the PBPK predictions of first-in-man studies.

3.2. **Introduction**

During drug development, a fundamental step in designing the first clinical trial (first-in-man, FIM) is to anticipate, with good accuracy, the expected systemic exposure in healthy volunteers at the adopted dose levels [Poulin et al., 2011]. The accurate prediction of systemic exposure in man allows an accurate definition of the conditions associated with tolerability issues identified via preclinical toxicological models, and consequently a more sensible choice of the initial dose to be administered to the volunteers. In addition, it permits anticipating the dose range that is expected to provide systemic exposures associated with a response in preclinical pharmacological models of efficacy. This knowledge allows a more efficient and informative dose escalation in FIM, which is of particular importance in therapeutic areas, such as oncology, in which the FIM is performed in patients: the dose can be efficiently escalated to clinically relevant values, and the number of patients exposed to ineffective treatment can thus be minimized [Kummar et al., 2006].

Numerous approaches have been proposed for predicting, in humans, the pharmacokinetic parameters (plasma clearance, CL, volume of distribution, V, and absolute bioavailability, F) allowing the estimation of the metrics of clinical systemic exposure at a certain dose level (maximum and minimal drug concentrations, and area-under-the-curve of the concentration time course, AUC) [Poggesi, 2004]. In many cases the allometric approach is used [Huang and Riviere, 2014], which assumes that the pharmacokinetic (PK) parameters are log-linear functions of body size and weight. With this approach, CL and V in humans can be estimated based on the regression of the values of the parameters obtained in the preclinical species. Numerous modifications and corrections (e.g., for maximum lifespan or for brain weight) have been suggested by different authors [Mahmood, 2007; Nagilla and Ward, 2004]. Moreover, the use of allometric concepts have been

proposed in the context of non-linear mixed effect modelling [Cosson et al., 1997], allowing to include inter-individual and inter-species variability terms.

In vitro-in vivo extrapolation approaches can be used and variously integrated in the prediction of human PK characteristics [Rostami-Hodjegan and Tucker, 2007]. The experiments leading to the estimation of the hepatic intrinsic clearance values based on measurements from liver preparations (microsomes and, even more relevant, hepatocytes) [De Buck et al., 2007; Lu et al., 2006; Obach, 1999; Obach et al., 1997] have been substantially improved in the last decade, and their capability to allow quantitative extrapolation to the whole human liver has been tested by many groups. Analogously, many approaches have been suggested for the estimation of the volume of distribution terms [Lombardo et al., 2004, 2002; Obach et al., 1997; Poulin and Theil, 2002a; Rodgers et al., 2005; Rodgers and Rowland, 2006; Berezhkovskiy, 2004], based on the physico-chemical properties of the compounds or on the combination of *in silico* and *in vitro* measurements.

Whole-body physiology-based pharmacokinetic (PBPK) modelling appears particularly suited to integrate knowledge of different origins (e.g., *in silico*, *in vitro*, and *in vivo*) in an anatomically and physiologically relevant framework. At variance from empirical compartmental models, in which compartments do not represent actual body districts, the actual volumes, compositions, and perfusions of the different organs and tissues are accounted for in a PBPK model. The structure of this model includes one or more compartments for each pharmacokinetically relevant organ or tissue. These compartments are interconnected via the arterial and venous systemic circulation, consistent with the known anatomical description of the body. Finally, basic physiological and biochemical principles are used to describe the details of the absorption and elimination processes [Jones and Rowland-Yeo, 2013; Rowland et al., 2011]. In recent years, the adoption of PBPK models in the applications related to drug development has been tremendously increasing [Jones et al., 2015, 2012; Zhao et al., 2012]. These models, often comprised in the more general systems-pharmacology approaches, allow a neat dissection of the system-related parameters from the drug-related parameters. Consequently, they provide a powerful tool for translating preclinical data into human PK predictions via the adoption of the parameter set for the relevant system.

Quite unfortunately and despite some reports indicating good predictions [Chen et al., 2012], an extensive blinded evaluation performed as part of a Phrma CPCDC initiative indicated that the pure PBPK predictive approach does not perform better than other methods [Poulin et al., 2011; Rowland and Benet, 2011]. Whilst on average, 69% and 90% of the AUC PBPK-predictions for drugs intravenously administered in humans were within 2 and 3 times the observations in humans, respectively, these percentages were substantially lower for oral drugs, as in this case only 21% and 37% of the predictions were within 2 and 3 times the observations, respectively. These results highlight the need for improved PBPK methods in the prediction of human exposure.

In this respect, it is worth noting that some basic parameters required as input to the PBPK models can be biased or known with substantial uncertainty. This translates into significant margins of error in the prediction of human PK. Thus, any further data generated during the development of the new molecular entity should be used, when possible, to remove this uncertainty and improve the predictive performance. The physiological nature of PBPK models makes them the ideal tool for implementing this operation, as these models have the possibility to "grow" when new knowledge is generated. For example, the parameters of a basic PBPK model (e.g., those based on simple *in silico* descriptors) can be adjourned based on the PK outcome in the rodent preclinical species; and the new values can be further updated when PK data in non-rodent species are produced.

This section tests this unexplored possibility on a panel of different compounds. Indeed, it first describes the performance of the PBPK approach in the prediction of the PK of 23 molecules after intravenous dosing in rats and of 15 of them following oral dosing to humans. Thereafter, it analyses whether the predictions in humans can be substantially improved via the identification of some critical input parameters and their systematic refinement based on the outcome of the PBPK predictions in rats.

3.3. **Materials and methods**

3.3.1. PBPK model

A whole-body PBPK model was implemented with SAAM II™ v1.1.2 (SAAM Institute, University of Washington, Seattle) and Berkeley Madonna™ v8.0.2 (Department of Molecular and Cellular Biology, University of California, Berkeley). The structure of the model consists of 13 compartments interconnected via the vasculature and representing different tissues, i.e., venous blood, arterial blood, adipose tissue, bone, brain, gut, heart, liver, lung, kidney, muscle, skin and spleen (Figure 1). The liver is considered the only site of drug metabolism and the kidney the only site of drug excretion. The venous blood is the site of input for intravascular (IV) doses, while the gut is the site of input for oral (PO) administration.

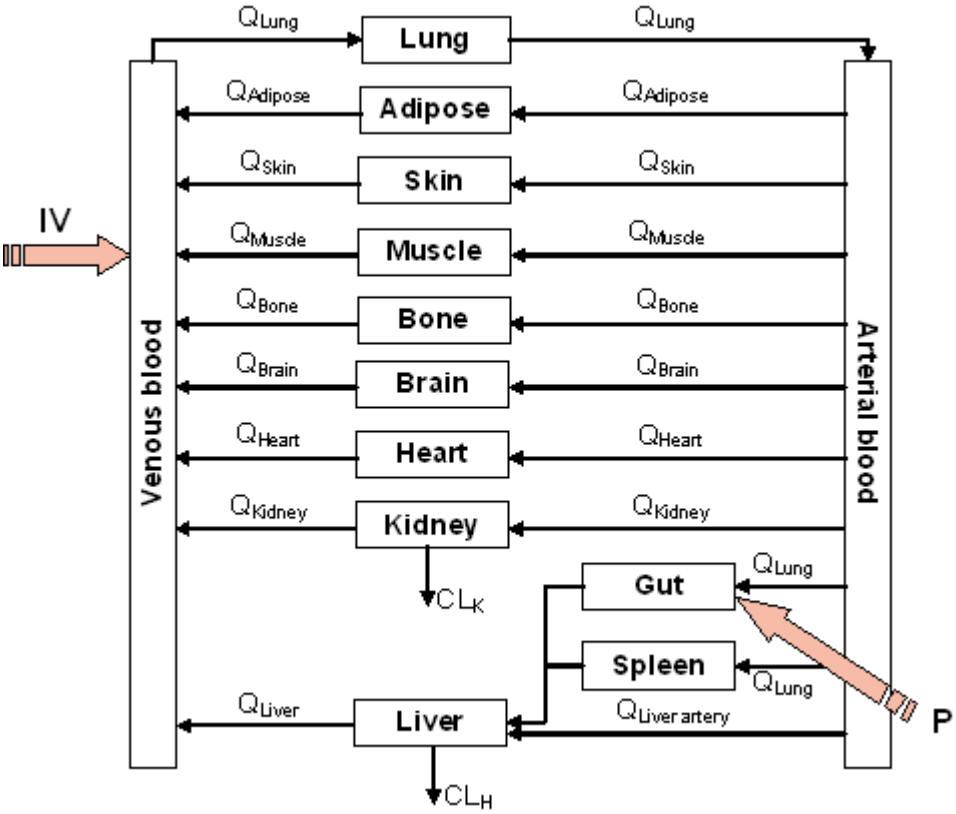

Figure 3.1. Schematics of the PBPK model.

Drug distribution in each tissue is hypothesized to be well-stirred. Permeability-limited uptake is excluded, as it may occur for compounds with low lipophilicity or high molecular weights (not the case here, see below). Binding into deep organ compartments is excluded as well.

The mass balance equation for a generic compartment describes the drug partition between the blood and the tissue, T, and the drug elimination by the tissue:

$$\frac{dC_T}{dt} = \frac{1}{V_T} \cdot \left(Q_T \cdot C_{input} - \frac{Q_T \cdot C_T}{\frac{P_{T:P}}{P_{B:P}}} - CL_T \cdot C_T \right), \qquad (1)$$

where C_T is the drug concentration in the tissue compartment T, V_T is the volume of the tissue compartment, Q_T is the blood flow to the compartment, C_{input} is the plasma concentration in input to the tissue, $P_{T:P}$ is the tissue-to-plasma partition coefficient at steady-state (i.e., the tissue-to-plasma concentration ratio), $P_{B:P}$ is the blood-to-plasma concentration ratio and CL_T is the intrinsic clearance of the tissue [Jones and Rowland-Yeo, 2013].

Partition coefficients ($P_{T:P}$) for adipose and non-adipose tissues at steady-state are estimated using a tissue composition model [Poulin and Theil, 2002b, 2000; Poulin et al., 2001]. The distribution of a compound into each tissue is assumed to depend on its partition into the lipids and water mixture

available in that tissue and on its reversible binding to the proteins in plasma and in the tissue interstitial space:

$$P_{T:P\_non\_Adipose} = \frac{P_{o:w} \cdot \left(V_{nlT} + 0.3V_{phT}\right) + \left(V_{wT} + 0.7V_{phT}\right)}{P_{o:w} \cdot \left(V_{nlP} + 0.3V_{phP}\right) + \left(V_{wP} + 0.7V_{phP}\right)} \cdot \left(\frac{f_{uP}}{f_{uT}}\right), \quad (2)$$

$$P_{T:P\_Adipose} = \frac{D_{vo:w} \cdot \left(V_{nlT} + 0.3V_{phT}\right) + \left(V_{wT} + 0.7V_{phT}\right)}{D_{vo:w} \cdot \left(V_{nlp} + 0.3V_{php}\right) + \left(V_{wp} + 0.7V_{php}\right)} \cdot f_{uP}, \quad (3)$$

Eq. 2 holds for non-adipose tissues and Eq. 3 holds for the adipose one; $P_{o:w}$ is the n-octanol:water partition coefficient of the non-ionized species, $D_{vo:w}$ is the vegetable oil:water distribution coefficient (partition coefficient of both the unionized and ionized species) at a pH value of 7.4; V_{wT}, V_{nlT}, V_{phT} are the fractional weights of water, neutral lipids and phospholipids in the tissue T, respectively, and V_{wP}, V_{nlP}, V_{phP} are the corresponding values in plasma; $f_{uP,}$ and f_{uT} are the fractions of unbound drug in plasma and in the tissue, respectively. The former is obtained experimentally, while the latter is calculated as reported in the literature [Poulin and Theil, 2000]:

$$f_{uT} = \frac{1}{1 + \left(1 - f_{uP}\right) / f_{uP} \cdot \alpha}. \quad (4)$$

where α is a constant assumed to be equal to 0.5 in all tissues [Poulin and Theil, 2000]. This assumption means that the tissue-to-plasma ratio of the binding macromolecules concentrations is equal to 0.5 in all tissues, which is in accordance with the amount of albumin, the major plasma binding protein, being in the order of 60% outside the plasma [Rowland and Tozer, 1994]. The model for calculating the tissue-to-plasma partition coefficients (Eq. 2, 3 and 4) has been successfully validated using *in vivo* estimates of volume of distribution obtained in rats for 123 unrelated drugs [Poulin and Theil, 2002b].

The values for $P_{o:w}$ and $D_{vo:w}$ in Equations 2 and 3 can be derived from experimental measures. If only one of them is available, the other one can be computed using the following equations:

- the empirical relation between partition coefficients relative to vegetable oil and n-octanol [Leo et al., 1971; Poulin and Theil, 2002b]:

$$log(P_{vo:w}) = 1.115 \cdot log(P_{o:w}) - 1.35; \quad (5)$$

- the Henderson-Hasselbalch equations, which require the knowledge of the values of the acid constants and tissue pH is assumed to be 7.4:

$log(D_{vo:w}) = log(P_{vo:w}) - log(1 + 10^{pH-pKa})$ for monoprotic acids
$log(D_{vo:w}) = log(P_{vo:w}) - log(1 + 10^{pKa-pH})$ for monoprotic bases
$log(D_{vo:w}) = log(P_{vo:w}) - log(1 + 10^{pH-pKa1+pH-pKa2})$ for diprotic acids
$log(D_{vo:w}) = log(P_{vo:w}) - log(1 + 10^{pKa1-pH+pKa2-pH})$ for diprotic bases
$log(D_{vo:w}) = log(P_{vo:w}) - log(1 + 10^{pKaBASE-pKaACID})$ for zwitterions
$log(D_{vo:w}) = log(P_{vo:w})$ for neutrals. (6)

In cases when both $P_{o:w}$ and $D_{vo:w}$ are available from experimental measures, the experimental values for $D_{vo:w}$ are not considered and their values derived from Equations 5 and 6 are instead used.

The ratio between (total) blood and plasma concentrations can be experimentally derived from the fraction of binding red blood cells, f_{bRBC}, and the species-specific haematocrit, H:

$$P_{B:P,\exp} = \frac{1-H}{1-f_{bRBC}}. \quad (7)$$

Since the $P_{B:P}$ ratio can be experimentally not available for some compounds, Eq. 2 can be rearranged to obtain its estimate (the "computed" one) as follows:

$$P_{B:P,comp} = \frac{P_{o:w}\cdot\left(V_{nlB}+0.3V_{phB}\right)+\left(V_{wB}+0.7V_{phB}\right)}{P_{o:w}\cdot\left(V_{nlP}+0.3V_{phP}\right)+\left(V_{wP}+0.7V_{phP}\right)}, \quad (8)$$

where the unbound fractions in blood and plasma are assumed to be the same.

The intrinsic hepatic clearance, CL_H, introduced into the mass balance equation for the liver compartment, is calculated considering a well-stirred model for the liver [Rowland et al., 1973; Wilkinson and Shand, 1975]:

$$CL_H = \frac{\beta\cdot CL_{app}\cdot LW\cdot Q_H}{\beta\cdot CL_{app}\cdot LW + Q_H}, \quad (9)$$

CL_{app} is the apparent in vitro intrinsic clearance obtained in liver preparations (microsomes or hepatocytes) of the species under consideration, expressed per gram of liver, LW is the liver weight, Q_H is the hepatic blood flow and β is the ratio between f_{uP} and the fraction unbound to microsomes or hepatocytes. It is assumed here that β is one, i.e., that the non-specific binding to the liver preparations is equivalent to the binding to plasma proteins [Poulin and Theil, 2002a]. CL_{app} is expressed as mL/min per gram of liver and has to be scaled to the entire liver value through the average liver weight for the considered species.

The intrinsic renal clearance, CL_K, introduced into the mass balance equation of the kidney compartment, is obtained from the glomerular filtration rate, GFR:

$$CL_K = \frac{GFR\cdot f_{uP}}{P_{B:P}}. \quad (10)$$

The other contributions to renal clearance, i.e., active tubular secretion and reabsorption [Rowland and Tozer, 1994], can be considered negligible or reciprocally compensating.

All the others tissues are assumed to be non-eliminating organs, therefore CL_T is assumed equal to zero in those cases.

In summary, in order to set up the described PBPK model, a few input parameters need to be retrieved from different sources, i.e., physicochemical analysis of the drug, *in vitro* experiments, *in silico* computations and *in vivo* or *ex vivo* measurements published in literature:

- the chemical nature of the compound (monoprotic acid, monoprotic base, diprotic acid, diprotic base, zwitterion or neutral molecule);
- experimental or *in silico* physicochemical data: pKa(s), $\log(P_{o:w})$ and/or $\log(D_{vo:w})$;

- *in vitro* data: f_{uP}, CL_{app} , $P_{B:P}$ (if available);
- physiological and biochemical data, taken from the literature: Q_T's, V_T's, V_{phT}'s, V_{nlT}'s, V_{wT}'s, GFR, LW, H.

Other input parameters are the individual body weight, used to scale blood flows and volumes, and the details about the administration of the drug (dose and rate). The rate of absorption into the gut after oral administration is computed using GenesiPK, a Matlab-based PBPK tool [Germani et al., 2007] which uses as inputs the parameters described above and the predicted jejunum permeability (solubility in water is not considered as all compounds are considered by the tool as highly soluble, i.e., BCS class I or III).

If expressed in plasma, the systemic clearance, CL, is computed as the sum of hepatic and renal clearances, and the volume of distribution at steady-state, V_{ss}, is computed as follows [Poulin and Theil, 2002a]:

$$V_{ssP} = \sum_i V_{Ti} \cdot P_{Ti:P} + V_P . \qquad (11)$$

Converting clearance and volume of distribution expressed in plasma to those expressed in blood is straight forward according to the following equations:

$$CL_P \cdot C_P = CL_B \cdot C_B , \quad (12)$$

$$V_{ssP} \cdot C_P = V_{ssB} \cdot C_B . \quad (13)$$

3.3.2. PK Predictions in Rats

3.3.2.1. Model Parameterization

The PBPK model was parameterized using anatomical and physiological parameters provided in the literature for rats [Brown et al., 1997; Poulin and Theil, 2002a, 2002b; Ritschel, 1992] and summarized within the Supplementary Material (Section S1). Each tissue blood flow was derived as a fraction of the total cardiac output (CO), which is also the blood flow perfusing the lungs. Its value for rats of different body weights (BW) was calculated through an allometric equation:

$$CO(mL/\min) = 0.235 \cdot BW(kg)^{0.75} . \quad (18)$$

Since the tissues considered in this PBPK implementation were not exhaustive of the entire composition of the body, and since the total CO had to equal the sum of each tissue blood flow to have an exact whole-body mass balance, the venous or arterial or lung blood flow was corrected through the following equation:

$$Q_B(L/\min) = 0.215 \cdot BW(kg)^{0.75} . \qquad (19)$$

The volumes of rat organs were taken from the literature [Brown et al., 1997] and are reported in the Supplementary Material (Section S1).

3.3.2.2. Data

The model was evaluated using a set of 23 drug candidates synthesized by the Psychiatric Centre of Excellence in Drug Discovery in GlaxoSmithKline. The characteristics of the different compounds are provided in Table 3.1. For 15 of these molecules (set A), PK was evaluated

also in humans and a systematic approach for refining this prediction is proposed and evaluated in this Chapter (see below). For the sake of comparison to the refined predictions, Table 3.1 provides summary statistics on set A and on the whole set of 23 compounds (set B) separately. Being part of psychiatric programs, all these molecules are designed to cross the blood-brain barrier. Consequently, none of them is an acid, only one of them is neutral, one is a zwitterion (within set B), the remaining being bases; all of them are small molecules with moderate to very strong lipophilic properties, characterized, with a couple of exceptions, by an extensive plasma protein binding. In all cases the blood-to-plasma partition coefficients were experimentally available, but simulations were performed also using $P_{B:P,comp}$, in order to evaluate the model performance in case of missing $P_{B:P,exp}$.

The compounds were administered IV, as a bolus or short infusion. Each molecule was administrated to multiple rats: N = 3 in all cases, apart from two compounds for which N = 6. For each rat, blood or plasma samples were submitted to non-compartmental analysis to derive *in vivo* estimates of systemic clearance, CL, and volume of distribution at steady-state, V_{ss}. Median values were then computed for each compound.

Table 3.1. Characteristics of the compounds used in the analysis

Compound	Molecular weight	log($P_{o:w}$)*	Chemical species†	pKa	P-gp substrate	Solubility	Predicted Human Jejunum permeability (*10^{-4}cm/s)	Rat $P_{B:P,exp}$	Rat $P_{B:P,comp}$	Rat f_{up}	Rat CL_{int} microsomes (mL/min/g liver)	Rat CL_{int} hepatocytes (mL/min/g liver)	Used value for rat CL_{int} (mL/min/g liver)	Human $P_{B:P,exp}$	Human $P_{B:P,comp}$	Human f_{up}	Human CL_{int} microsomes (mL/min/g liver)	Human CL_{int} hepatocytes (mL/min/g liver)	Used value for human CL_{int} (mL/min/g liver)
GSK1	416	3.48	db	5.9; 6.9	y	low	3.624	0.71	1.12	0.041	0.8	0.47	0.8	0.74	1.20	0.041	1.2	NA	1.2
GSK2	433	4.63	b	9.3	NA	high	14.09	2	1.18	0.019	[<0.5-0.9]	NA	0.7	2.1	1.23	0.028	1	NA	1.0
GSK3	489	4.87	b	8.63	y	high	19	1.6	1.18	0.02	0.9	NA	0.9	0.8	1.23	0.006	1	NA	1.0
GSK4	407	3.8	b	5.41	n	low	4.079	0.8	1.15	0.031	0.9	NA	0.9	0.71	1.22	0.061	[<0.5,<0.5, 0.6]	NA	0.4
GSK5	469	2.93	db	3.61; 6.04	y	low	1.649	1.2	0.87	0.029	[<0.5-0.6]	NA	0.25	1	1.15	0.013	0.8	NA	0.8
GSK6	632	4.41	b	7.86	NA	high	4.84	0.65	1.17	0.012	0.6	NA	0.6	0.62	1.23	0.028	1.3	NA	1.3
GSK7	407	3.2	b	7.9	n	high	7.22	0.82	1.09	0.056	[<0.5-0.5]	NA	0.5	0.78	1.18	0.085	0.6	NA	0.6
GSK8	334	2.91	n	-	n	low	6.446	0.7	0.97	0.133	0.7	NA	0.7	0.8	1.14	0.092	[<0.5-1]	NA	0.5
GSK9	351	2.53	b	7.6	n	high	high	0.6	0.84	0.06	1	NA	1	0.6	1.06	0.032	[<0.5-0.6]	NA	0.5
GSK10	607	7.1	b	9.2	y-n	high	high	0.8	1.18	0.028	[<0.5-0.6]	NA	0.5	0.9	1.23	0.06	2.2	NA	2.2
GSK11	617	4.56	b	7.13	n	high	high	0.74	1.17	0.012	2.4	11	11	0.61	1.23	0.005	0.9	0.5	0.5
GSK12	665	3.9	b	5.89	NA	high	23	0.81	1.16	0.01	0.9	5.55	0.9	NA	1.22	0.0013	[<0.5-<0.5]	NA	0.3
GSK13	404	3.9	b	6.6	n	low	5.789	1.17	1.16	0.01	1.9	[0.05-0.96]	1.9	0.94	1.23	0.004	0.6	NA	0.6
GSK14	478	5.05	b	1.39	y-n	low	6.27	0.5	1.18	0.01	8.7	0.22	8.7	0.49	1.23	0.003	15.1	0.5	0.5
GSK15	508	5.03	b	8.69	n	NA	1	2.1	1.18	<0.01‡	1.1	NA	1.1	1.3	1.23	<0.01‡	0.9	NA	0.9
average	481	4.2	-	-	-	-	-	1.0	1.1	0.03	-	-	2.0	0.9	1.2	-	-	-	0.8
min	334	2.5	-	1.39	-	low	1	0.5	0.8	0.01	-	-	0.3	0.49	1.06	0.001	-	-	0.3
Max	665	7.1	-	9.2	-	high	14.09	2.1	1.2	0.133	-	-	11	2.1	1.23	0.092	-	-	2.2

* Experimental value if available, otherwise computed based on Equations 5 and 6

† db: diprotic base; b: monoprotic base; n: neutral; ‡ Value used for predictions: 0.005

3.3.3. PK Predictions in humans

3.3.3.1. Model Parameterization

The model was also parameterized using anatomical and physiological parameters provided in the literature for humans [Brown et al., 1997; Poulin and Theil, 2002a; Ritschel, 1992] and summarized within the Supplementary Material (Section S1). A correction for the CO in humans of different ages was applied. Similarly to what done for rats, the venous or arterial or lung blood flow was corrected through the following equation:

$$Q_B(L/\min) = 0.899 \cdot CO(L/\min)$$

The volumes of human organs were calculated as for rats.

The computed values of the partition coefficients between blood and plasma were used, as it was found within this work that they improve the prediction of PK in rats (see Section 3.4.1).

3.3.3.2. Data

Fifteen of the molecules used for PK prediction in rats (set A) were administered to humans as well, as part of different FIM studies performed in GlaxoSmithKline. The compounds were administered orally to multiple individuals (N between 8 and 19). For each subject, plasma samples were submitted to non-compartmental analysis to derive, from the plasma concentration time courses, estimates of systemic exposure [maximum concentration (C_{max}) and AUC calculated using the trapezoidal rule and extrapolated to infinity via the terminal half-life ($t_{1/2}$)] and the pharmacokinetic parameters [oral apparent plasma clearance ($CL_{P,PO}$ = Dose/AUC) and oral apparent volume of distribution at steady state ($V_{ss,P,PO}$ = $CL \cdot t_{1/2}/\ln(2)$, assuming rapid absorption]. Median values of the parameters were then computed for each compound.

3.3.4. Accuracy of Predictions

The accuracy of the PBPK-predicted parameters (CL and V_{ss} for rats or C_{max} and AUC for humans) was expressed in terms of fold-error, fe [Wajima et al., 2002):

$$fe(P_{pred,i}) = \begin{cases} \dfrac{P_{pred,i}}{P_{OBS,i}} & if \quad P_{pred,i} > P_{OBS,i} \\ \\ \dfrac{P_{OBS,i}}{P_{pred,i}} & if \quad P_{pred,i} \le P_{OBS,i} \end{cases} \qquad (20)$$

where $P_{OBS,i}$ is the observed parameter calculated for the i^{th} compound and $P_{pred,i}$ is the corresponding prediction.

Correlations between observations and predictions were computed as Spearman rank correlation coefficients. Any systematic bias was evaluated with the 2-sided Wilcoxon Signed-Rank test. Correlations and bias were considered significantly different from zero when $p \le 0.05$.

3.3.5. Alternative equations and factors influencing model predictivity

The physicochemical and *in vitro* characteristics of the 23 compounds given IV to rats were analysed by principal components analysis [Gabrielsson et al., 2002; Wold et al., 1987] (PCA), in order to identify whether any specific cluster of values can be related to the goodness of the predictive performance of the implemented whole-body PBPK model.

PCA was performed only on the basic molecules of the dataset, as only one neutral compound and one zwitterionic compound were included in the whole set of considered molecules. All the compound-related input parameters (i.e., $\log(P_{o:w})$, pKa, f_{uP}, CL_{int}) as well as other structural descriptors, such as the molecular weight (MW) and the solubility in water (S_w) were considered in the analysis. Before performing PCA, the 6 variables in the data matrix were scaled to unit variance. PCA was performed using R v3.2.2 (R Core Team, 2016), via the *princomp* function.

3.3.6. Sensitivity analysis

The whole-body PBPK model was investigated through sensitivity analysis in order to verify the relevance of the input parameters in determining the predictions in the rat (set B) of the major PK parameters. The built-in sensitivity analysis tool provided by Berkeley Madonna™ v8.0.2 was used. This tool determines the sensitivity of an output y_i to an input parameters p_j as follows:

1. the model runs with all parameters at their specified values, producing the output y_{i1};
2. the parameters p_j is modified by adding an amount Δ_j equal to $0.001*p_j$, and the model runs again producing the output y_{i2};
3. the sensitivity $s_{i,j}$ is computed using:

$$s_{i,j} = \frac{y_{i2} - y_{i1}}{\Delta_j}. \quad (19)$$

The investigated outputs were plasma CL_{PO} and $V_{ss,PO}$ (both expressed per kg of body weight). The investigated parameters were the drug-specific physicochemical and *in vitro* input data, i.e., $\log(P_{o:w})$, pKa, f_{uP}, and CL_{app}. The parameter α was also included in the analysis as it represents a numeric model assumption. As for PCA, sensitivity analysis was performed on the basic molecules of the dataset. For the sake of clarity of the following section, it is anticipated here that CL_{PO} was found to be mostly sensitive to CL_{app} (especially with low values of CL_{app}) and to f_{uP}, and that V_{ss} was found to be mostly sensitive to f_{uP}, to α, and to $\log(P_{o:w})$.

3.3.7. Improvements of Predictions in humans

This section describes the innovative part of this work. It depicts a method for improving the prediction of human PK, based on the knowledge produced in the pre-clinical phase of drug development. Once the real PK data are obtained from rats, the PK profiles simulated with the PBPK model

introduced above are fitted to those data, by allowing some parameters in the model equations to change their values. The updated values are then used to predict the PK profiles in man with greater confidence.

The parameters whose values were allowed to be modified were the ones that sensitivity analysis proved to influence the model predictions to the biggest extent: f_{uP}, α, $\log(P_{o:w})$ and CL_{app}. Besides the indications gathered through sensitivity analysis, a conceptual rationale does exist for allowing these parameters to change. The values of f_{uP} and $\log(P_{o:w})$ are obtained in vitro ($\log(P_{o:w})$ may actually be computed in silico from the experimentally available $\log(D_{vo:w})$), therefore they are associated with some experimental uncertainty. The value for α is 0.5 by assumption. The value for CL_{app} is again known with experimental uncertainty, and it is multiplied by the constant β, which is considered equal to one by assumption. The fact that CL_{app} and β are multiplied by each other implies that, when fitting the data, allowing CL_{app} or β to change is equivalent: this analysis used the latter as modifiable parameter, as this can be viewed as a multiplicative factor of CL_{app} and is thus more easily interpretable. In the fitting operation, the experimental (or in silico) values for f_{uP} and $\log(P_{o:w})$ and the default values for α and β were used as priors, in order not to lose the a priori knowledge on these parameters. The standard deviation expressing the priors strength was fixed to 0.25 for α, $\log(P_{o:w})$ and β, and to 10% of the prior value for f_{uP}. $P_{B:P,comp}$ was used for the blood-to-plasma-ratio. The fit was performed with SAAM IITM v1.1.2.

The modulated values of the parameters were used to produce new PK profiles in man, and the predictive performance was evaluated de novo in order to assess whether the new values improve the accuracy of the PK predictions. Since experimental values for f_{uP} were available for both rats and humans, the ratio between the modulated value obtained through fitting and the prior value in the rat was used as multiplying factor of the experimental value in man to obtain the new PK prediction.

3.4. **Results**

3.4.1. PK Predictions in Rats

The observed and predicted values of CL and V_{ss} after intravenous dosing in rats are reported in Table 3.2 for each compound, together with the correspondent fold-errors. The predictive performance of the model is similar considering set A alone (those molecules for which oral PK was available in humans) or all of the drug candidates. The focus here is on set A. The performance is slightly better using $P_{B:P,comp}$ instead of $P_{B:P,exp}$, with fe being ≤ 2 in 80% of the cases and ≤ 3 in 93% of the cases for V_{ss}, using $P_{B:P,comp}$. The percentages are similar for CL (80% and 87%, respectively, using both $P_{B:P,comp}$ and $P_{B:P,exp}$). The correlation between observed and predicted values of V_{ss} is non-significant using $P_{B:P,exp}$ and is 0.509 (p = 0.0066) using $P_{B:P,comp}$. With respect to CL, the correlation is 0.602 (p =

0.0015) using $P_{B:P,exp}$ and 0.689 (p = 0.0002) using $P_{B:P,comp}$. No significant bias is detected between observations and predictions of both V_{ss} and CL, using both $P_{B:P,comp}$ and $P_{B:P,exp}$. These outcomes made us choose $P_{B:P,comp}$ as the parameter to be used for the following analyses.

Table 3.2. Predicted and observed PK parameters in rats.

Compound	CL (mL/min/kg)					V_{ss} (L/kg)				
	observed	$predicted_{exp}$	$predicted_{comp}$	fe_{exp}	fe_{comp}	observed	$predicted_{exp}$	$predicted_{comp}$	fe_{exp}	fe_{comp}
GSK1	39	24.2	24.2	1.6	1.6	2.0	0.9	0.7	2.2	3.0
GSK2	4	17.9	17.9	4.5	4.5	1.6	7.0	4.7	4.4	3.0
GSK3	12	21.1	21.1	1.8	1.8	2.7	6.2	4.0	2.3	1.5
GSK4	32	19.5	19.5	1.6	1.6	8.0	2.3	3.9	3.4	2.0
GSK5	36	23.1	23.1	1.6	1.6	6.1	3.3	4.4	1.9	1.4
GSK6	27	18.2	26.1	1.5	1.0	9.4	4.9	4.9	1.9	1.9
GSK7	10	9.2	9.2	1.1	1.1	2.9	2.6	3.0	1.1	1.0
GSK8	18	17.6	17.6	1.0	1.0	4.3	7.2	4.0	1.7	1.1
GSK9	23	15.6	15.6	1.5	1.5	1.9	4.5	3.4	2.4	1.8
GSK10	5.4	20.1	20.0	3.7	3.7	2.4	5.3	3.6	2.2	1.5
GSK11	37	36.3	60.0	1.0	1.6	3.2	4.8	4.9	1.5	1.5
GSK12	29	18.7	26.8	1.5	1.1	3.7	4.5	4.5	1.2	1.2
GSK13	19	39.1	39.0	2.1	2.1	2.4	4.6	4.6	1.9	1.9
GSK14	24	48.3	48.3	2.0	2.0	1.1	9.6	4.1	8.8	3.8
GSK15	15	25.8	25.8	1.7	1.7	7.0	2.2	3.9	3.1	1.8
average	22	23.6	26.3	1.9	1.9	3.9	4.7	3.9	2.7	1.9
min	4	9.2	9.2	1.0	1.0	1.1	0.9	0.7	1.1	1.0
max	39	48.3	60.0	4.5	4.5	9.4	9.6	4.9	8.8	3.8
fe ≤ 2 (%)	-	-	-	80	80	-	-	-	47	80
fe ≤ 3 (%)	-	-	-	87	87	-	-	-	73	93

* Predicted values and fe are computed using the experimental and computed values of blood-to-plasma partition coefficient (subscript “exp” and “comp”, respectively).

Figure 3.2, providing a visual representation of the correspondence between observed and predicted PK parameters, clarifies that systemic clearance is predicted with higher precision than steady-state volume of distribution (R^2 = 0.18 and 0.08, respectively).

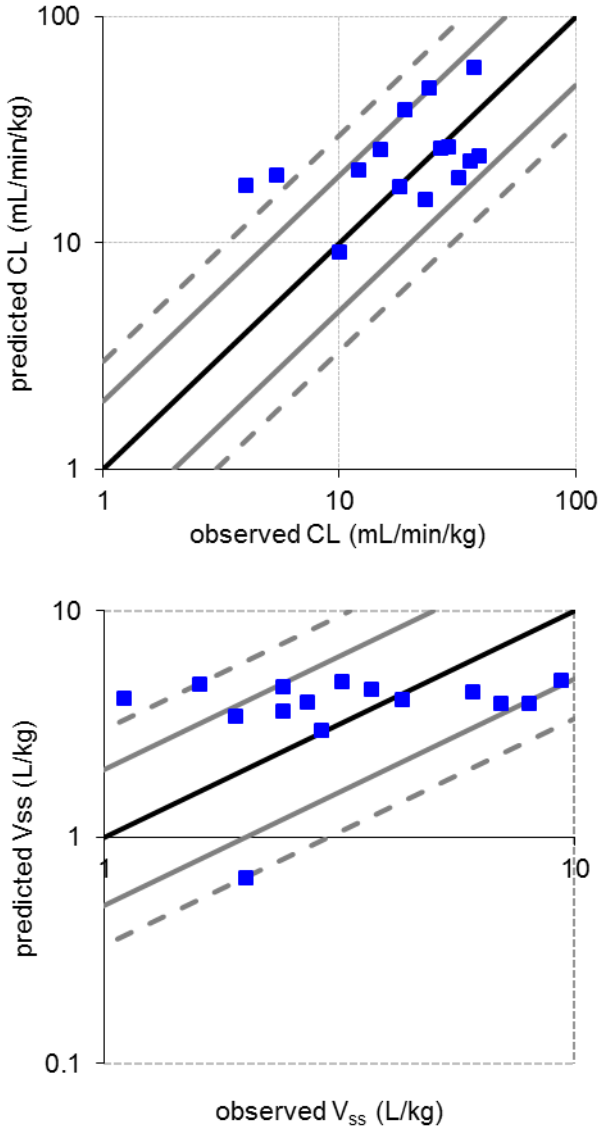

Figure 3.2. Correlation between observed and predicted values of systemic clearance (CL) and of steady-state volume of distribution (V_{ss}) for the implemented PBPK model. The black line is the identity line, the area between the two grey solid lines verifies the condition fold-error < 2 and the area between the two grey dashed lines verifies the condition fold-error < 3.

Both the compounds for which fe on CL is greater than 3 (GSK2 and GSK10) are imprecisely characterized in terms of hepatic intrinsic clearance, as its value is close to the lower limit of quantification: the range is <0.5 -

0.9 and <0.5 - 0.6 mL/min/g liver, respectively. The 90% prediction interval on the V_{ss} predictions goes from 2.3 to 4.9 L/kg while the correspondent observed range is considerably wider (1.5 to 8.4 L/kg). Nevertheless, as anticipated in the previous paragraph, the number of unacceptable predictions for V_{ss} (fe > 3) is low (7%, i.e., one compound) and under-predictions and over-predictions are balanced. The compound with fe > 3, GSK14, is characterized by high lipophilicity.

3.4.2. PK Predictions in Humans

The observed and predicted values of C_{max} and AUC in man are reported in Table 3.3 for each compound, together with the correspondent fold-errors. The model predictive performance is poor (fe ≤ 3 in 67% and 33% of the cases, respectively). However, the correlation between observations and predictions is significantly different from zero for all parameters (0.889 for C_{max}, $p < 0.0001$, $R^2 = 0.81$; 0.918 for AUC, $p < 0.0001$, $R^2 = 0.62$). AUC is almost consistently underpredicted by the PBPK model, as shown by Figure 3.3, bottom left panel.

The fold error is greater than 10 in one case for C_{max} and 2 cases for AUC (GSK8 and GSK14). It has to be noted that for GSK8 the quantification of hepatic intrinsic clearance is imprecise (between <0.5 and 1 mL/min/g liver), and for GSK8 the difference between intrinsic clearance as derived from microsomes and from hepatocytes is large (15.1 vs 0.46 mL/min per gram of liver, respectively).

Table 3.3 Observed, PBPK predicted and revised values for humans.

Compound	C_{max} (ng/mL)					AUC (ng*h/mL)				
	observed	predicted	revised	fe on predicted	fe on revised	Observed	predicted	revised	fe on predicted	fe on revised
GSK1	2.03	3	6	1.5	3.1	38.3	7	16	5.4	2.3
GSK2	26.6	318	99	11.8	3.6	569	717	194	1.3	2.9
GSK3	46.3	96	40	2.1	1.2	795	214	79	3.7	10.1
GSK4	274	151	93	1.8	2.9	3302	549	430	6.0	7.7
GSK5	3.47	16	12	5.3	4.0	82.5	40	30	2.1	2.7
GSK6	81	27	24	3.0	3.4	429	56	50	7.7	8.5
GSK7	397	456	387	1.1	1.0	4848	1274	560	3.8	8.7
GSK8	5	1	3	5.0	2.0	166	3	21	55.3	7.8
GSK9	1273	1170	872	1.1	1.5	13752	2994	1337	4.6	10.3
GSK10	26.3	45	212	1.7	8.2	182.2	84	417	2.2	2.3
GSK11	211	190	355	1.1	1.7	1183	883	2034	1.3	1.7
GSK12	404	446	536	1.1	1.3	2443	2092	1922	1.2	1.3
GSK13	520	452	1041	1.2	2.0	9205	1223	4463	7.5	2.1
GSK14	522	103	413	5.1	1.3	3850	324	3170	11.9	1.2
GSK15	8.14	57	57	7.1	7.1	433	130	285	3.3	1.5
Average	253	235	277	3.3	2.9	2752	706	1000	7.8	4.7
Min	2	1	3	1.1	1.0	38	3	16	1.2	1.2
Max	1273	1170	1041	11.8	8.2	13752	2994	4463	55.3	10.3
fe ≤ 2 (%)	-	-	-	53	47	-	-	-	20	27
fe ≤ 3 (%)	-	-	-	67	60	-	-	-	33	60

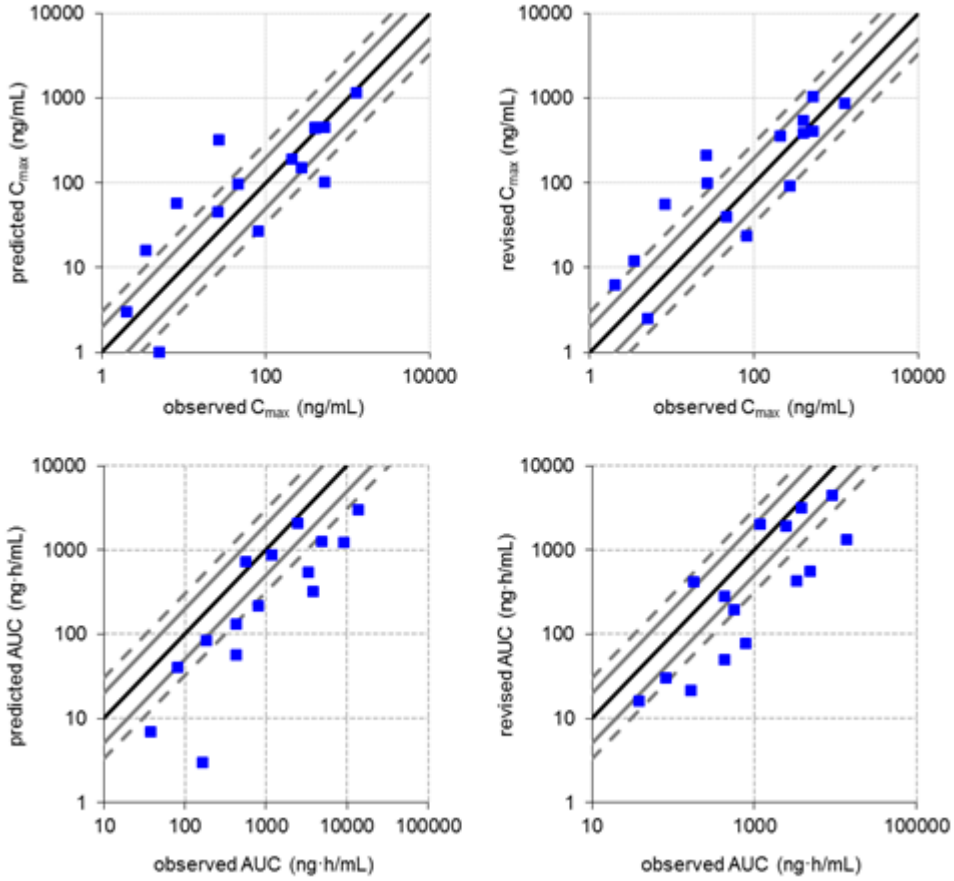

Figure 3.3. Correlation between observed and predicted values (left panels) or revised values (right panels) of maximum concentration (C_{max}) and area-under-the-curve (AUC) for the implemented PBPK model. The black line is the identity line, the area between the two grey solid lines verifies the condition fold-error < 2 and the area between the two grey dashed lines verifies the condition fold-error < 3.

3.4.3. Improvements of PK Predictions in Humans

3.4.3.1. Principal Component Analysis

Two score plots are provided in order to analyse the goodness of the prediction of CL and V_{ss} separately (Figure 3.4, left and right, respectively). The compounds are coded, based on the fold error between the predicted and observed parameter (CL or V_{ss}), as "over-predicted" (fe > 2 and prediction > observation), "correctly predicted" (fe < 2) and "under-predicted" (fe > 2 and prediction < observation). Such thresholds are chosen because a 2-fold error in the prediction of CL or V_{ss} is considered the upper bound in the identification of a good predictions, and because this threshold is suitable to identify a limited but sufficient number of relatively poor predictions useful to recognize possible clusters in the score plots (4 in both the CL and V_{ss} score plots). The values for the two principal components, i.e., the coordinates of the points in the score plots, are provided in the

Supplementary Material (Section S2). The loading plot is shown in Figure 3.4, centre panel.

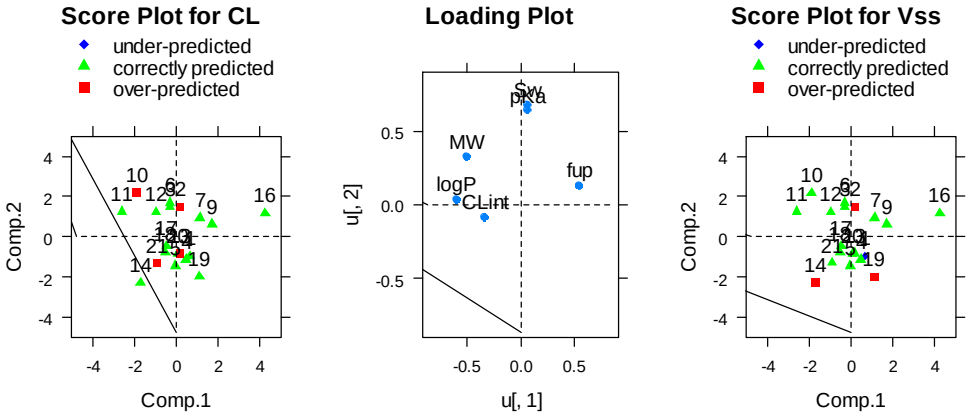

Figure 3.4. Loading and score plot from the principal component analysis for CL and V_{ss}.

The first two principal components explain 65% of the total variance. The four compounds for which CL is over-predicted stay in the second and third quadrants of the score plot. The loading plot shows that this placement corresponds to high $\log(P_{o:w})$and CL_{app}, and to low f_{uP}. These results are in agreement with those reported by Germani et al. [Germani et al., 2007), especially for what concerns lipophilicity and protein binding. Therefore, when the CL of a new compound is predicted with the implemented PBPK model, a potential over-prediction can be expected if the drug is highly lipophilic and highly bound to proteins. With respect to V_{ss}, since no cluster can be recognized in the score plot, it can be inferred that according to our dataset there are no drug properties, among the considered ones, which may anticipate a bias in V_{ss} prediction.

3.4.3.2. Sensitivity Analysis

Table 3.4 shows the values of the sensitivity coefficients $s_{i,j}$ (Eq. 19) for each input parameter considered in the analysis and for all compounds. The reader needs to consider that, for each input parameter, the ratio between its relative change (0.001), used to perform sensitivity analysis, and the input parameter range calculated from the considered compounds set and divided by the average parameter value, has the same order of size. Therefore, the values provided by Table 3.4 can be considered comparable when contrasting the effects of the different parameters on CL, or the effects of the different parameters on V_{ss}.

The average values show that systemic clearance is mostly influenced by CL_{app}, and to a lesser extent by f_{uP}. Principal components analysis performed on the values in Table 3.4 shows that the effect of CL_{app} is stronger when CL_{app} is low (see Figure S2.1 in the Supplementary Material): indeed, from

Eq. 9, increasing values for hepatic intrinsic clearance determine the gradual saturation of hepatic clearance (which reaches the level of the liver blood flow).

Steady-state volume of distribution is sensitive to f_{uP}, α, log($P_{o:w}$) and pka, from the highest to the lowest impact. In particular, principal components analysis (see Figure S2.1 in the Supplementary Material) reveals that, in the considered set of drug candidates: when log($P_{o:w}$) is low or f_{uP} is high, variations in log($P_{o:w}$) are not relevant; when log($P_{o:w}$) is high or f_{uP} is low, variations in log($P_{o:w}$) are less relevant; decreasing values of log($P_{o:w}$) or increasing values of f_{uP} increase the effect of variations in α; the small effect of pKa variations seems to appear at higher values of pKa itself.

Table 3.4 Sensitivity coefficients ($s_{i,j}$) for all compounds.

Compound	CL (mL/min/kg)					V_{ss} (L/kg)				
	log($P_{o:w}$)	pKa	f_{uP}	CL_{int} (mL/min/g liver)	α	log($P_{o:w}$)	pKa	f_{uP}	CL_{int} (mL/min/g liver)	α
GSK1	-0.0034	0	0.9	16	0	1.539	-0.003	15.0	0	6.4
GSK2	0.0000	0	0.8	18	0	0.230	-0.140	7.4	0	7.3
GSK3	-0.0004	0	1.0	15	0	0.415	-0.319	19.8	0	7.3
GSK4	-0.0015	0	0.9	14	0	0.997	-0.005	21.0	0	6.9
GSK5	0.0000	0	1.0	30	0	0.000	0.000	6.8	0	5.1
GSK6	-0.0012	0	1.0	20	0	1.425	-0.037	4.9	0	5.9
GSK7	-0.0076	0	0.9	22	0	1.573	-0.193	5.2	0	5.8
GSK8	-0.0315	0	1.2	18	0	3.075	0.000	6.8	0	4.6
GSK9	-0.0131	0	1.1	13	0	2.167	-0.060	2.7	0	3.6
GSK10	0.0000	0	1.0	23	0	0.020	-0.018	32.9	0	7.3
GSK11	-0.0007	0	1.0	0	0	0.023	-0.005	32.9	0	7.3
GSK12	-0.0005	0	1.0	15	0	0.521	-0.005	22.6	0	7.1
GSK13	0.0000	0	0.8	7	0	0.377	-0.019	25.1	0	7.2
GSK14	0.0000	0	1.2	1	0	0.047	0.000	32.4	0	7.4
GSK15	-0.0004	0	0.8	12	0	0.118	-0.077	21.8	0	7.4
GSK16	-0.0740	0	1.3	7	0	1.688	0.000	0.9	0	0.9
GSK17	0.0000	0	1.0	15	0	0.046	-0.007	32.4	0	7.4
GSK18	0.0000	0	0.7	30	0	0.023	0.000	32.7	0	7.4
GSK19	-0.0209	0	1.2	31	0	2.666	0.000	6.7	0	4.8
GSK20	-0.0003	0	0.8	30	0	0.635	-0.002	19.0	0	6.9
GSK21	0.0000	0	0.0	3	0	0.005	0.000	33.1	0	7.5
GSK22	0.0000	0	0.9	2	0	0.085	-0.009	31.3	0	7.4
GSK23	0.0000	0	1.1	15	0	0.032	-0.004	32.5	0	7.4
Average	**-0.0068**	**0**	**0.9**	**16**	**0**	**0.770**	**-0.039**	**19.4**	**0**	**6.4**
Min	**-0.0740**	**0**	**0.0**	**0**	**0**	**0.000**	**-0.319**	**0.9**	**0**	**0.9**
Max	**0.0000**	**0**	**1.3**	**31**	**0**	**3.075**	**0.000**	**33.1**	**0**	**7.5**

3.4.3.3. Improvement of the PK predictions in humans

The results of the modulation of the parameters f_{uP}, log($P_{o:w}$), α and β achieved by fitting the PK data (set A) in rats are presented in Table 3.5. The median ratio between modulated and prior values of log($P_{o:w}$) is significantly less than one ($p = 0.0039$). The median ratios for the other three parameters are not significantly different from one ($p > 0.1$).

Table 3.5 Modulated values of the parameters modified by fitting of the PK data in rats.

	Modulated values				Ratio between modulated and prior values			
Compound	**Rat f_{uP}**	**log($P_{o:w}$)**	**α***	**β†**	**Rat f_{uP}**	**log($P_{o:w}$)**	**α**	**B**
GSK1	0.038	2.83	0.50	0.50	0.94	0.81	1.00	0.50
GSK2	0.019	4.49	0.77	3.78	0.99	0.97	1.54	3.78
GSK3	0.021	5.15	0.71	2.77	1.06	1.06	1.43	2.77
GSK4	0.028	3.18	1.50	1.47	0.90	0.84	2.99	1.47
GSK5	0.028	2.76	0.79	1.35	0.95	0.94	1.58	1.35
GSK6	0.011	3.86	0.57	1.15	0.94	0.88	1.14	1.15
GSK7	0.054	2.72	0.27	2.44	0.97	0.85	0.54	2.44
GSK8	0.130	2.55	0.50	0.20	0.98	0.87	1.00	0.20
GSK9	0.059	2.53	0.34	2.24	0.99	1.00	0.69	2.24
GSK10	0.030	7.11	0.08	0.20	1.06	1.00	0.16	0.20
GSK11	0.011	3.22	0.49	0.23	0.93	0.71	0.98	0.23
GSK12	0.010	3.26	0.50	1.35	0.96	0.84	1.00	1.35
GSK13	0.010	3.91	0.23	0.28	1.00	1.00	0.46	0.28
GSK14	0.011	5.07	0.08	0.10	1.05	1.00	0.15	0.10
GSK15	0.005	5.15	1.07	0.48	1.02	1.02	2.15	0.48
average	0.03	3.85	0.56	1.23	0.98	0.92	1.12	1.23
min	0.01	2.53	0.08	0.10	0.90	0.71	0.15	0.10
max	0.13	7.11	1.50	3.78	1.06	1.06	2.99	3.78

* Before fitting this is assumed equal to 1
† Before fitting this is assumed equal to 0.5

The revised values of C_{max} and AUC in man are reported in Table 5.3 for each compound, together with the correspondent fold-errors. With respect to the comparison between observations and predictions, the average fe decreases from 3.3 to 2.9 for C_{max} (fe is ≤ 3 in 60% *vs* 67% of cases) and from 7.8 to 4.7 for AUC (with fe ≤ 3 in 60% *vs* 33% of cases). The correlation between observations and revised predictions slightly increases for C_{max} and AUC (0.913 for C_{max}, $p < 0.0001$, $R^2 = 0.64$; 0.903 for AUC, $p < 0.0001$, $R^2 = 0.23$). As visible from Figure 3.3 (bottom panel on the right), the under-prediction of AUC is reduced but still significant ($p = 0.01$ and $p = 0.04$, respectively).

With respect to predictions with fe > 10, the integrated PBPK approach improved both the Cmax prediction (the compound with fe = 11.8 got a revised fe of 3.6) and the AUC prediction (two cases of fe > 10 without using the prior knowledge, with values 55.3 and 11.9, vs two cases after integrating the priors, but with smaller values, 10.1 and 10.3, respectively).

Figure 3.5 shows how the proposed integrated approach for human PBPK prediction works in a representative case (GSK13). The fit of the rat IV plasma concentration data produces a change of the modifiable parameter values (see Table 3.5) and a consequent improvement of the PBPK prediction. However, the model structure, the fixed values for most model

parameters, and the prior knowledge on the values of the modifiable parameter, together with the measurement errors affecting the observations, still do not allow to achieve a perfect match between data and model predictions. The reduction of the values of α and β decreases the predicted values of both CL and Vss in rat, thus reducing the fold errors on these PK parameters (from 2.1 to 1.3 and from 1.9 to 1.0, respectively). When the modulated parameter values take the place of the original values in the human PBPK model, the predicted values for Cmax and AUC increase, producing a slight decrease in the fold-error in Cmax, but a more consistent decrease in the fold-errors for AUC.

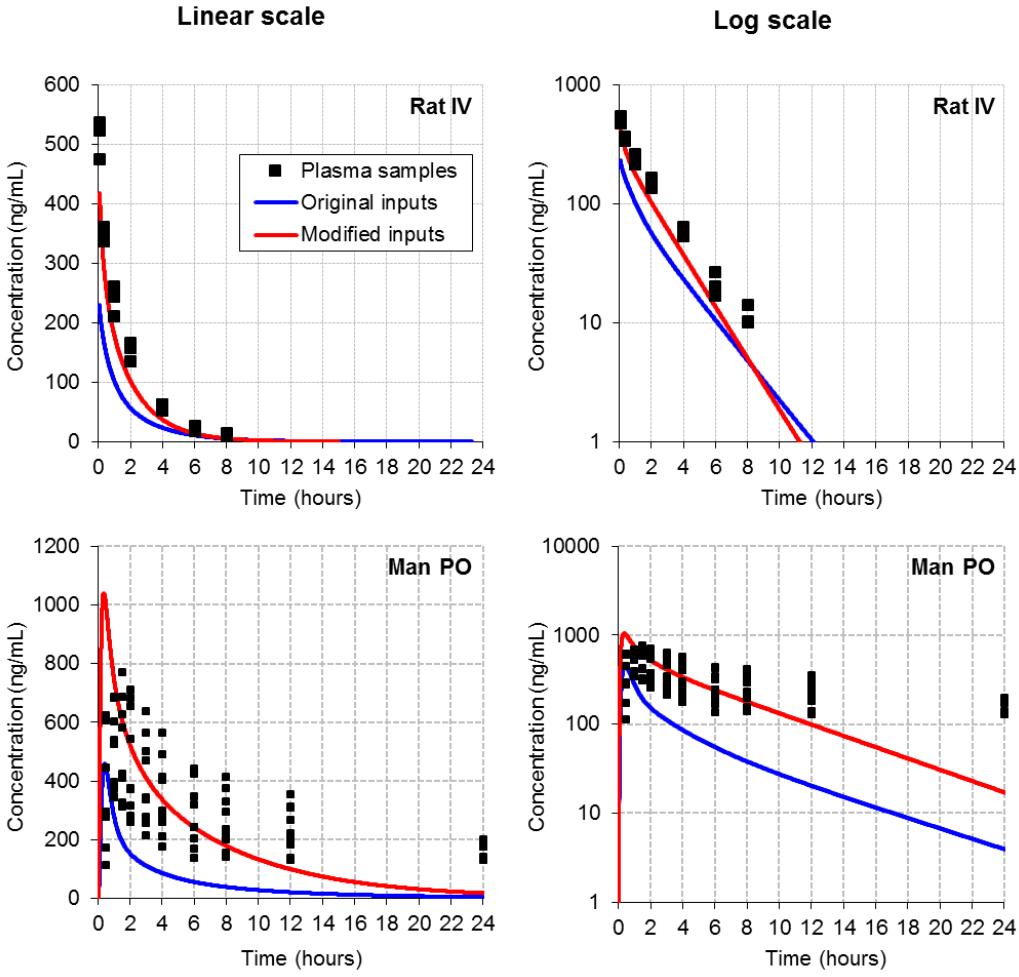

Figure 3.3. Improvement of the prediction of PK profiles for compound GSK13 using the integrated PBPK approach. The original parameter values produce the plasma concentration profiles in blue. The fit of the rat plasma concentration data using prior knowledge as priors produce new parameter values and the profiles in blue shown in the upper panels. The modulated parameter values are used in the human PBPK model and produce the profiles in blue shown in the lower panels.

3.5. **Discussion**

As a rule of thumb, a PK prediction from non-clinical assessment is considered good (both for animal and human PK predictions) when the main metrics of systemic exposure and parameters are predicted within a factor of 2 or lower from the average experimental value. When instead the fe between prediction and observation is larger than 3, the prediction is considered poor.

In the current assessment for the prediction of PK parameters in rats following IV dosing, the fe for CL is < 2 in 80% of the examined compounds and < 3 in 87% of them. The fe statistics are also good for the volume of distribution, being < 2 in 80% of the examined compounds and < 3 in 93% of them. However, the implemented computational model provides V_{ss} predictions that are constrained within a narrow range, whilst the actual observations are characterized by a wider range of values. This indicates that the equations for the tissue partition coefficients still need to be refined, and possibly complemented with additional considerations (effect of transporters, permeability limitations, etc.) that are lacking in the currently implemented mathematical model and that may allow to differentiate among the considered set of molecules. In any case, the model seems to be relatively accurate for this dataset, even in case the blood-to-plasma ratio is not experimentally available. These observations essentially confirm the behaviour of the whole-body PBPK model for predicting the PK in animals obtained in previous assessments in analogous conditions [Germani et al., 2007]. It is interesting to notice that, with the available data, the use of other approaches to predict the tissue partition coefficients [Berezhkovskiy, 2004; Rodgers et al., 2005; Rodgers and Rowland, 2006] did not provide additional benefit to the prediction (data not shown). It may be that this data set, obtained from a single therapeutic area, characterized by relatively homogeneous physical-chemistry and biochemical properties (mostly basic, with high lipophilicity and protein binding), is better described by an approach that is compressing the dynamic range of the predicted volumes of distribution, such as the one adopted here [Paulin and Theil, 2002b].

The predictions are substantially worsening when the predictions concern the human PK following oral dosing. The basic PBPK approach allows to determine the overall systemic exposure (AUC) after oral dose with a fe within 2 and 3 only in 20% and 33% of the examined compounds, respectively. The use of the input parameters modulated using the proposed integrated approach based on the Bayesian fitting of *in vivo* data obtained in rats after IV dosing substantially improves the predictions, the fe on AUC predictions being within 2 and 3 in 27% and 60% of the cases, respectively, indicating that the fitting approach, although not fully suited to correct the inaccuracies, substantially improves the predictive outcome. It can be speculated what are the quantitative assumptions underlying this procedure, i.e., whether the error in the estimates of the input parameters in rats should be similar to that in human. Without getting that far, the basic consideration is that preclinical data contain information that can be extracted to provide

more accurate predictions. It is particularly interesting that, in this particular case, the fitting concerns extravascular dosing of compounds in rats (and thus disposition: distribution and elimination), whilst the benefit on human predictions concerns oral dosing (thus including in the PK processes also the absorption, for which the rat data did not provide any basic information). An even more comprehensive integration of preclinical data (including oral administration, and different species) would likely be even more efficient in improving the predictions.

In the vast majority of our cases, the predicted exposures under-estimate the observed values suggesting that oral CL is overpredicted in this set of compounds. The same bias does not appear to be present for C_{max} values. The absolute bioavailability of the PBPK model is based on many assumptions (complete absorption, linear pharmacokinetics and metabolism occurring only in the liver), which may be faulty in this case. Unfortunately, actual F values were not available for these compounds, so that it could not be checked whether the under-prediction of the exposure can be due over-prediction of the oral clearance or to the underprediction of the absolute bioavailability. Over-prediction of clearance can be particularly severe for compounds, such as those used for this evaluation, characterized by high lipophilicity and avid protein binding, as shown by the PCA and previously in the literature [Germani et al., 2007]. An analogous over-prediction of oral clearance was reported in the extensive blinded evaluation performed as part a Phrma initiative, which indicated the limitation of the PBPK approach when considered on its own [Poulin et al., 2011].

These general, blinded assessments, however, do not consider the knowledge on a specific compound that can emerge from the involvement in drug research project teams. An interesting example in this respect is the prediction for GSK9, a compound in which in vitro clearance was at the lower limit of determination of the system. Based on the knowledge derived from other candidates of the same project, it was found that in vivo monkey data were predictive for human PK. The assessment based on the human predicted clearance obtained from allometric scaling of monkey clearance was substantially improved (with fold error decreased from 4.6-10.1 down to 1-1.5).

It must be highlighted that for most of the compounds analysed here, CLapp was measured in liver microsomes, which was reported to be less accurate that that obtained in hepatocytes, in which a more comprehensive battery of drug metabolizing enzymes is accounted for [Ito and Houston, 2004].

The exercise reported in this Chapter does not intend to provide a receipt to success for the human PK prediction: from this assessment, only emerges that it is always advisable to proceed with the most comprehensive integration of the knowledge obtained from non clinical assessments (*in silico, in vitro, in vivo)* using the PBPK approach. In this way the intrinsic uncertainty of some parameters can be accounted for or the robustness of some of the assumptions of the more basic PBPK model can be tested on experimental data.

3.6. **References**

Berezhkovskiy LM. Volume of distribution at steady state for a linear pharmacokinetic system with peripheral elimination. J. Pharm. Sci. 2004, 93: 1628–1640.

Brown RP, Delp MD, Lindstedt SL, Rhomberg LR, Beliles RP. Physiological Parameter Values for Physiologically Based Pharmacokinetic Models. Toxicol. Ind. Health 1997,13: 407–484.

Chen Y, Jin JY, Mukadam S, Malhi V, Kenny JR. Application of IVIVE and PBPK modeling in prospective prediction of clinical pharmacokinetics: strategy and approach during the drug discovery phase with four case studies. Biopharm. Drug Dispos. 2012, 3: 85–98.

Cosson VF, Fuseau E, Efthymiopoulos C, Bye A. Mixed effect modeling of sumatriptan pharmacokinetics during drug development. I: Interspecies allometric scaling. J. Pharmacokinet. Biopharm. 1997, 25: 149–167.

De Buck SS, Sinha VK, Fenu LA, Nijsen MJ, Mackie CE, Gilissen RAHJ. Prediction of human pharmacokinetics using physiologically based modeling: a retrospective analysis of 26 clinically tested drugs. Drug Metab. Dispos. 2007, 35: 1766–1780.

Germani M, Crivori P, Rocchetti M, Burton PS, Wilson AGE, Smith ME, Poggesi I. Evaluation of a basic physiologically based pharmacokinetic model for simulating the first-time-in-animal study. Eur. J. Pharm. Sci. 2007, 31: 190–201.

Huang Q, Riviere JE. The application of allometric scaling principles to predict pharmacokinetic parameters across species. Expert Opin. Drug Metab. Toxicol. 2014, 10: 1241–1253.

Ito K, Houston JB. Comparison of the use of liver models for predicting drug clearance using in vitro kinetic data from hepatic microsomes and isolated hepatocytes. Pharmaceutical research. 2004, 21:785-92.

Jones H, Rowland-Yeo K. Basic concepts in physiologically based pharmacokinetic modeling in drug discovery and development. CPT Pharmacomet. Syst. Pharmacol. 2013, 2: e63.

Jones HM, Dickins M, Youdim K, Gosset JR, Attkins NJ, Hay TL, Gurrell IK, Logan YR, Bungay PJ, Jones BC, Gardner IB. Application of PBPK modelling in drug discovery and development at Pfizer. Xenobiotica 2012, 42: 94–106.

Jones HM, Chen Y, Gibson C, Heimbach T, Parrott N, Peters SA, Snoeys J, Upreti VV, Zheng M, Hall S.D. Physiologically based pharmacokinetic modeling in drug discovery and development: a pharmaceutical industry perspective. Clin. Pharmacol. Ther. 2015, 97: 247–262.

Kummar S, Gutierrez M, Doroshow JH, Murgo AJ. Drug development in oncology: classical cytotoxics and molecularly targeted agents. Br. J. Clin. Pharmacol. 2006, 62: 15–26.

Leo A, Hansch C, Elkins D. Partition coefficients and their uses. Chem. Rev. 1971, 71: 525–616.

Lombardo F, Obach RS, Shalaeva MY, Gao F. Prediction of Volume of Distribution Values in Humans for Neutral and Basic Drugs Using Physicochemical Measurements and Plasma Protein Binding Data. J. Med. Chem. 2002, 45: 2867–2876.

Lombardo F, Obach RS, Shalaeva MY, Gao F. Prediction of Human Volume of Distribution Values for Neutral and Basic Drugs. 2. Extended Data Set and Leave-Class-Out Statistics. J. Med. Chem. 2004, 47: 1242–1250.

Lu C, Li P, Gallegos R, Uttamsingh V, Xia CQ, Miwa GT, Balani SK, Gan, L-S. Comparison of intrinsic clearance in liver microsomes and hepatocytes from rats and humans: evaluation of free fraction and uptake in hepatocytes. Drug Metab. Dispos. 2006, 34: 1600–1605.

Mahmood I. Application of allometric principles for the prediction of pharmacokinetics in human and veterinary drug development. Adv. Drug Deliv. Rev. 2007, 59: 1177–1192.

Nagilla R, Ward KW. A comprehensive analysis of the role of correction factors in the allometric predictivity of clearance from rat, dog, and monkey to humans. J. Pharm. Sci. 2004, 93: 2522–2534.

Obach RS. Prediction of human clearance of twenty-nine drugs from hepatic microsomal intrinsic clearance data: An examination of in vitro half-life approach and nonspecific binding to microsomes. Drug Metab. Dispos. Biol. Fate Chem. 1999, 27: 1350–1359.

Obach RS, Baxter JG, Liston TE, Silber BM, Jones BC, MacIntyre F, Rance DJ, Wastall P. The prediction of human pharmacokinetic parameters from preclinical and in vitro metabolism data. J. Pharmacol. Exp. Ther. 1997, 283: 46–58.

Poggesi I. Predicting human pharmacokinetics from preclinical data. Curr. Opin. Drug Discov. Devel. 2004, 7: 100–111.

Poulin P, Theil F-P. A priori prediction of tissue: plasma partition coefficients of drugs to facilitate the use of physiologically-based pharmacokinetic models in drug discovery. J. Pharm. Sci. 2000, 89: 16–35.

Poulin P, Theil F-P. Prediction of pharmacokinetics prior to in vivo studies. 1. Mechanism-based prediction of volume of distribution. J. Pharm. Sci. 2002a, 91: 129–156.

Poulin P, Theil F-P. Prediction of pharmacokinetics prior to in vivo studies. II. Generic physiologically based pharmacokinetic models of drug disposition. J. Pharm. Sci. 2002b, 91: 1358–1370.

Poulin P, Schoenlein K, Theil F-P. Prediction of adipose tissue: plasma partition coefficients for structurally unrelated drugs. J. Pharm. Sci. 2001, 90: 436–447.

Poulin P, Jones HM, Jones RD, Yates JWT, Gibson CR, Chien JY, Ring BJ, Adkison KK, He H, Vuppugalla R, Marathe P, Fischer V, Dutta S, Sinha VK, Björnsson T, Lavé T, Ku MS. PhRMA CPCDC initiative on predictive models of human pharmacokinetics, part 1: goals, properties of the PhRMA dataset, and comparison with literature datasets. J. Pharm. Sci. 2011, 100: 4050–4073. Ritschel WA. Handbook of basic pharmacokinetics-- including clinical applications, 4th ed. 1992, Drug Intelligence Publications.

Rodgers T, Rowland M. Physiologically based pharmacokinetic modelling 2: Predicting the tissue distribution of acids, very weak bases, neutrals and zwitterions. J. Pharm. Sci. 2006, 95: 1238–1257.

Rodgers T, Leahy D, Rowland M. Physiologically based pharmacokinetic modeling 1: Predicting the tissue distribution of moderate-to-strong bases. J. Pharm. Sci. 2005, 94: 1259–1276.

Rostami-Hodjegan, A, Tucker GT. Simulation and prediction of in vivo drug metabolism in human populations from in vitro data. Nat. Rev. Drug Discov. 2007, 6: 140–148.

Rowland M, Benet LZ. Lead PK Commentary: Predicting Human Pharmacokinetics. J. Pharm. Sci. 2011, 100: 4047–4049.

Rowland M, Tozer TN. Clinical pharmacokinetics: Concepts and applications, 3rd edition. 1994. Baltimore: Lea & Febiger.

Rowland M, Benet LZ, Graham GG. Clearance concepts in pharmacokinetics. J. Pharmacokinet. Biopharm. 1973, 1: 123–136.

Rowland M, Peck C, Tucker G. Physiologically-Based Pharmacokinetics in Drug Development and Regulatory Science. Annu. Rev. Pharmacol. Toxicol. 2011, 51: 45–73.

Wajima T, Fukumura K, Yano Y, Oguma T. Prediction of human clearance from animal data and molecular structural parameters using multivariate regression analysis. J. Pharm. Sci. 2002, 91: 2489–2499.

Wilkinson GR, Shand DG. Commentary: a physiological approach to hepatic drug clearance. Clin. Pharmacol. Ther. 1975, 18: 377–390.

Zhao P, Rowland M, Huang S-M. Best practice in the use of physiologically based pharmacokinetic modeling and simulation to address clinical pharmacology regulatory questions. Clin. Pharmacol. Ther. 2012, 92: 17–20.

SUPPLEMENTARY MATERIAL TO CHAPTER 3

S1. Species-specific anatomical and physiological parameters

Table S1.1. Tissue compositions. Data taken from the literature [Poulin and Theil, 2002a, 2002b).

Tissue	Water fractional weight		Neutral lipids fractional weight		Phospholipids fractional weight	
	Rat	Man	Rat	Man	Rat	Man
Adipose tissue	0.12	0.18	0.853	0.79	0.002	0.002
Bone	0.446	0.439	0.0273	0.074	0.0027	0.0011
Brain	0.788	0.77	0.0392	0.051	0.0533	0.0565
Gut	0.749	0.718	0.0292	0.0487	0.0138	0.0163
Heart	0.779	0.758	0.014	0.0115	0.0118	0.0166
Kidney	0.771	0.783	0.0123	0.0207	0.0284	0.0162
Liver	0.705	0.751	0.0138	0.0348	0.0303	0.0252
Lung	0.79	0.811	0.0219	0.003	0.014	0.009
Muscle	0.756	0.076	0.01	0.0238	0.009	0.0072
Skin	0.651	0.718	0.0239	0.0284	0.018	0.0111
Spleen	0.771	0.788	0.0077	0.0201	0.0136	0.0198
Plasma [a]	0.96	0.945	0.00147	0.0035	0.00083	0.00225
Blood	0.78642	0.766	0.001295	0.0031	0.002445	0.00684

[a] A similar composition is assumed for the arterial and venous plasma.

Table S1.2. Tissue volumes. Data taken from the literature [Brown et al., 1997; Poulin and Theil, 2002a).

Tissue	Volume (mL/kg)[a]		
	Rat	Dog	Man
Adipose tissue	70.012	138.00	110.0044
Bone	73.005	142.56	143.0021
Brain	5.7	8.0	20.0
Gut	27.0	37.0	17.1
Heart	3.3	8.0	8.0
Kidney	7.3	5.0	4.4
Liver	36.6	33.0	26.0
Lung	5.0	5.0	7.6
Muscle	404.0	457.0	400.0
Skin	190.0	91.0	37.1
Spleen	2.0	35.0	2.6
Arterial blood	27.2	30.0	25.7
Venous blood	54.4	60.0	51.4

[a] Values to be scaled allometrically.

Table S1.3. Tissue blood flows. Data taken from the literature [Brown et al., 1997; Poulin and Theil, 2002a).

Tissue	Blood flow		
	Rat[a]	Dog[b]	Man[c]
Adipose tissue	16.450	36	52
Bone	28.670	120	42
Brain	4.700	45	114
Gut	30.785	216	157
Heart	11.515	54	40
Kidney	33.135	216	175
Liver	41.125	312	227
Lung	214.555	1149	899
Muscle	65.330	264	191
Skin	13.630	102	58
Spleen	4.700	24	24

[a] Values expressed as mL/min/kg.

[b] Values expressed as mL/min for a 10 kg-dog.

[c] Values to be multiplied by -6.846 * log10(age) + 16.775 to obtain the blood flow expressed as mL/min.

Table S1.4 - Haematocrit, liver weight and glomerular filtration rate. Data taken from the literature [Brown et al., 1997; Poulin and Theil, 2002a; Ritschel, 1992).

Species	Rat	Dog	Man
Haematocrit (vol/vol %)	47.4	45.1	44.8
Liver weight (g/kg of body weight)	44	32	26
Glomerular filtration rate (mL/min)	0.36	61.3	120

S2. Details on Principal Component and Sensitivity Analyses

Table S2.1. First and second principal components for each compound considered in the PCA

Compound	Comp.1	Comp.2	CL: fe with sign	Vss: fe with sign
GSK1	0.65	-0.96	-1.6	-3
GSK2	0.17	1.47	4.5	3
GSK3	-0.30	1.47	1.8	1.5
GSK4	0.47	-1.14	-1.6	-2
GSK5	-0.05	-1.44	-1.6	-1.4
GSK6	-0.30	1.69	-1	-1.9
GSK7	1.13	0.94	-1.1	1
GSK9	1.70	0.62	-1.5	1.8
GSK10	-1.89	2.17	3.7	1.5
GSK11	-2.60	1.26	1.6	1.5
GSK12	-0.97	1.23	-1.1	1.2
GSK13	0.17	-0.83	2.1	1.9
GSK14	-1.71	-2.28	2	3.8
GSK15	NA	NA	1.7	-1.8
GSK16	4.26	1.17	1.3	-1.5
GSK17	-0.47	-0.46	1.1	-1.8
GSK18	-0.52	-0.79	-1	-1.2
GSK19	1.12	-1.99	-1.9	2.3
GSK20	0.07	-0.83	-1.5	-2
GSK21	-0.91	-1.30	2.2	-1.2
GSK22	NA	NA	-1.1	1.1

NA: not computable as solubility in water is not available

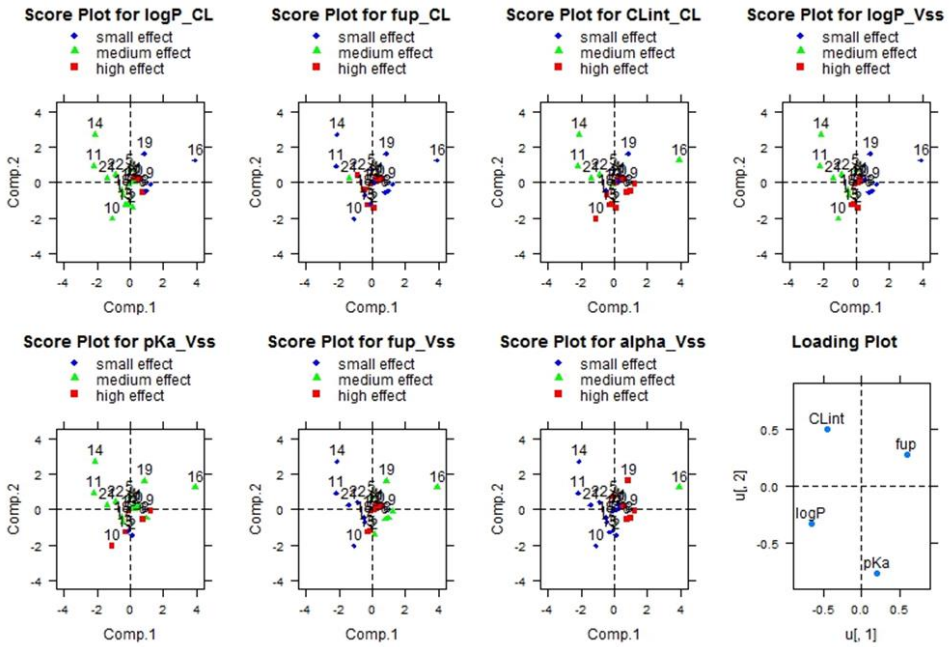

Figure S2.1. Score plots and loading plot for the first two principal components identified by principal components analysis on the values of $s_{i,j}$ (Eq. 23) provided with Table 3.4. The two components explain 71% of the total variance. Score plots: the compounds have different colour codes depending on the size of the effect of the considered input parameter (e.g., logP in the top left score plot) on the considered output (e.g., CL in the top left score plot), as determined by sensitivity analysis. The thresholds on the effect size are provided by Table S2.2. Loading plot: fup is the fraction of unbound drug in plasma, pKa is the association constant (the highest for diprotic bases), logP is the logarithm of the n-octanol:water partition coefficient of the non-ionized species, CLint is the hepatic intrinsic clearance.

Table S2.2. Thresholds on the effect size to be used in the principal components analysis in Fig. S.2.1

Output	**CL (mL/min/kg)**					**V_{ss} (mL/kg)**				
Input	**$\lvert\log(P_{o:w})\rvert$**	**pKa**	**f_{uP}**	**CL_{int}**	**α**	**$\log(P_{o:w})$**	**$\lvert pKa \rvert$**	**f_{uP}**	**CL_{int}**	**α**
1st threshold	0.001	-	0.6	10	-	0.1	0.01	10	-	1.0
2nd threshold	0.010	-	1.0	25	-	1.0	0.10	30	-	6.5

REFERENCES

Brown RP, Delp MD, Lindstedt SL, Rhomberg LR, Beliles RP. Physiological Parameter Values for Physiologically Based Pharmacokinetic Models. Toxicol. Ind. Health 1997, 13: 407–484.

Poulin P, Theil F-P. Prediction of pharmacokinetics prior to in vivo studies. 1. Mechanism-based prediction of volume of distribution. J. Pharm. Sci. 2002a, 91: 129–156.

Poulin P, Theil F-P. Prediction of pharmacokinetics prior to in vivo studies. II. Generic physiologically based pharmacokinetic models of drug disposition. J. Pharm. Sci. 2002b, 91: 1358–1370.

Ritschel WA. Handbook of basic pharmacokinetics-- including clinical applications, 4th ed. 1992. Drug Intelligence Publications.

Chapter 4

PBPK considerations for predicting PK in liver disease[3]

Another field in which PBPK is sometime failing is the prediction of the PK in subjects suffering from liver impairment. In the experience of the author, the extent of the PK changes are often overestimated using the PBPK models implemented in the commercial platforms, especially for the mild and moderate stage of liver disease. In the following Chapter, some of the reasons for these discrepancies are examined. After developing a database of marketed drug with information on the PK changes in liver disease, this Chapter proposes the utility of multivariate regression techniques to improve the accuracy of the predicted changes. Analogous techniques could be implemented in a more comprehensive PBPK approach.

4.1. Abstract

4.1.1. Introduction

The liver is one of the most important organs responsible for the elimination of xenobiotics and there is considerable regulatory pressure to characterize the in vivo pharmacokinetic (PK) changes in subjects with liver disease (LD). Despite this, predictions of the potential effect of LD on the PK of compounds presents several limitations.

[3] This chapter is based on the paper: Gonzalez M, Goracci L, Cruciani G, Poggesi I. Some considerations on the predictions of pharmacokinetic alterations in subjects with liver disease, published in Expert Opin Drug Metab Toxicol 2014, 10: 1397-408. Please note that the conclusion section has been named 'Expert Opinion' following the journal requirements.

4.1.2. Methods

We examined a list of marketed drugs with the aim to identify compound PK characteristics potentially correlated with PK changes in LD.

4.1.3. Expert opinion

Extensive renal elimination (>40%) was the only predictor of the lack of significant changes in PK in subjects with LD. Parameters related to hepatic extraction (extraction ratio, clearance, oral clearance) were only weakly correlated to PK changes. The interplay of the effects of liver impairment on bioavailability and systemic clearance may prevent compound characteristics predictive of large increases of systemic exposure in subjects with LD compared to healthy subjects from being highlighted. A wider knowledge-base and a deeper scientific understanding may be needed to obtain predictive assessments of PK alterations in these conditions. The use of multivariate analysis can provide a stimulus for a more detailed mechanistic understanding of the absorption and disposition changes to be expected in LD.

4.2. Introduction

4.2.1. Background

The liver is one of the most important organs responsible for the elimination of xenobiotics [Peters, 2008]. The high activity of the liver's metabolizing enzymes combined with a large blood flow (approximately 25% of the cardiac output [Luttringer et al. 2003]) makes the liver the most important site of metabolism.

Liver disease is on the rise worldwide, with sharp increases in hepatitis C [Ly et al., 2012, Davis et al., 2010]. The incidence of cirrhosis due to alcohol consumption is also high (approximately 1/10000 [Featherstone, 2008]. It is therefore important to have information regarding the potential changes in the drug pharmacokinetic (PK) behavior induced by liver disease and the subsequent dose changes to be adopted in these cases.

It must be emphasized that liver disease is not a single disease and that different indications may have different impacts on the PK of a drug. A guidance on the design of PK studies in subjects with hepatic impairment and the subsequent impact on drug labeling was finalized by the United States Food and Drug Administration (FDA) in 2003 [FDA Guidance on liver impairment, 2006]. Since then, regulatory authorities are requesting these studies more frequently than in the past, also as part of post-marketing commitments. Pharmacokinetic studies in subjects with hepatic impairment are difficult to design: these assessments are not typically conducted in the

patient population for which the drug is proposed. In most cases, these studies enroll few subjects per group (both healthy subjects and subjects with mild, moderate and severe hepatic impairment), if possible with similar age and body mass index. The goal of these studies is to identify the dose level that is able to realize in subjects with hepatic impairment a similar drug systemic exposure (for instance, described by the area under the plasma concentration-time curve) compared to healthy subjects. The recruitment of subjects in these studies may be slow and unbalanced across subjects with different stages of liver disease. In addition, there are ethical limitations concerning the treatment of very ill patients with drugs that are not necessary for the treatment of their disease. Despite these difficulties, based on the results of these studies, some conclusions can be drawn regarding the need for a dosage change in these liver disease conditions: drug labels report these conclusions and physicians can rely on the achievement of similar systemic exposure to adjust the dose when patients suffering of a certain disease are also affected by some degree of hepatic impairment. This approach, surrogating efficacy and safety endpoints with a PK endpoint, may be too simplistic due to many unknowns (dependency of the drug effects on peak or average, total or unbound concentrations, etc.) and, even in presence of a relatively well designed study, the accompanying drug information (for instance regarding the involvement of hepatic metabolism) may be limited or the label language may be vague [Chang et al., 2013].

In two recent papers, the effects of liver disease on the disposition of drugs have been assessed in light of physiologically-based pharmacokinetic (PBPK) modeling [Edginton and Willlmann, 2008, Johnson et al., 2010]. In this system pharmacology-related approach, the body is represented as a collection of compartments, representing real organs and anatomical spaces, with their interconnectivity via the vasculature. In vitro and in vivo data are considered in such models, for instance, using tissues and organs compositions and volumes, blood perfusions, and all the knowledge related to system processes governing absorption and disposition of drugs [Rowland et al, 2011]. Using this approach, the modifications of the system parameters associated with hepatic impairment (anatomical-physiological characteristics such as liver size, liver enzyme activity, liver blood flow, protein levels, etc.) can be considered to anticipate the effect to be expected on the absorption and disposition of a drug approaches [Holt and Smith, 2008; Vaghjiani, 2008]. Unfortunately, based on the experience of the authors and of other groups (Jan Snoeys, personal communication) the PBPK models, as implemented in the currently available commercial platforms, do not always provide accurate predictions. In particular, the extent of the PK changes are sometimes overestimated, especially in the population of subjects characterized by the mild and moderate stages of liver disease.

The main objective of this Chapter was to examine a list of marketed drugs with the aim to identify compound PK characteristics potentially correlated to the extent of PK changes in LD in order to have a predictive assessment of new drug exposure in these conditions prior to in vivo assessment. The approach highlighted here could be used for a better parameterization of

PBPK models or could help prioritize programs for PBPK modeling in view of liver impairment studies. Some considerations will be drawn to determine whether the science may be considered adequate to allow anticipating the PK alterations to be expected in subjects with hepatic impairment based on PBPK approaches.

4.2.2. Anatomical changes in LD

The liver is the largest internal organ of the body; its weight represents approximately 2% of the body weight in adult subjects. The healthy liver receives approximately 1.3 L/min of blood (approx. 25% of the cardiac output [Luttringer et al., 2003]), 75% of which is provided by the portal circulation arriving from the gut and the remaining provided by the hepatic artery. The majority of the weight of the liver is represented by hepatocytes, the cells responsible for most of the liver functions [Holt and Smith, 2008]. Among other things, hepatocytes are responsible for the synthesis of plasma proteins, including immune factors, the metabolism of amino acids and other nitrogen compounds, the regulation of the excess glucose via formation and storage of glycogen, the synthesis and metabolism of different kind of lipids, and the conjugation and excretion of bilirubin [Vaghjiani, 2008]. Last, but not least, the liver is responsible for the metabolism of xenobiotics and the subsequent excretion into the bile of catabolism products [Vaghjiani, 2008].

Liver disease can be classified as acute or chronic depending on the duration of the symptoms (≤6 months and >6 months, respectively) [Chang et al., 2013]. Based on the pattern of damage, the liver disease can be cholestatic (when there is retention of the bile in the bile ducts that may be due to disruption of the intrahepatic biliary ductules network or to extrahepatic obstruction) or hepatocellular (when there is a direct injury to the hepatocytes, that can result in fat infiltration [steatosis] or inflammation [hepatitis]). It is important to underline that in cases of mild condition (compensated liver disease) the amount of hepatocytes is enough to perform the function of a normal liver. Sustained hepatocellular disease may further degenerate in necrosis: this event is then followed by deposition of scar tissue, resulting in fibrosis. If the fibrosis is extensive, the regeneration of hepatocytes is erratic and further disrupts the liver architecture: small nodules (cirrhosis) are formed that impair the blood flow into the liver, giving rise to increased blood pressure in the liver portal system (portal hypertension) and liver dysfunction, which typically leads to severe impairment of the drug disposition [Davis et al., 2010]. This condition (decompensated liver disease) is a vicious cycle which leads to the progressive worsening of the liver condition (see scheme reported in Fig. 4.1). Johnson et al. [Johnson et al, 2010] and Edginton & Willman [Edginton & Willman, 2008] described in their papers the changes in the anatomical and physiological liver characteristics in subjects with hepatic impairment compared to those of normal hepatic function. A comparison of these data, which represent the basis of their PBPK models, is shown in Table 4.1.

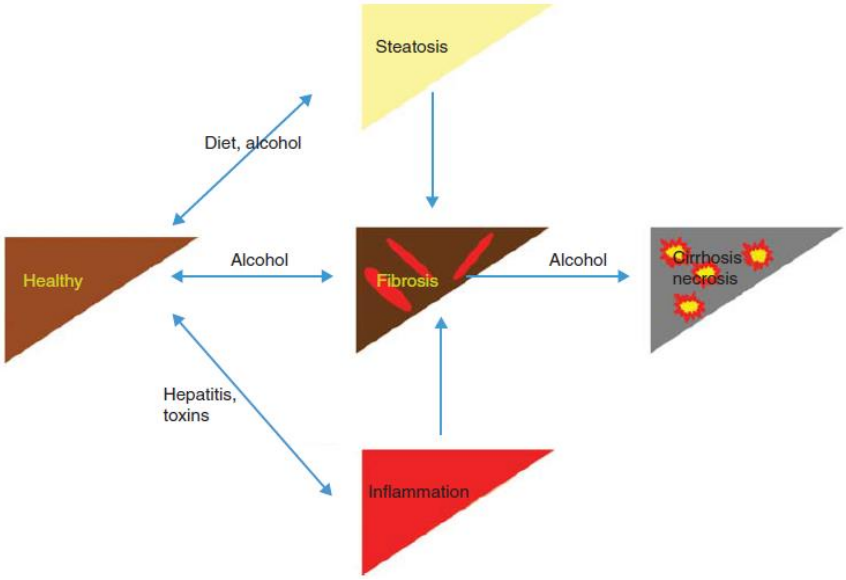

Figure 4.1. Different pattern of liver disease. Two-sided arrows represent potentially reversible processes, one-sided arrows represent irreversible processes.

Table 4.1. Examples of liver-related anatomical and physiological characteristics (expressed in fraction of a normal liver) in subjects with different degrees of hepatic impairment (Child-Pugh classification).

Characteristics	Authors	Liver disease*		
		Mild	Moderate	Severe
Liver mass	Johnson et al. 2008	0.81	0.65	0.53
	Edginton et al. 2010	0.69	0.55	0.28
Portal blood flow	Johnson et al. 2008	0.91	0.63	0.55
	Ediginton et al. 2010	0.40	0.36	0.05
Enzyme activity				
CYP1A2	Johnson et al. 2008	0.63	0.26	0.12
	Edginton et al. 2010	1.00	0.10	0.10
CYP2E1	Johnson et al. 2008]	0.74	0.48	0.11
	Edginton et al. 2010	1.00	0.83	0.83
CYP3A4	Johnson et al. 2008	0.59	0.39	0.25

Numerous factors may lead to liver disease. Alcohol consumption is the most important cause of chronic liver disease, while viral infections and drug reactions are the main causes of acute liver disease. In some cases, the hepatitis condition may become chronic (for instance in approximately 5% of hepatitis B) leading to a higher probability of developing cirrhosis and hepatocellular carcinoma with aging [Featherstone. 2008].

4.2.3. Assessments tools and tests

A number of quantitative tests are available to estimate the degree of hepatic impairment and liver function. For this purpose, liver function tests (LFT) related to synthetic (such as urea synthesis, ammonia metabolism, albumin, etc.) or excretory liver functions (e.g., serum bilirubin) have been proposed [Hughes, 2008]. Other markers (such as alanine (ALT) and aspartate aminotransferases (AST), alkaline phosphatase), indicative of acute hepatotoxicity, can be used [Hughes, 2008]. More comprehensive diagnostic or prognostic LFT (Child-Pugh classification [Child and Turcotte, 1964; Pugh et al., 1973], National Cancer Institute-Organ Dysfunction Working Group [Patel et al., 2004]) have been devised. In addition, the use of probe compounds (for instance, galactose, sorbitol, erythromycin, antipyrine, caffeine, erythromycin, and midazolam [Dourakis, 2008; Albarmawi et al, 2013]) has also been proposed to describe the impairment of specific metabolic and excretory liver functions.

Table 4.2. Child-Pugh and NCI-ODWG classification criteria [Hughes, 2008; Child and Turcotte, 1964; Pugh et al., 1973]

<table>
<tr><td colspan="4">Classification</td><td colspan="3">Liver disease</td></tr>
<tr><td colspan="4"></td><td>Mild</td><td>Moderate</td><td>Severe</td></tr>
<tr><td colspan="7">Child-Pugh score, calculated considering:</td></tr>
<tr><td>Criteria</td><td>1 point</td><td>2 points</td><td>3 points</td><td rowspan="6">5-6</td><td rowspan="6">7-9</td><td rowspan="6">10-15</td></tr>
<tr><td>Total serum bilirubin (mg/dL)</td><td><2</td><td>2-3</td><td>>3</td></tr>
<tr><td>Serum albumin (g/dL)</td><td></td><td></td><td></td></tr>
<tr><td>Prothrombin time (sec > controls)</td><td><4</td><td>4-6</td><td>>6</td></tr>
<tr><td>Encephalopathy (grade)</td><td>None</td><td>1-2</td><td>3-4</td></tr>
<tr><td>Ascites</td><td>Absent</td><td>Slight</td><td>Moderate</td></tr>
<tr><td colspan="7">NCI-ODWG</td></tr>
<tr><td colspan="4">Total bilirubin</td><td>≤1,5 ULN</td><td>>1,5-3 ULN</td><td>>3-10 ULN</td></tr>
<tr><td colspan="4">AST</td><td>> ULN</td><td>Any</td><td>Any</td></tr>
</table>

It must be underlined that no individual LFT, diagnostic or prognostic tests, or probe compounds can be used to describe all possible liver disease situations. To specify the different profiles of liver dysfunction, different LFT may be characterized by a significant rate of false positives (i.e., a significant movement of the LFT may not be accompanied by a significant reduction of the assessed liver function, for instance the efficiency in metabolizing a certain drug) or false negatives (i.e., a LFT may not be moving, but a certain liver function can be significantly impaired). Composite scores or combination of these tests can also be used. Currently Child-Pugh Score (see Table 2) [Child and Turcotte, 1964; Pugh et al., 1973] is the most commonly used method to assess hepatic impairment.

Following the FDA guidance, the Child-Pugh Score classification system is used to design the clinical pharmacology studies in which the effect of

liver impairment on the pharmacokinetics of a certain drug is assessed [FDA Guidance on liver impairment, 2006]. However, the Child-Pugh Score classification system was developed as prognostic index, and does not necessarily reflect the effect of the hepatic impairment on xenobiotic disposition. For instance, it does not differentiate between liver disease due to hepatitis or cirrhosis [Albarmawi et al., 2013], each having different effects on specific metabolizing enzymes within the liver. For subjects with cancer, the National Cancer Institute Organ Dysfunction Working Group introduced a classification based on total serum bilirubin and aspartate transaminase (AST) (Table 4.2) [Patel et al., 2004; Ramanathan et al., 2008]. However, the scope of the classification was not specifically related to be prediction of changes in drug elimination.

4.2.4. Effect of hepatic impairment on the PK of drugs

Liver disease is not a unique condition, depending on its specific characteristics (acute or chronic, typology and severity) it may affect different elimination pathways in different ways. The effect of liver disease on pharmacokinetics will also depend on the elimination pathway for a particular drug.

A number of excellent reviews have been published on this matter, either general [Edginton and Willlmann, 2008, Johnson et al., 2010, Johnson and Thomson, 2008; Verbeeck 2008; Rodighiero, 1999] or dedicated to specific therapeutic areas or group of compounds [Wyles and Gerber, 2005; Sheen, 2014; Budingen et al., 2014; Superfin et al., 2007; Bosilkovska et al., 2012; Schlatter et al., 2009]. Other papers were dedicated to the general suggestions when prescribing drugs to subjects with hepatic impairment [Branch, 1998, Spray, 2007].

In cirrhosis, the disruption of the liver vascular architecture may lead to increased blood flow resistance which limits blood flow through the liver and causes portal vein pressure to rise (portal hypertension) [Le Couteur et al., 2005]. As a consequence, formation of portocaval shunts may occur that allow the drug to bypass the first pass in the liver, with subsequent higher drug exposure [Johnson and Thomson, 2008]. Chronic disease causes damage to hepatocytes which in turn may cause a decreased intrinsic clearance of the drug metabolizing liver enzymes. Different cytochromes P450 may be affected differently by the hepatocyte damage [Branch, 1998; Frye et al, 2006] and in addition, the damage may also be different in the different regions of the liver. Cholestasis will impair the elimination of drugs that are excreted in the bile [Johnson and Thomson, 2008]. Liver disease causes a decrease of albumin in serum, which implies variation of the binding of drugs to the circulating proteins, which can potentially affect the distribution volume of certain drugs [Verbeeck, 2008]. In general, a complex interplay of these modifications need to be considered. Some of the potential situations are shown in Fig. 4.2.

Hepatic extraction	Hepatic clearance CL_H	Fraction escaping hepatic first pass F_H	AUC_{IV}	AUC_{PO}
Low $E_H \leq 0.3$	$CL_H \sim f_u \cdot CL_{int}$	$F_H \sim 1$	$AUC \sim \frac{1}{f_u \cdot CL_{int}}$	$AUC \sim \frac{1}{f_u \cdot CL_{int}}$
Moderate $0.3 < E_H \leq 0.7$	$CL_H = \frac{Q_H \cdot f_u \cdot CL_{int}}{Q_H + f_u \cdot CL_{int}}$	$F_H = 1 - \frac{CL_H}{Q_H} = \frac{Q_H}{Q_H + f_u \cdot CL_{int}}$	$AUC \sim \frac{Q_H + f_u \cdot CL_{int}}{Q_H \cdot f_u \cdot CL_{int}}$	$AUC \sim \frac{1}{f_u \cdot CL_{int}}$
High $E_H > 0.7$	$CL_H \sim Q_H$	$F_H \sim \frac{Q_H}{f_u \cdot CL_{int}}$	$AUC \sim \alpha \frac{1}{Q_H}$	$AUC \sim \frac{1}{f_u \cdot CL_{int}}$

Figure 4.2. Physicologically based PK characteristics for drugs with low, moderate or high hepatic extration (EH) and potential alterations in liver disease, depicted by the red arrows.

4.3. **Methods**

4.3.1. Data search methods

An extensive list of marketed medications, PK changes, and corresponding recommended dosage adjustments for subjects with hepatic impairment was prepared with data obtained from drug labels via Daily Med [NCI Daily Med website]. Additional information was collected from other literature sources (references are available in the supplementary material). The list was reduced to include only marketed drugs (small molecules) given orally or intravenously, for which the relevant PK information was available. Drugs with inconsistent or incomplete records were discarded. The change in pharmacokinetics in subjects with hepatic impairment was summarized using the ratio of the average area under the plasma concentration-time curve (AUC) obtained in subjects with hepatic impairment to the average AUC in subject with normal hepatic function. If data was available, the ratio was calculated for all categories of subjects with hepatic impairment (Child-Pugh A: mild; Child-Pugh B: moderate; Child-Pugh C: severe). In case of studies in which Child-Pugh classification was not used, reference to more generic terms (such as mild, moderate or severe hepatic impairment) was used. Some studies included indications on mixed group (i.e., mild and moderate hepatic impairment) and in this case, the same AUC ratio was attributed to both the categories. For each compound the minimum amount of PK information needed for analysis was: intravenous plasma clearance (CL) (or oral clearance (CL/F) and absolute bioavailability (F)), amount excreted unchanged in urine (Ae), and binding to plasma or serum protein. An estimation of the hepatic extraction ratio (E_H) was obtained using the ratio

of non-renal intravenous clearance to the hepatic blood flow. In absence of this, the intravenous clearance was calculated assuming that the (non-renal) oral clearance is a good estimator of the intrinsic clearance, using the formula $CL_{IV} = \frac{Q_H \cdot CL_{PO}}{Q_H + CL_{PO}}$.
For this aim, no limitation due to plasma protein binding restrictions was assumed. Also, it was assumed that non-renal clearance was due to hepatic metabolism or biliary excretion only and blood to plasma ratio was not much different from 1. To test that these assumptions were reasonable the estimated bioavailability (calculated using 1-E_H) was checked to be within ±30% of the observed, if this condition was not met, the compound was not considered. Other PK descriptors where also collected (i.e., whether the compound was under the control of a single metabolic route, CYP versus non-CYP, etc.) and the data were explored graphically.

The final list included the information for 84 drugs; for approximately half of them, the study of liver disease was done by characterizing the hepatic impairment using the Child-Pugh Score classification system, as suggested by the FDA guideline [FDA Guidance on liver impairment, 2006]. Graphical exploration of the correlations between the AUC ratio in the different categories of liver disease and the various PK descriptors were assessed using SigmaPlot 12.5 (Systat Software, San Jose, CA). Multivariate analysis was also carried out by PCA using a non-linear estimation by iterative partial least squares (NIPALS) approach [Wold, 1966], as implemented in the VolSurf software [Cruciani et al., 2000], to explore the potential relationships between AUC ratio and the continuous variables (total and unbound CL and CL/F, F, Ae, protein binding, E_H).

4.4. **Results**

Some of the collected data are reported in Table 4.3. The estimate of hepatic extraction ratio, E_H, is a reasonable candidate summary parameter to describe quantitatively how much the disposition of a compound is dependent on hepatic elimination. The univariate correlation between E_H ratio and the AUC ratio is reported in Fig. 4.3. Considering the population of subjects with mild hepatic impairment, no evident trend between the two variables was observed. When evaluating the subjects characterized by moderate or severe hepatic impairment, there is a tendency towards an increase of the AUC ratio with an increase of the E_H. The correlation was significant (based on p-value) for the moderate to normal and severe to normal AUC ratio; however, considering the relative position of the observations compared to the regression line, this model cannot be used for prediction purposes. However, a predictive quantitative assessment of the expected changes in AUC cannot be based on this. Indeed, despite the observed trends, it can be appreciated that there are some drugs with low E_H (≤0.3) that show a significant increase of AUC (AUC ratio>2) in subjects with hepatic impairment compared to those with normal hepatic function,

and vice versa, some compounds with moderate (0.3<EH≤0.7) or high EH (>0.7) show no relevant changes of AUC (AUC ratio ≤2) in subjects with hepatic impairment. Similar behaviors were observed considering other PK parameters (CL and CL/F, total and unbound, data not shown). Also the involvement of a unique versus many disposition pathways, as well as the involvement of certain drug metabolizing enzymes (e.g., CYP3A, 2D6, etc.) in the metabolism of a drug was not able to provide a clear-cut discrimination of drugs with large increases of AUC in subjects with hepatic impairment (AUC ratios>2) from those for which the increase was mild (AUC ratio<2). Extensive renal elimination was the only significant (and relatively trivial) determinant predictive of the lack of significant changes in PK in subjects with hepatic impairment. Considering the whole dataset, AUC ratio in subjects with hepatic impairment of any severity was ≤2 when Ae>40%.

Table 4.3. The PK characteristics and AUC ratio in subjects with hepatic impairment versus subjects with normal hepatic function for 83 different drugs.

Generic name	F (%)	CL/F (l/h)	CL (l/h)	Ae (%)	Plasma protein binding (%)	Estimated E_H	AUC ratio		
							Mild LD/ normal	Moderate LD/ normal	Severe LD/ Normal
Abacavir	83	56	NA	1	50	0,36	1,89	NA	NA
Abiraterone	5	1550	NA	0	99	0,94	1,1	3,6	6,976
Alvimopan	6	NA	24	35	80	0,16	1,5	2	NA
Anidulafungin	NA	NA	0,9	0	99	0,01	NA	NA	1
Argatroban	NA	NA	22	16	54	0,18	2,5	2,5	NA
Aripiprazole	87	4	NA	0	99	0,03	1,31	1,08	0,8
Asenapine	35	146	NA	NA	95	0,59	1	1	7
Atomoxetine	63	26	NA	3	98	0,29	NA	2	4
Axitinib	58	38	NA	0	99	0,28	NA	2	NA
Bortezomib	NA	NA	23	NA	83	0,23	NA	1,6	NA
Budesonide	11	NA	84	0	87,5	0,84	1	2,5	NA
Caspofungin	NA	NA	0,7	1	96	0,01	1,2	1,76	NA
Cefditoren	14	NA	5,0	100	88	0,00	1,1	1,1	NA
Cinacalcet	27,7	273	76	NA	95	0,76	NA	2,4	4,2
Ciprofloxacin	70	56	NA	30	30	0,25	1	1	NA
Conivaptan	44	NA	15	1	99	0,15	NA	2,8	NA
Cyclobenzaprine	44	NA	42	0	95	0,42	2	NA	NA
Dasatinib	23	294	NA	0	96	0,75	NA	1,08	0,72
Didanosine	42	NA	21	18	2,5	0,17	NA	1,13	1,13
Diltiazem	40	NA	50	3	75	0,49	NA	1,69	NA
Docetaxel	NA	NA	36	4	94	0,35	NA	1,38	NA
Dofetilide	92	NA	24	78	65	0,05	1	1	NA
Dronedarone	15	NA	140	0	98	1,00	NA	1,3	NA
Eletripan	50	NA	28	10	85	0,25	1,34	1,34	NA
Entacapone	36	118	43	0	98	0,43	2	2	NA
Entecavir	100	28	28	100	13	0,00	1	1	1
Epirubicin	NA	NA	65	6	77	0,61	1,43	2	NA

Generic name	F (%)	CL/F (l/h)	CL (l/h)	Ae (%)	Plasma protein binding (%)	Estimated E_H	AUC ratio		
							Mild LD/ normal	Moderate LD/ normal	Severe LD/ Normal
Eplerenone	69	10	NA	5	50	0,09	NA	1,42	NA
Eribulin	NA	NA	3,2	9	57	0,03	1,8	2,5	NA
Erlotinib	60	NA	NA	9	93	0,00	NA	1	NA
Escitalopram	80	36	NA	8	55	0,24	NA	1,5	NA
Eszopiclone	78	16	NA	10	55	0,12	1	1	2
Ezogabine	60	NA	35	36	80	0,22	1	1,5	2
Famciclovir	77	NA	NA	NA	10	0,23	1	1	NA
Fenoldopam	5,7	NA	160	1	88	1,00	NA	NA	1
Fingolimod	93	NA	6,3	0	99	0,06	1,12	1,44	2,03
Fluvastatin sodium	25	NA	68	0	99	0,75	NA	2,5	NA
Hydromorphone	24	484	NA	7	27	0,77	NA	4	NA
Icatibant	NA	NA	18	5	44	0,17	1	1	1
Lacosamide	100	NA	2,8	40	15	0,02	NA	1,6	NA
Lamivudine	85	30	21	75	36	0,05	1	1	NA
Lamotrigine	98	2,2	NA	78	60	0,00	1,23	1,54	1,76
Lansoprazole	85	17	NA	0	97	0,14	NA	6	NA
Letrozole	100	2,2	NA	4	60	0,02	1,37	1,37	2
Meropenem	NA	NA	15	74	2	0,04	1	1	1
Miglitol	59	NA	7,2	100	4	0,00	1	1	1
Montelukast	64	NA	2,7	0	99	0,03	1,41	1,41	NA
Moxifloxacin	89	15	13	23	48	0,10	0,78	1,02	NA
Naratriptan	78	38	27	50	29	0,13	1,43	1,43	NA
Nelfinavir	75	50	38	2	98	0,37	1	1,62	NA
Olmesartan medoxomil	26	NA	1,3	13	99,7	0,01	NA	1,6	NA
Paliperidone	282	72	27	60	74	0,11	NA	1	NA
Palonosetron	NA	NA	11	40	62	0,07	NA	1	NA
Pantoprazole	77	NA	7,0	0	98	0,07	1,5	1,5	1,5
Paricalcitol	80	NA	2,7	6	99,8	0,03	1	1	NA
Perindopril erbumine	80	NA	31	9	60	0,29	NA	1,5	NA
Quetiapine	9	NA	80	20	83	0,64	NA	1,43	NA

Generic name	F (%)	CL/F (l/h)	CL (l/h)	Ae (%)	Plasma protein binding (%)	Estimated E_H	AUC ratio		
							Mild LD/ normal	Moderate LD/ normal	Severe LD/ Normal
Ribavirin	52	NA	25	28	0	0,18	1	1	1
Riluzole	64	NA	48	0	96	0,48	1,7	3	NA
Risperidone	66	NA	43	1	90	0,42	1	1	1
Rivaroxaban	90	10	NA	30	94	0,06	1,15	2,27	NA
Roflumilast	80	10	NA	0	95	0,09	1,51	1,92	NA
Romidepsin	NA	NA	15	NA	93	0,09	1	NA	NA
Rosuvastatin	20	NA	44	NA	88	0,44	1,05	1,21	NA
Saxagliptin	67	73	NA	24	0	0,32	1,77	1,77	1,77
Sildenafil	41	NA	NA	2	96	0,60	1,85	1,85	NA
Solifenacin	88	NA	10	7	98	0,09	NA	1,35	NA
Tapentadol	32	NA	92	3	20	0,70	1,7	4,2	NA
Telavancin	NA	NA	0,9	68	90	0,01	NA	1	1
Telbivudine	NA	21	18	42	3	0,10	1	1	1
Telithromycin	57	64	59	7	65	0,54	1	1	1
Temozolomide	100	NA	12	NA	15	0,00	1	1	NA
Teriflunomide	100	NA	0,03	0	99	0,00	1	1	NA
Tolcapone	65	NA	7,0	0	99,9	0,15	NA	2	NA
Triptorelin	NA	NA	13	40	0	0,08	3	3	NA
Trovafloxacin	88	NA	6,0	10	76	0,05	1,45	1,5	NA
Valproic acid	100	NA	0,5	3	90	0,00	NA	2	NA
Valsartan	25	NA	2,0	13	95	0,01	2	2	NA
Vardenafil	15	NA	56	4	95	0,54	1,17	2,6	NA
Vilazodone	72	34	NA	1	98	0,25	1	1	1
Voriconazole	96	NA	16	2	58	0,16	2,3	3,2	NA
Zaleplon	30	266	70	0	60	0,70	NA	4	7
Zolmitriptan	40	141	NA	8	25	0,54	NA	NA	3
Zolpidem	70	NA	18	0	92	0,18	NA	5	NA

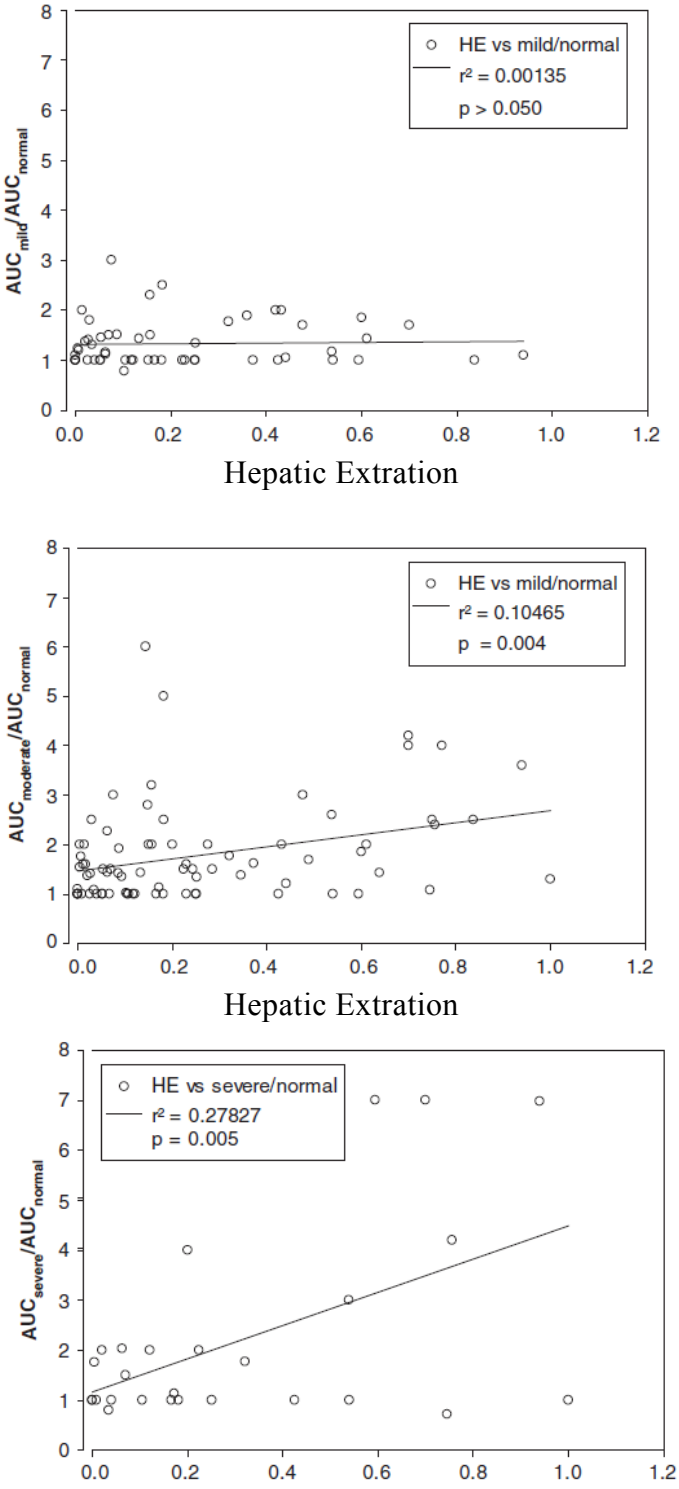

Figure 4.3. correlation of the ratio AUC in subjects with hepatic impairment to AUC in subjects with normal hepatic function with EH, from top to bottom: mild/normal, moderate/normal and severe/normal, respectively. In the plot, the regression line, correlation coefficient and Pearson p-value are shown.

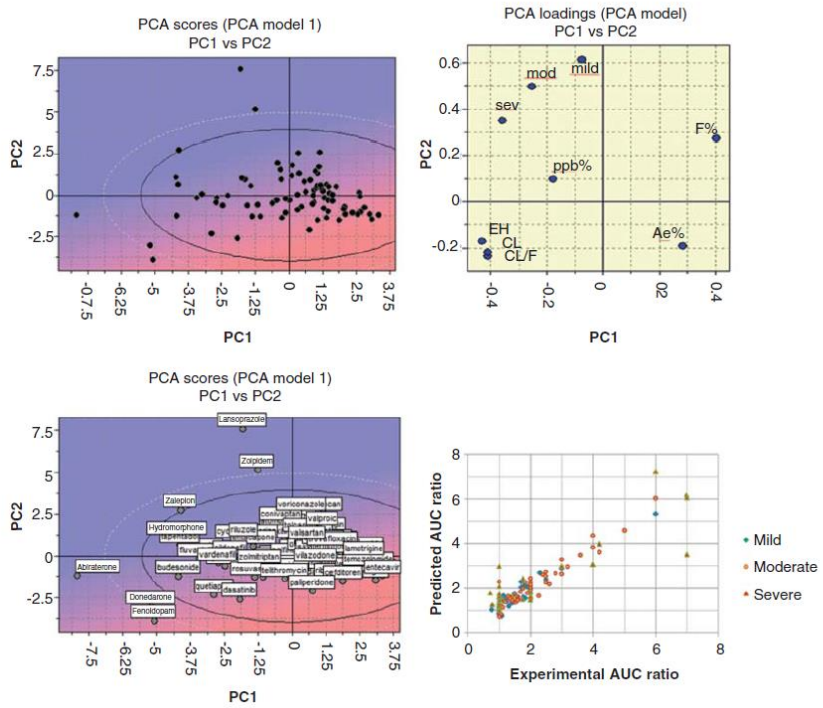

Figure 4.4. Outcome of the PCA-NIPALS model. Upper left panel: score plot (lower flet panel reports the name of the compounds in the score plot); upper right panel: loading plot; lower right panel: correlation between the observed and predicted AUC ratio in mild, moderate or severe hepatic disease.

The outcome of this multivariate analysis is reported in Figure 4.4. This approach, particularly indicated in case of matrices of data with missing data, is a multivariate regression technique in which the variables are projected on principal components (PCs), which are linear combinations of the variables, with the aim of reducing the dimensionality of the problem and accounting for the collinearity of the original set of variables. The outcome of PCA-NIPALS can be summarized into two plots, the score and the loading plots, both depicted in the space of the PCs (Figure 4.4, upper left and right panels). The score plot represents the position of the compounds, and it is reported with background color, which corresponds to the moderate to normal AUC ratio values that linearly increase from red (low AUC ratios) to blue (high AUC ratios). The loading plot represents the relationships among the descriptors. The latter can be used to interpret the position of the compounds in the score plot. A compound in the score plot will be characterized by high values of the properties reported in the corresponding position of the loading plot, and vice versa, low values of the properties reported in the opposite quadrant of the loading plot. Additional details on NIPALS and on the other multivariate analysis tools based on projection techniques can be found in [Varmuza and Filzmoser, 2009]. The NIPALS model was able to describe

well the AUC ratio of the training dataset: model-predicted AUC ratio were in good agreement with the observations (see Fig. 5.4, bottom right panel). Using an AUC threshold ratio of 2 to discriminate between a relevant AUC increase in subjects with hepatic impairment, the model was able to correctly classify the compounds in approximately 90% of the cases. Being located in opposite quadrants of the loading plot, and as underlined by the univariate analysis, the amount excreted unchanged in urine is a strong determinant of the absence of large AUC ratio values

It can be appreciated that clearance and hepatic extraction and oral bioavailability are also in opposite quadrants and both are adjacent to the quadrant in which the AUC ratio values properties are located, suggesting some interplay between the effects of these characteristics on the outcome variables. A limited external validation of the approach was performed for assessing the predictive ability of this approach based on the AUC ratio for 4 compounds (chosen randomly while avoiding similar PK characteristics and not included in the original dataset): the comparison between observed and predicted AUC ratios are shown in Table 4.4. The NIPALS approach was able to predict the effect of liver disease on the PK of these compounds with reasonable accuracy.

Table 4.4. The PK characteristics and observed and model-predicted AUC ratio in subjects with hepatic impairment versus subjects with normal hepatic function for 4 drugs (test dataset)

Generic name	F (%)	CL/F (l/h)	CL (l/h)	Ae (%)	Plasma protein binding (%)	Estimated E_H	AUC ratio					
							Mild LD/ normal		Moderate LD/ normal		Severe LD/ Normal	
							observed	Predicted	Observed	Predicted	Observed	Predicted
Midazolam Dundee et al, 1984	NA	27,60	NA	0,5	95,5	0,27	1	1,3	2,21	1,7	2,92	2,5
Omeprazole Piquè et al, 2002	35	NA	33	0	95	0,12	1,57	1,6	1,83	1,8	2,10	2,3
Rosuvastatin Simonson et al., 2003; Martin et al., 2003	NA	48,9	NA	28	88	0,35	1,05	1,0	1,21	1,4	NA	1,9
Sildenafil Muirhead et al., 2008	41	NA	85	0	96	0,35	1.84	1,6	1,84	2,1	NA	2,9

4.5. **Expert opinion**

The analysis performed in this review showed that the quantitative prediction of the increase of the AUC ratio based on the PK characteristics cannot be done with a reasonable degree of accuracy using a univariate regression analysis. In some previous papers it was suggested that significant change of the pharmacokinetics in liver disease could be anticipated for drugs with high hepatic extraction [Schlatter et al., 2009], but these trends could not be used for a predictive approach as this was not consistently observed in the behavior of drugs included in the present assessment. Individual PK determinants (E_H, for instance) are able to provide only weak hints of the expected PK changes in subjects with hepatic impairment.

It is possible that drug PK characteristics show a complex interplay that is responsible for the overall effect of the change in exposure observed in these liver disease conditions, providing a confounded picture. Some limitations in the design of these studies may contribute to this situation: for instance, in many of the reported studies in subjects with hepatic impairment there was no assessment of the unbound concentrations. Also, for oral drugs, the characterization of the PK in subjects with hepatic impairment after IV dosing is almost never done, despite the fact that it would provide precious information for the study of the changes of the disposition in these liver disease conditions. Another important aspect of this problem is that liver disease may be characterized by different presentations (cholestatic, inflammatory, fibrotic, cirrhotic) and this is likely to differently modify the expression and function of hepatocyte membrane transporters and metabolic enzymes which characterize the intrinsic hepatic clearance of the liver.

Some physiological information related to the characterization of subjects with hepatic impairment is still missing or uncertain. An appreciation of this aspect can be obtained from the comparison of the sometime different PBPK parameters used in the two papers assessing the use of PBPK in this patient population (see Table 4.1) [Edginton and Willlmann, 2008, Johnson et al., 2010]. More experiments are needed to try and consolidate the characteristics of the system “subjects with hepatic impairment”.

The application of multivariate techniques, especially those that can deal with incomplete data, may overcome part of the uncertainties and missing information underlined above and can provide momentum for a more detailed mechanistic understanding of the absorption and disposition changes to be expected in the different pathological conditions linked to liver disease. In the example we showed here, NIPALS approach was able to provide a model characterized by adequate accuracy in approximately 90% of the cases and this was also confirmed based on the outcome of an external dataset. The loading plot (Figure 4.4, upper right panel) provided some suggestion related to the previously mentioned interplay between the PK characteristics responsible for the outcome variable. Compounds with either low or high extraction ratios can undergo significant increases in exposure

in subjects with hepatic impairment via different mechanisms (for instance, portocaval shunts may significantly increase the exposure [AUC] of drugs characterized by high hepatic extraction via an increased oral bioavailability, while the decreased liver enzyme activity may affect in the same sense the exposure of drugs with low hepatic extraction).

In conclusion, for their predictive use (for instance, for the parameterization of PBPK approaches), the assessments of PK alterations in subjects with hepatic impairment are still limited by some uncertainties partially attributable to constraints in the study design and conduct. In absence of additional information that may contribute to fix these aspects, a smarter statistical analysis, making use of the overall pattern of information available, may provide useful guidance for designing the studies of new compounds and for highlighting the specific physiological aspects that need additional investigations.

4.6. **References**

Albarmawi A, Czock D, Gauss A, Ehehalt R, Bermejo JL, Burhenne J et al. CYP3A activity in severe liver cirrhosis correlates with Child-Pugh and model for end-stage liver disease (MELD) scores. British J Clin Pharmacol 2013,77:190-9.

Bosilkovska M, Walder B, Besson M, Daali Y, Desmeules J. Analgesics in patients with hepatic impairment. Pharmacology and clinical implications. Drugs 2012, 72:1645-69.

Branch RA. Drugs in liver disease. Clin Pharmacol Ther 1998, 64:462-4.

Budingen FV, Gonzalez D, Tucker AN, Derendorf H. Relevance of liver failure for anti-infective agents: from pharmacokinetic alterations to dosage adjustments. Ther Advan Infectious Disease 2014,2:17-42.

Chang Y, Burckart GJ, Lesko LJ, Dowling TC. Evaluation of hepatic impairment dosing recommendations in FDA-approved product labels. J Clin Pharmacol 2013, 53:962-6.

Child CG, Turcotte JC. Surgery and portal hypertension. Major Probl Clin Surg, 1964: 1:1-85.

Cruciani G, Crivori P, Carrupt PA, Testa B. Molecular Fields in Quantitative Structure-Permeation Relationships: The VolSurf Approach. J Mol Struct: THEOCHEM 2000, 503: 17–30.

Davis GL, Alter MJ, El-Serag H, et al. Aging of hepatitis C virus (HCV)-infected persons in the United States: a multiple cohort model of HCV prevalence and disease progression. Gastroenterology 2010; 138(2):513-21

Dourakis SP. Drug therapy in liver diseases. Annals Gastroenterol 2008, 21:215-7.Edginton AN, Willmann S. Physiology-based simulation of a

pathological condition. Prediction of pharmacokinetics in patients with liver cirrhosis. Clin Pharmacokinet 2008, 47:743-52.

Dundee JW, Halliday NJ, Harper KW, Brogden RN. Midazolam A Review of its Pharmacological Properties and Therapeutic Use. Drugs 1984, 28: 519-543

Featherstone B. Causes of liver disease and dysfunction. In: Drugs and the liver, North Lewis P (editor), Pharmaceutical Press, London, 2008.

Frye RF, Zgheib NK, Matzke GR, Chaves-Gnecco D, Rabinovitz M, Shaikh OS, Branch RA. Liver disease selectively modulates cytochrome P450-mediated metabolism Clin Pharmaco Ther 2006, 80:235-45.

Holt A, Smith A. An introduction to the anatomy of the liver. In: Drugs and the liver, North Lewis P (editor), Pharmaceutical Press, London, 2008.

Hughes C. Assessing liver function. In: Drugs and the liver, North Lewis P (editor), Pharmaceutical Press, London, 2008.Johnson TN, Boussery K, Rowland-Yeo K et al. A semi-mechanistic model to predict the effects of liver cirrhosis on drug clearance. Clin Pharmacokinet 2010; 49:189-206.

Johnson TN, Thomson AH. Pharmacokinetics of drugs in liver disease. In: In: Drugs and the liver, North Lewis P (editor), Pharmaceutical Press, London, 2008.

Le Couteur DG, Fraser R, Hilmer S, Rivory LP, McLean AJ. The hepatic sinusoid in aging and cirrhosis. Clin Pharmacokinet 2005, 44:187-200.

Luttringer O, Theil FP, Poulin, P, Schmitt-Hoffmann A H, Guentert TW, Lavé T. Physiologically based pharmacokinetic (PBPK) modeling of disposition of epiroprim in humans. J Pharm Sci, 2003, 92(10): 1990-2007.

Ly KN, Xing J, Klevens RM, Jiles RB, Ward JW, Holmberg SD. The increasing burden of mortality from viral hepatitis in the United States between 1999 and 2007. Ann Intern Med. 2012;156(4):271–8

Martin PD, Warwick MJ, Dane AL, Brindley C, Short T. Absolute oral bioavailability of rosuvastatin in healthy white adult male volunteers. Clinical Therapeutics 2003, 25 :2553-63

Muirhead GJ, Rance DJ. Walker DK. Wastall P. Comparative human pharmacokinetics and metabolism of single-dose oral and intravenous sildenafil citrate. Br J Clin Pharmacol 2002, 3, 13S-20S

National Cancer Institute Daily Med. http://dailymed.nlm.nih.gov/dailymed/about.cfm last accessed March 5, 2014.

Patel H, Egorin MJ, Remick SC, Mulkerin D, Takimoto CHM, Doroshow JH et al. Comparison of Child-Pugh (CP) criteria and NCI organ dysfunction working group (NCI-ODWG) criteria for hepatic dysfunction (HD): Implications for chemotherapy dosing. J Clin Oncol 2004,22(14S):6051.

Peters SA. Physiologically-based pharmacokinetic (PBPK) modeling and simulations: principles, methods, and applications in the pharmaceutical industry. John Wiley & Sons, Hoboken (NJ), 2008.

Piqué JM, Feu F, de Prada G, Röhss K, Hasselgren G. Pharmacokinetics of omeprazole given by continuous intravenous infusion in patients with varying degrees of hepatic dysfunction. Clin Pharmacokinet 2002, 41: 999-1004.

Pugh RN, Murray-Lyon IM, Dawson JL, Pietroni MC, Williams R. Transection of the oesophagus for bleeding oesophageal varices. Br J Surg 1973, 60:646-9.

Ramanathan RK, Egorin MJ, Takimoto CHM, Remick SC, Doroshow JH, LoRusso PA et al. Phase I and pharmacokinetic study of imatinib mesylate in patients with advanced malignancies and varying degrees of liver dysfunction: A study by the national Cancer Institute Organ Dysfunction Working Group, J Clin Oncol 2008, 26:563-9.

Rodighiero V. Effects of liver disease on pharmacokinetics. An update. Clinical Pharmacokinet 1999, 37:399-431.

Rowland M, Peck C, Tucker G. Physiologically-based pharmacokinetics in drug development and regulatory science. Annu Rev Pharmacol Toxicol 2011; 51:45-73.

Scheen AJ. Pharmacokinetics and toxicological considerations for the treatment of diabetes in patients with liver disease. Expert Opin Drug Metab Toxicol 2014, 6. Early online doi:10.1517/17425255.2014.902444.

Schlatter C, Egger SE, Tchambaz L, Krahenbuhl S. Pharmacokinetic changes of psychotropic drugs in patients with liver disease. Implications for dose adaptation. Drug Safety 2009, 32-561-78.

Simonson SG, Martin PD, Mitchell P, Schneck DW, Lasseter KC, Warwick MJ. Pharmacokinetics and pharmacodynamics of rosuvastatin in subjects with hepatic impairment. Eur J Clin Pharmacol 2003, 58: 669–675

Spray JW, Willet K, Chase D, Sindelar R, Connelly S. Dosage adjustment for hepatic dysfunction based on Child Pugh scores. Am J Health Syst Pharm 2007, 64:690-3.

Superfin D, Iannucci AA, Davies AM. Commentary: oncologic drugs in patients with organ dysfunction: a summary. The oncologist 2007, 12:1070-1083.

U.S. Food and Drug Administration. Guidance for industry pharmacokinetics in patients with impaired hepatic function: study design, data analysis, and impact on dosing and labeling, U.S. Department of Health and Human Services Food and Drug Administration Center for Drug Evaluation and Research (CDER), Center for Biologics Evaluation and Research (CBER), May 2003. Clinical Pharmacology. Available from

http://www.fda.gov/downloads/Drugs/GuidanceComplianceRegulatoryInformation/Guidances/ucm072123.pdf, accessed March 31, 2014.

Vaghjiani S. Functions of the liver. In: Drugs and the liver, North Lewis P (editor), Pharmaceutical Press, London, 2008.

Varmuza, K.; Filzmoser, P., Introduction to multivariate statistical analysis in chemometrics. CRC Press/Taylor & Francis: Boca Raton, Fla., 2009

Verbeeck RK. Pharmacokinetics and dosage adjustment in patients with hepatic dysfunction. Eur J Clin Pharmacol 2008, 64:1147-61.

Wold H. Estimation of principal components and related models by iterative least squares. In Krishnaiah PR (ed.) Multivariate Analysis Academic Press, NY, 1966, 391–420.

Wyles, DL, Gerber JG. Antiretroviral drug pharmacokinetics in hepatitis with hepatic dysfunction. Clin Infectious Diseases 2005, 40:174-81.

Chapter 5

Predictive assessments of PK in renal disease[4]

This is the natural companion to the previous Chapter, dealing with the prediction of PK changes in subjects with renal disease. Analyses were performed based on the same database previously considered. Regression analyses suggested that the relevant descriptors for predicting the effect of renal impairment on PK of drugs were the amount excreted unchanged in urine and fraction unbound in plasma, which is expected based on the physiology of renal excretion. Whilst the accuracy of the predictions of the PK changes in renal impairment is better than in case of liver disease (as well as the predictive performance of PBPK models), there are still cases in which the reason for the PK changes are escaping the current physiological description. The use of more sophisticated multivariate techniques was not as successful as in the previous case to correct these discrepancies.

5.1. Abstract

Renal disease has important effects on the pharmacokinetics of drugs. Ad hoc pharmacokinetic studies are required by the regulatory authorities in subjects with renal impairment for proposing dose adjustments to be adopted in subjects with renal disease, in order to obtain similar systemic exposures compared to healthy subjects. To establish a predictive model of the effect of renal impairment on the exposure of drugs in development, we considered 73 marketed drugs, for which studies in subjects with different degrees of renal impairment were available in the literature. Multivariate analysis was performed using the principal pharmacokinetic parameters and physiological

[4] This chapter is essentially based on the manuscript: Borella E, Poggesi I. Magni P. Predictive assessments of pharmacokinetic alterations in subjects with renal disease, that is being submitted to Clinical Pharmacokinetics.

considerations. As expected based the basic physiological description of the renal clearance processes, stepwise multivariate regression analyses revealed that the fraction of dose excreted unchanged in urine and plasma protein binding were primarily related to the change in exposure for subjects with renal impairment versus subjects with normal renal function. Other methodologies, including data mining and machine learning techniques, were used to propose models based on a categorical definition of the exposure changes, providing similar results. The predictions were however not always satisfactory, especially to describe drugs which, despite the negligible renal excretion, are characterized by significant increases in the systemic exposure. This phenomenon, interpreted considering the accumulation of endogenous metabolism inhibitors in subjects with moderate and severe renal disease (uremic toxins), cannot be fully described likely due to an incomplete understanding of the physiopathological phenomena and to some limitations of the clinical studies.

5.2. **Introduction**

Kidneys, together with the liver, are between the main organs responsible for the elimination of drugs. Renal disease, which affects glomerular blood flow and filtration, tubular secretion and reabsorption, alters the renal excretion of unchanged drug and/or their metabolites. The changes accompanying renal disease can also lead to other modifications of pharmacokinetic processes, for instance, changes in the distribution, transport, and biotransformation of drug substances [Yeo et al., 2014; Velenosi and Urquhart, 2014; Verbeeck and Musuamba, 2009; Poggesi et al., 2009].

Renal failure is a medical condition in which the kidneys fail to adequately filter waste products from the blood. The two main forms are Acute Kidney Injury (AKI), often due to immunologic reactions, oxygen deprivation, and exposure to chemical agents, which is often reversible with adequate treatment, and Chronic Kidney Disease (CKD), which is often not reversible, progressing to end-stage renal failure over a period of months to years [Levey et al., 2005]. The incidence of CKD is increasing in western countries, the prevalence of CKD among the U.S. adult population recently being estimated around 13% [Coresh et al, 2007]. CKD is characterized by glomerulosclerosis, interstitial leukocyte infiltration, tubular atrophy and tubulointerstitial fibrosis. Given the sequential renal microvasculature structure, a decrease in preglomerular or glomerular blood flow due to the loss of glomerular capillary loops will inevitably be associated with a reduction in postglomerular, peritubular blood flow and, consequently, with tubular ischemia and general hypoxia of renal tissue [Schlondorff , 2008].

In 2002 the Kidney Disease Outcomes Quality Initiative (K/DOQI) of the National Kidney Foundation has published guidelines [Eknoyan et al., 2003] to define CKD and to classify stages in its progression (Table 5.1). This classification is based on the glomerular filtration rate (GFR), typically

expressed using serum creatinine concentration values via the Cockroft-Gault formula:

$$\text{CrCL}= \frac{(140\text{-Age}) \text{x Weight (kg)}}{72 \text{ x Creatinine}_{serum} \left(\frac{mg}{dL}\right)} \text{ x } 0.85 \text{ if female}$$

or, if available, using the more precise values provided by the actual measurements of creatinine clearance (CrCL). When GFR is impaired, less creatinine is excreted by the glomerulus, causing serum creatinine concentrations to increase and CrCL to decrease in patients with acute or chronic renal insufficiency. Despite some polemics centred on the fact that CrCL may be somewhat biased as a descriptor for GFR (inuline clearance may be a more accurate one) and that GFR may not be a comprehensive descriptor of renal disease [Kliger et al., 2013], this appears to be a very reasonable candidate as descriptor of pharmacokinetic changes.

Table 5.1. Classification of Chronic Kidney Disease.

Stage	Description	GFR (mL/min/1.73m^2)
1	Kidney damage with normal or increased GFR	≥90
2	Kidney damage with mildly decreased GFR	60-89
3	Moderately decreased GFR	30-59
4	Severely decreased GFR	15-29
5	Kidney failure	<15 or dialysis

For a drug eliminated primarily via renal excretory mechanisms, impaired renal function may alter its pharmacokinetic to an extent that the dosage regimen needs to be changed from that used in patients with normal renal function [Poggesi et al., 2009]. Although the most obvious change arising from renal excretion or metabolism of both drug and metabolites, renal impairment may also be associated with other changes, such as changes in absorption, plasma protein binding, and drug distribution [http://www.fda.gov/downloads/Drugs/.../Guidances/UCM204959.pdf, accessed Aug 1, 2016].

The time at which the maximum plasma concentration occurs was found slightly increased for drugs given to patients with severe renal dysfunction [Verbeeck and Musuamba, 2009]. Drug absorption may also be altered in these subjects due to vomit or diarrhoea; use of antacids or uraemia can increase the gastric pH with further effects on absorption time.

The plasma protein binding of many acidic drugs is decreased in patients with renal dysfunction due to hypoalbuminemia or accumulation of endogenous substances which competitively displace acidic drugs from albumin. Besides, an increased volume of distribution may be the result of fluid overload, decreased protein binding, or altered tissue binding [Verbeeck and Musuamba, 2009]. While acidic drugs usually bind to albumin, basic drugs have often a high affinity for α_1-acid glycoprotein

(AGP). AGP has been found increased in certain patients with renal disease; subsequently, differently from the drug binding to albumin, the plasma protein binding of basic drugs may be increased in these patients.

Pharmacokinetic studies in patients with renal dysfunction have shown that also non-renal clearance is reduced for many drugs providing indirect evidence that the also hepatic metabolism of these drugs is impaired in these patients. Many in vivo and in vitro studies, using rat models of both acute and chronic renal failure, have shown a down-regulation of the activity of not only CYP450 enzymes, but also other drug-metabolizing enzymes, such as N-acetyltransferase. Besides, endogenous inhibitors (sometimes called uremic toxins) accumulating in the body as a result of the chronic renal failure have been shown to be implicated in these alterations in drug-metabolizing enzyme activities [Poggesi et al., 2009]. The kidney also expresses many of the same drug metabolizing enzymes as those found in the liver, even if the efficiency of elimination in this organ is typically lower than the liver as a result of the lower blood flow and thus, the lower rate of presentation to the eliminating organ.

Renal disease affects all renal excretory processes: glomerular filtration, active tubular secretion and passive tubular reabsorption. Therefore, independently of whether a drug is filtered or actively secreted, the loss of excretory function in the diseased kidney can be quantified by GFR, a measure of glomerular function, such as creatinine clearance [Verbeeck and Musuamba, 2009]. In general, renal clearance (CL_R), the proportionality constant between the rate of renal elimination and the concentration in systemic circulation, can be quantified from a physiological point of view as:

$$CL_R = CL_{filtration} + CL_{active\ secretion} - reabsorption$$

Where $CL_{filtration}$ is the clearance due to the process of glomerular filtration, $CL_{active\ secretion}$ is the renal excretion clearance component which is under the control of active processes and reabsorption is the (negative) clearance component accounting for the tubular reabsorption. Filtration is a passive process, the efficiency of which is directly proportional to the fraction unbound to plasma proteins (f_u) and GFR:

$$CL_{filtration} = f_u \cdot GFR$$

Active secretion is under the control of active transporters and, whilst its extent is decreasing with the decrease of renal function, the effect of renal disease on this process is less easily precisely quantified. Reabsorption, as filtration, is essentially a passive process.

Efficacy and safety profile of a drug is established in phase III studies in a well-defined patient population, which may not be fully representative of the patient population in which the drug will be used once it is on the market. For this reason, ad hoc pharmacokinetic and pharmacodynamic studies are performed in special population in order to estimate the drug exposure in these subpopulations whose characteristics may affect drug exposure, such as patients with renal impairment. Both the Food and Drug Administration (FDA) and the European Medicines Agency (EMEA) promote pharmacokinetic studies to assess the pharmacokinetic characterization of

drugs in patients with renal dysfunction. A traditional two-stage method, in which, in the first stage a detailed pharmacokinetic study is carried out in selected subjects to obtain estimates of individual pharmacokinetic parameters, such as plasma clearance, volume of distribution, plasma half-life, etc. In the second stage, the relationships between patient characteristics and the estimated pharmacokinetic parameters are established by categorization or regression techniques [Verbeeck and Musuamba, 2009]. Based on the results of these studies, conclusions can be drawn for dosage adjustments in renal disease conditions and potential dosing advice for renal impairment is provided in the label.

The main objective of this work is to find approaches capable of describing the changes in exposure of a series of marketed drugs observed in subjects with renal impairment using their pharmacokinetic attributes via multivariate analysis to evaluate whether these approaches can be used as predictive tools. This could be a starting point to identify the basic molecular, biochemical or biological determinants that influence the pharmacokinetics (and thus systemic exposure) changes in subjects with renal disease compared to those with normal renal function. When these attributes are identified, and their effect quantified, they can be used in a more quantitative manner to drive comprehensive physiology-based pharmacokinetic (PBPK) models.

5.3. **Methods**

5.3.1. Data Collection

For an extensive list of marketed drugs, pharmacokinetic (PK) parameters and recommendations in case of renal impairment were collected from DailyMed [https://dailymed.nlm.nih.gov/dailymed/, from the U.S. National Library of Medicine, National Institutes of Health, Health & Human Services] and other literature resources [Dowell et al., 2007; Mallikaarjun et al., 2008; Drusano et al., 1987; Roy et al., 2013; Boike et al., 1994; Johnson et al., 1998; Wootton et al., 1997; Delhotal-Landes et al., 1993; Christenssen et al., 1992; Snoeck et al., 1995; Kubitza et al., 2010; Boulton et al., 2011]. Only drugs given orally or intravenously were selected. To represent the change in PK in subjects with renal impairment, the ratio between the average area under the plasma concentration-time curve (AUC) in renal impaired subjects to the average AUC in subjects with normal renal function was considered. If data were available, the ratio was calculated for the three categories of renal impairment (mild, moderate and severe) according to the classification reported in Table 5.1. Some studies included indications only for mixed groups (for instance, for mild and moderate renal impairment), so, for these cases, the same AUC ratio was attributed to both the categories. If AUC changes in renal impaired population were not reported, the ratio between the oral clearance of healthy subjects to the oral clearance of

subjects with renal impairment was used instead. If no change in pharmacokinetics was observed, the AUC ratio was set to 1. For each drug, the following principal PK parameters were collected, as available: intravenous plasma clearance (CL), absolute bioavailability (F), oral clearance (CL/F), fraction of dose excreted unchanged in urine (Ae, expressed as fraction of dose), and fraction of dose bound to plasma serum protein (ppb). An estimation of the hepatic extraction ratio (EH) was calculated using the ratio of non-renal CL after intra-venous dosing to the hepatic blood flow (Q_h), or, in absence of this, it was calculated from the non-renal oral clearance ($CL_{nr,PO}$) using the following formula:

$$CL_{nr,\,IV} = \frac{Q_H \cdot CL_{nr,PO}}{Q_H + CL_{nr,PO}}$$

assuming complete absorption, non-renal clearance only occurring in the liver, and no restrictions due to protein binding and blood to plasma ratio not significantly different from unit [Germani et al., 2007]. Other information was also recorded: the main way of extraction, whether the compound was under the control of a single metabolic route, information about the cytochrome mainly involved in the metabolism processes or, if no cytochrome was involved, the type of enzyme or membrane transport proteins involved.

The full dataset includes information about 73 drugs and it is reported in Table 5.9 at the end of this chapter. Summary statistics for PK parameters and AUC ratios are reported in Table 5.2.

Table 5.2. Summary statistics of PK parameters and AUC ratios.

	CL/F (L/h)	F (%)	CL (L/h)	Ae (%)	ppb (%)	EH (-)	AUC ratio mild	AUC ratio moderate	AUC ratio severe
Min	2.20	0.79	0.03	0.00	0.00	0.00	0.80	0.98	0.67
1st Qu.	15.20	29.50	6.22	1.00	50.00	0.04	1.00	1.00	1.00
Median	34.00	61.50	16.73	7.20	83.00	0.15	1.00	1.00	1.10
Mean	138.60	57.23	25.98	19.11	68.34	0.23	1.13	1.39	1.85
3rd Qu.	129.80	85.00	32.30	29.42	97.00	0.29	1.12	1.45	2.00
Max	1550.00	100.00	140.00	100.00	99.90	1.00	2.49	4.33	10.91
NA's	46	13	21	7	0	0	13	6	7

5.3.2. Data Analysis

To explore the potential relationships between the AUC ratios and the PK attributes selected (CL, CL/F, F, Ae, ppb, EH), two different types of analyses have been performed. In the first analysis univariate single regressions, multiple linear regression, and non-linear iterative partial least squares (NIPALS) multivariate regression [Bastien and Tenenhaus, 2003, Abdi, 2010, Preda et al., 2010] were performed for each of the three levels of renal impairment and their performances in predicting the AUC ratios given the PK parameters were compared. For the univariate single regression

each PK parameter was individually tested, while only the most informative parameters selected through a stepwise procedure were used as regressors for the univariate multiple regression. The following graphical analyses were performed for model evaluation: data vs. predictions, fold changes vs. predictions, residuals vs. predictions, residuals vs. regressor. The first analysis was performed in R v.3.0.3 [R Core Team (2014). R: A language and environment for statistical computing. R Foundation for Statistical Computing, Vienna, Austria. URL http://www.R-project.org/] using lm function for linear regression, nipals (available in mixOmics package) and plsreg2 function (available in plsdepot package) functions for NIPALS regression. The second analysis consisted of a classification approach. Two types of classification problems were considered. For this aim, the following classification criteria was chosen according to expert's opinion: an administration is considered safe if the AUC ratio is below 1.25; associated with low risk if the AUC ratio is between 1.25 and 2; associated with medium risk if the AUC ratio is between 2 and 5, and with high risk if the AUC ratio is above 5. As a first step, each drug was assigned to a three-level class: 0 for drugs that are classified as safe, 1 for drugs with low risk, and 2 for drugs with medium/high risk. In a second step, each drug was assigned to a binary class: 0 for those drugs whose administration is considered safe and 1 for those drugs whose administration is associated with some risk (low, medium or high) of increased exposure in subjects with renal disease. The following data mining and machine-learning methods were tested: Naïve Bayes (NB) and Classification Tree (CT) [Fung, 2001]. The analyses were performed in Orange v.2.7 [Demsar et al., 2013]. Since NB requests discrete attributes, all the six continuous attributes have been discretized through an entropy-MDL discretization. Gain Ratio was chosen as attribute selection criterion for CT, exhaustive search for optimal split was set as binarization method; for the pre-pruning the minimum number of instances in leaves was set to 10; recursively merge leaves with same majority and pruning with m-estimate (m=2) were used for post-pruning.

A 10-fold cross validation was adopted to compare the performances of the regression and the two classifiers. In a 10-fold cross validation the dataset is divided in ten subsets of the same dimension through a stratified sampling (in this way the same class distribution is maintained in each subset). At the first iteration, nine folds are used to train the classifiers and one is used as test set; in the following iterations, the folds are interchanged. A set of scores represents the goodness of the classifier: accuracy, AUC of the Receiver Operating Characteristic (ROC) curve, sensitivity and specificity. Two-way analysis of variance (ANOVA) was used to check if there were significant differences among the accuracies calculated with the ten folds of the tested classifiers and the majority classifier, with the significance limit (α) set to 0.01. Then, if a significant difference was detected via two-way ANOVA, post-hoc analysis was conducted using the Tukey's test ($\alpha = 0.01$), to perform comparisons between classifiers. The proportion of false positive (FP) and false negative (FN) were calculated and compared to the ones obtained with the multiple linear regression, using a paired t-test to check if

they were significantly different ($\alpha = 0.01$). A validation analysis was also performed: the proportions of FP and FN obtained on a test set of five drugs not included in the original list of 73 drugs were used to compare the best classifier with the regression model. Statistical analyses were performed in R v.3.0.3 using anova, t.test and glht (available in the multcomp package) R functions to carry out the tests above.

5.4. **Results**

5.4.1. Regression Analysis

Among all the PK parameters, only Ae and ppb showed a correlation with the AUC ratios. Univariate regressions with Ae as descriptor for the three levels of renal impairment are shown in Fig. 5.1, while the univariate regressions with plasma protein binding (ppb) as regressor are reported in Fig. 5.2.

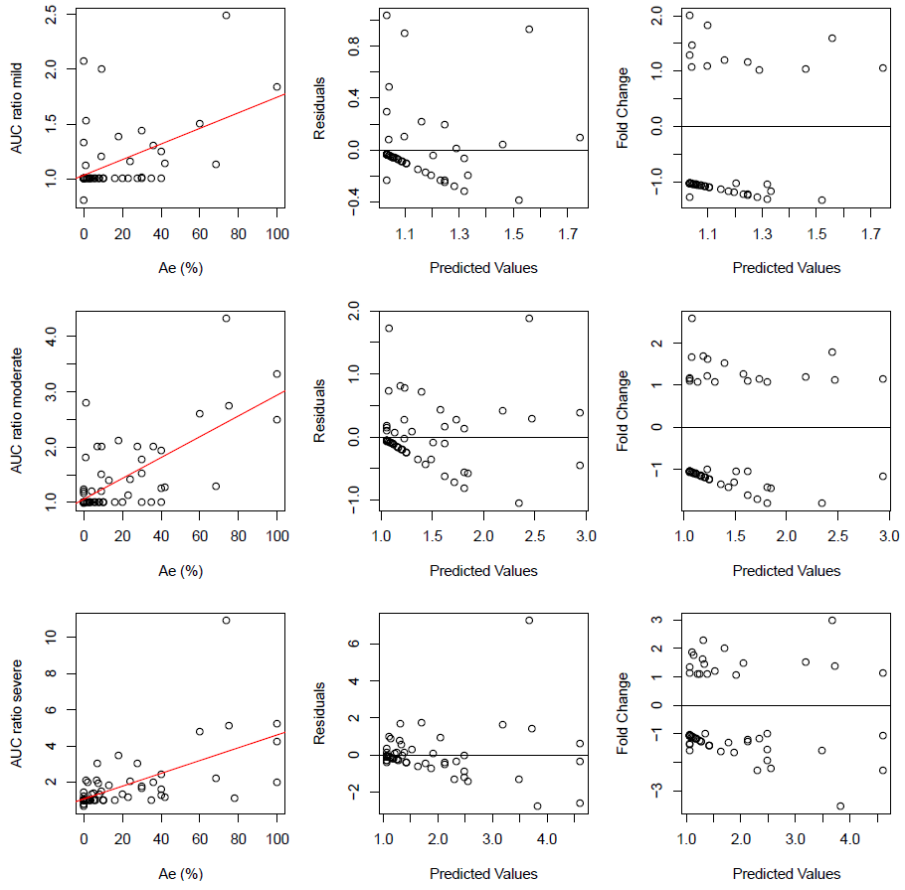

Figure 5.1. Univariate regression analysis of the renally impaired to normal subject AUC ratio with the amount excreted in urine (left) and goodness of fit plots (residuals, center; fold error, right); from top to bottom: mild/normal, moderate/normal and severe/normal AUC ratio.

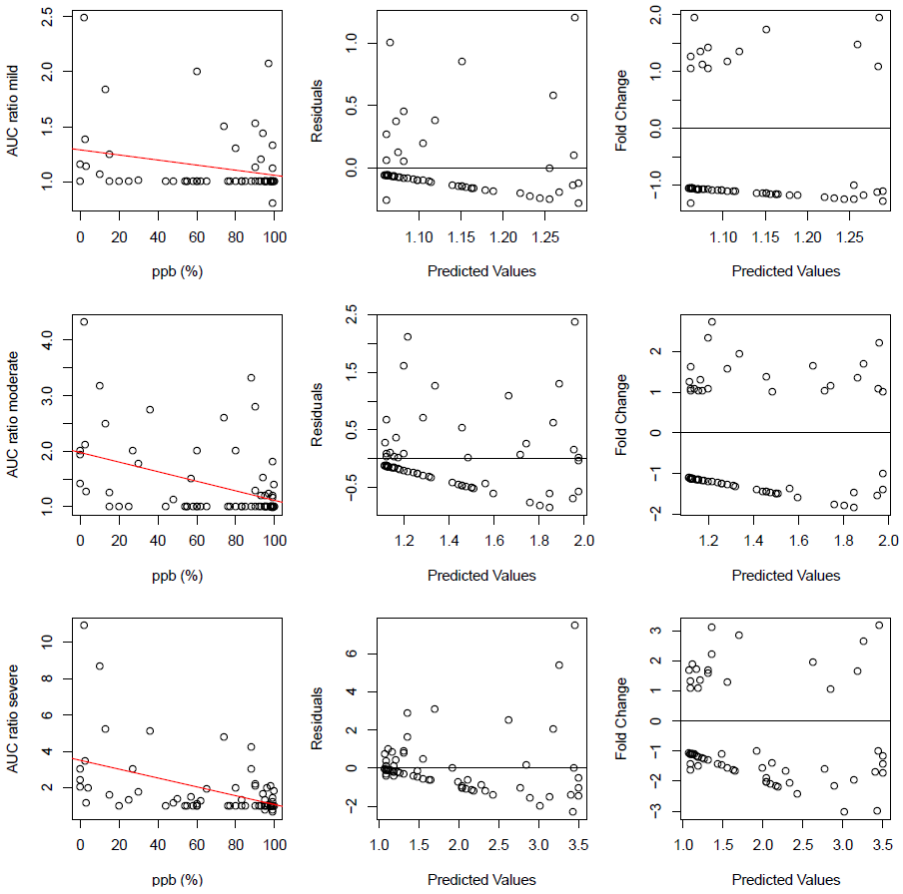

Figure 5.2. Univariate regression analysis of the renally impaired to normal subject AUC ratio with the protein binding (left) and goodness of fit plots (residuals, center; fold error, right); from top to bottom: mild/normal, moderate/normal and severe/normal AUC ratio.

The AUC ratio tends to increase with an increase of Ae, and to decrease with an increase of ppb (and in turn, a decrease of fraction unbound to plasma protein), particularly in case of moderate and severe renal impairment. However, these two PK parameters alone were not able to predict accurately the expected changes in the AUC ratios.

Assuming that the CL_R can be approximated by the filtration clearance ($CL_R \sim f_u \cdot GFR$, with fu=1-ppb) and $CL_R = Ae \cdot CL$ (where Ae is expressed as fraction of administered dose), AUC can be expressed as:

$$AUC = \frac{F \cdot Dose}{CL} = \frac{Dose \cdot F \cdot Ae}{f_u \cdot GFR}.$$

The potential correlation between the AUC ratios and the ratio $F \cdot Ae/f_u$ was therefore explored and the corresponding regressions are reported in Fig. 5.3.

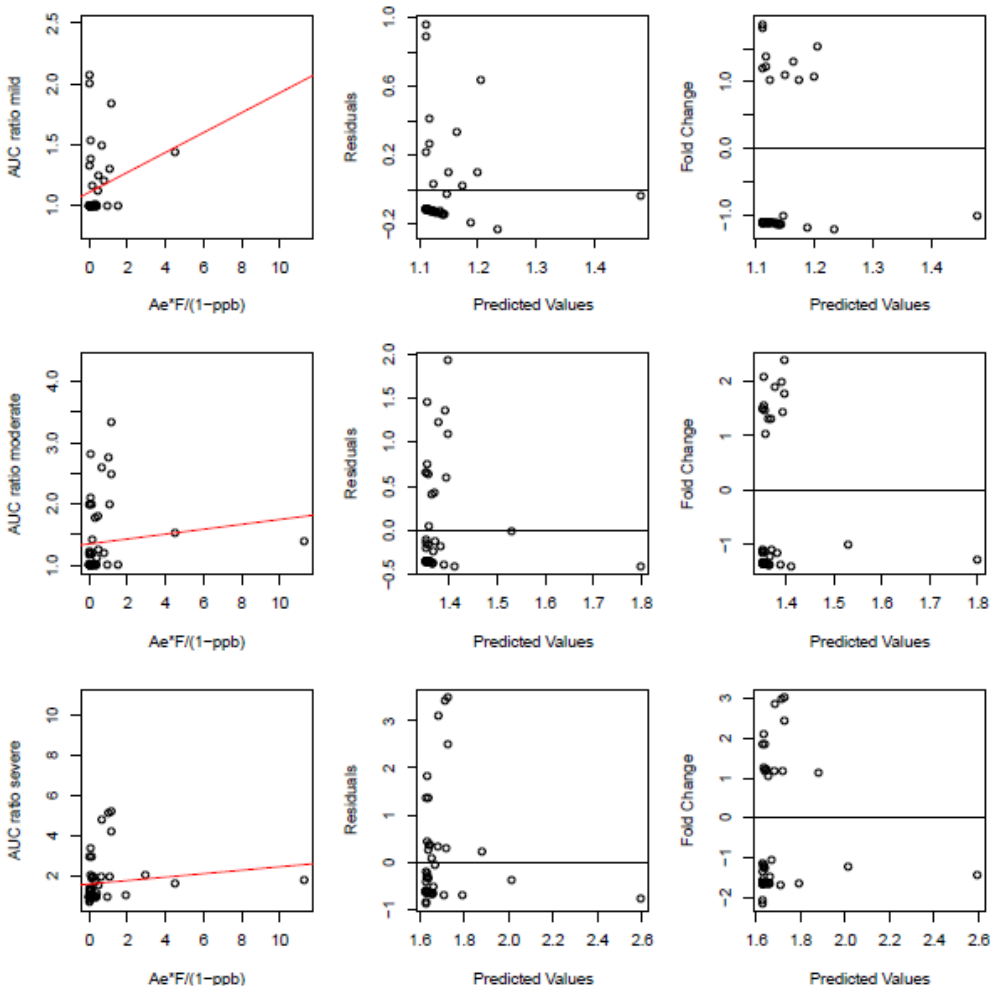

Figure 5.3. Univariate regression analysis of the renally impaired to normal subject AUC ratio with the amount excreted to fraction unbound ratio (left) and goodness of fit plots (residuals, center; fold error, right); from top to bottom: mild/normal, moderate/normal and severe/normal AUC ratio.

According to this outcome, a combination of backward elimination and forward selection was performed for each level of renal impairment using as initial possible regressors only Ae, ppb, and EH. Other regressors, such as CL, CL/F and F, were not considered due to the large number of missing values and the estimated EH summarizes well the information contained in the available CL and CL/F data. This procedure confirmed the results of the previous analysis. Indeed, for the mild and moderate levels, only Ae was selected, instead for the most severe level of renal impairment, both Ae and ppb were chosen. This approach was able to provide a more consistent trend between the change in AUC and the PK parameters as reported in Fig. 5.4 where can be observed that all the fold-changes remain inside the interval of 2-fold.

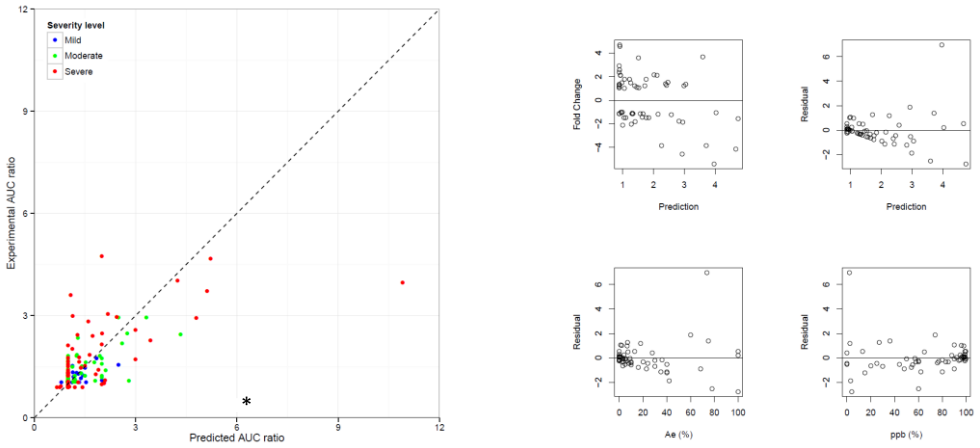

Figure 5.4. Multivariate regression analysis. Left: observed and predicted data; right: goodness of fit.

To test the predictability of this approach, the AUC ratios for four compounds in subjects with renal impairment, which were not included in the original dataset, have been estimated: the comparison between the observed and predicted AUC ratios are shown in Table 5.3. The MLR approach was able to predict the effect of renal disease on the PK of these compounds with reasonable accuracy. To be noticed that, for drugs such as exemestane, that are cleared mainly by metabolism and are highly bound to plasma proteins, the model underestimates the AUC ratio and, as consequence, the risk.

Table 5.3. Predictions obtained with the following regression models: $y1 = 1.034004 + 0.007116 \cdot Ae$, $y2 = 1.058059 + 0.018823 \cdot Ae$ and $y3 = 1.736347 + 0.030453 \cdot Ae - 0.008548 \cdot ppb$, with y1, y2, y3 representing the AUC ratios relative to mild, moderate and severe renal impairment, respectively. Obs: observed; Pred: predicted.

Generic name	Ae (%)	ppb (%)	AUC ratio					
			mild/normal		moderate/normal		severe/normal	
			obs	pred	obs	pred	obs	predcted
Rivaroxaban [1]	36	95	1.44	1.29	1.52	1.73	1.64	2.02
Lenalidomide [1,23]	82	30	1.30	1.61	3.20	2.60	3.90	3.98
Dabigatran etexilate mesylate [1,24]	80	35	1.50	1.05	3.20	2.56	6.30	3.87
Capecitabine [1,25]	3	60	1.00	1.05	1.13	1.11	1.18	1.31
Exemestane [1,26]	1	90	-	-	2.70	1.11	1.89	0.997

Since in the dataset there were some missing data, a multivariate NIPALS approach was tested, which is particularly indicated in this case. This technique is a multivariate regression where the variables are projected on principal components (PCs), which are linear combinations of the variables.

NIPALS is an algorithm to impute the missing data in the original variables. The aim of this approach is to reduce the dimensionality of the problem and to avoid collinearity between the original set of variables. The outcome of PLS-NIPALS can be summarized into the circle of correlations (Fig. 5.5). It shows the correlation of the original variables with the two axes that represent the first two principal components (PCs) that are the most informative ones. In this case, the first two PCs are mostly correlated with Ae and ppb and this is a confirmation of the importance of these two regressors. From the circle of correlations is evident that Ae is a strong determinant of the presence of large AUC ratio, in fact, Ae is related to the degree of severity of the renal impairment which affects the excretion of drug extracted mainly through the renal way. CL, EH and CL/F are close to each other, suggesting some interplay between them. The regressor ppb, located in the opposite quadrant, is a strong determinant of the absence of large AUC ratios, in fact, drug avidly bound to plasma protein are usually not extracted through the renal way to a large extent.

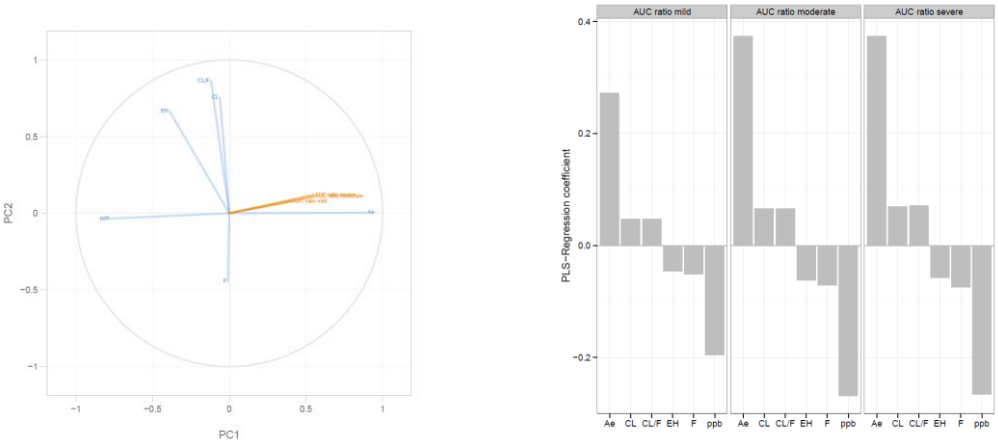

Figure 5.5. NIPALS. Left: circle of correlation; right: goodness of fit; right: histogram of the regression coefficients.

5.4.2. Classification Problem

To perform the second type of analysis the three dependent variables were firstly transformed from continuous to categorical in three class of risk: no risk, low, medium-high risk. The moderate and severe classes of risk were merged together because of the presence of a small number of drugs in these classes, which could worsen the accuracy of the classificators. The missing values were imputed with NIPALS method otherwise all the rows with at least one missing value would have been discarded, resulting in a massive reduction of the dataset. The classification methods selected for this analysis were: Naïve Bayes (NB) and Classification Tree (CT). Results are showed only for the most severe level of renal impairment. As it can be seen in Table

5.4, NB showed less accuracy compared to the majority classifier, while the accuracies of the CT in each of the ten folds were not significantly different according to a paired t-test of difference with a significance limit set to α=0.01.

Table 5.4. Results in terms of accuracy, AUC of the ROC curve, sensitivity and specificity relative to the classification problem with a three-levels class and to the most severe renal impairment. A: Values designated by the same letter are not significantly different by paired t-test (p-value=0.04127).

Method	Accuracy	AUC	Sensitivity	Specificity
Majority	0.49-0.50[A]	0.5	1	0
	0.49-0.50	0.5-0.5	1-1	0-0
	0.49 (0.01)	0.50 (0)	1 (0)	0 (0)
Naïve Bayes	0.48-0.53	0.62-0.68	0.61-0.68	0.52-0.58
	0.43-0.55	0.59-0.75	0.55-0.72	0.48-0.62
	0.50 (0.04)	0.65 (0.04)	0.65 (0.06)	0.55 (0.04)
Classification	0.50-0.58[A]	0.62-0.70	0.64-0.72	0.58-0.74
Tree	0.39-0.60	0.54-0.74	0.59-0.79	0.52-0.85
	0.54 (0.06)	0.66 (0.06)	0.68 (0.06)	0.66 (0.13)

These low performances could be due to a disproportion of examples in the three classes; to overcome this, a binary-class classification problem was also tested. The AUC ratios were discretized in a binary class: 0 for those drugs with AUC ratio less than 1.25, and 1 for those drugs with AUC ratio greater than 1.25. Results are showed in Table 5.5.

Table 5.5. Results in terms of accuracy, AUC of the ROC curve, sensitivity and specificity relative to the classification problem with a binary-levels class (threshold 1.25) and to the most severe renal impairment. A, B, C: Values designated by the same letter are significantly different by post-hoc analysis using Tukey's test (p-value <0.001).

Method	Accuracy	AUC	Sensitivity	Specificity
Majority	0.46-0.49[B,C]	0.5	0.18-0.48	0.43-0.77
	0.46-0.51	0.5-0.5	0-0.64	0.27-1
	0.47 (0.02)	0.5 (0)	0.33 (0.24)	0.60 (0.27)
Naïve Bayes	0.64-0.67[A,B]	0.68-0.74	0.66-0.70	0.61-0.65
	0.59-0.69	0.66-0.79	0.62-0.72	0.58-0.67
	0.65 (0.03)	0.71 (0.05)	0.68 (0.03)	0.63 (0.03)
Classification	0.67-0.75[A,C]	0.68-0.77	0.65-0.74	0.68-0.78
Tree	0.58-0.78	0.55-0.80	0.55-0.78	0.55-0.79
	0.71 (0.06)	0.73 (0.07)	0.69 (0.07)	0.73 (0.08)

In this case, both the classifiers were significantly different (p-value<0.001) compared to the majority classifier according to a Tukey's test. CT proved to be the best classifier in terms of accuracy since its accuracy was significantly different (p-value<0.001) compared to NB.

The same analysis was repeated with a threshold of 2 rather than 1.25 to test if the results were not affected by the proportion of cases in the two classes. The results in terms of accuracy, AUC, sensitivity and specificity for this binary-class problem obtained with a threshold of 2 are shown in Table 5.6.

Table 5.6. Results in terms of accuracy, AUC of the ROC curve, sensitivity and specificity relative to the classification problem with a binary-levels class (threshold 2) and to the most severe renal impairment. A: Values designated by the same letter are significantly different by a paired t-test (p-value<0.001).

Method	Accuracy	AUC	Sensitivity	Specificity
Majority	0.71[A]	0.5	1	0
	0.71-0.72	0.5-0.5	1-1	0-0
	0.71 (0)	0.5 (0)	1 (0)	0 (0)
Naïve Bayes	0.76-0.79[A]	0.80-0.83	0.85-0.88	0.51-0.60
	0.75-0.81	0.78-0.86	0.83-0.91	0.47-0.68
	0.78 (0.02)	0.81 (0.03)	0.87 (0.02)	0.56 (0.08)
Classification	0.64-0.70	0.55-0.64	0.79-0.86	0.24-0.34
Tree	0.59-0.74	0.47-0.70	0.72-0.87	0.21-0.42
	0.67 (0.05)	0.59 (0.08)	0.82 (0.05)	0.29 (0.08)

NB proved to be the only classifier better than majority; for this reason, it was considered the best classifier for this analysis since the performances of CT showed to be dependent on the chosen threshold. The corresponding percentages of FP and FN were calculated, and then compared to the ones of the regression model as reported in Table 5.7.

To test the predictability of this approach, the previously reported AUC ratios of the five compounds, which were not included in the original dataset, were calculated using the multiple regression. For the most severe level of renal impairment, the predictions were discretized using thresholds 1.25 and 2, and the proportions of FP and FN were compared with the same proportions obtained with NB (Table 5.8). For this analysis, the classifier was firstly trained on all the 73 drugs and then tested only on the new five drugs.

Table 5.7. Proportions of FP and FN calculated as $\left(\frac{FP}{FP+TN}\right) * 100$ and $\left(\frac{FN}{TP+FN}\right) * 100$ respectively, for multiple regression and NB for classification problems with thresholds 1.25 and 2. A, B, C, D: Values designated by the same letter are not significantly different by a paired t-test.

Method	**FP (%)**		**FN (%)**	
Threshold	1.25	2	1.25	2
Regression	31.03-43.97[A] 0-100 37.5 (33.03)	12.35-17.98[B] 0-40 15.17 (14.35)	12.51-19.82[C] 0-50 16.17 (18.66)	22.04-39.07[D] 0-100 30.56 (39.09)
Naïve Bayes	6.98-48.02[A] 0-100 27.5 (33.11)	-1.15-8.48[B] 0-20 3.67 (7.77)	4.74-30.26[C] 0-50 17.5 (20.58)	20.39-66.28[D] 0-100 43.33 (37.02)

Table 5.8. Proportions of FP and FN calculated as $\frac{FP}{FP+TN}$ and $\frac{FN}{TP+FN}$ respectively, using the validation dataset for multiple regression and NB for classification problems with thresholds 1.25 and 2; the list of drugs resulted as FP or FN are reported below.

Method	**FP/(FP+TN)**		**FN/(FN+TP)**	
Threshold	1.25	2	1.25	2
Regression	1/1 Capecitabine	1/3 Rivaroxaban	1/4 Exemestane	0/2 /
Naïve Bayes	1/1 Capecitabine	0/3 /	1/4 Exemestane	0/2 /

5.5. **Conclusions**

The results of this assessment, aiming to the quantitative prediction of the increase of the AUC in subjects with renal impairment compared to subjects with normal renal function showed that AUC ratio was directly correlated with the amount excreted unchanged in urine and inversely related to the protein binding (which is a factor that again limits the urinary excretion). This is also expected based on physiological considerations. Anyway the predictions could not be done with an appropriate level of granularity and precision. The use of more sophisticated statistical analysis seems not to help

in providing more accurate predictions; in fact, there are compounds for which also the classifier is not providing accurate results. In particular, it appears that the compounds for which renal excretion is low and protein binding is high, a small change in AUC (inhibited vs un-inhibited) is consistently predicted, whilst there are compounds, such as exemestane, in which a relatively large AUC change was observed, probably as a results of the uremic toxins inhibiting the metabolic pathway of this compound. There were recent reports [Yoshida et al., 2014] suggesting that CYP2D6 activity, but not CYP3A activity, decreased in subjects with CKD. The absence of a lack of effect of CKD on CYP2C0 and CYP3A4 activity was confirmed in another paper [Joy et al., 2014], where the potential inhibitory effect of uremic toxins was however indicated for transporters. It is interesting to notice that exemestane is metabolized via CYP3A and direct conjugation pathways, indicating that, still, there is not a full understanding of the determinants related to the involvement of uremic toxins in case of compounds that are eliminate in urine for a minor extent. Further in vivo and in vitro studies are therefore warranted to fully understand the physiological bases of the alterations of ADME characteristics in patients with renal impairment.

Another aspect that should be carefully considered are the limitations related to the experimental studies and the available databases. Regarding the first aspect, it should be considered that, in the vast majority of cases, an intravenous assessment of oral drugs is lacking, which may help disentangling the effect of renal impairment on the various ADME characteristics. Concerning the availability of accurate databases, whilst this was a limitation in the past, tools are starting to become available to the scientists to test their approaches and hypotheses [Yeung et al., 2015].

In conclusion, the predictive assessments of PK alterations in subjects with renal impairment are still limited by a variety of factors (incomplete characterization of the compound characteristics, constraints in the conduct of clinical studies, lack of a fully mechanistic understanding). In the absence of additional information that may contribute to fix these aspects, more sophisticated statistical analysis (especially those able to deal with missing data) may provide useful guidance for a better understanding of the problem, setting up meaningful hypotheses, and helping the design of the clinical studies for assessing these effects.

Table 5.9. Characteristics of the analysed compounds

Compound	CL/F	F	CL	Ae	ppb	EH	AUC ratio AUC ratio mild	AUC ratio moderate	AUC ratio severe	Re
Abiraterone Acetate	1550	5		0	99	0.94	1	1	1	[1]
Alvimopan		6	24.12	35	80	0.16	1	1	1	[1]
Anidulafungin			0.87	0	99	0.01	0.8	0.98	0.67	[2]
Argatroban			21.7	16	54	0.18	1	1	1	[1]
Aripiprazole	3.6	87		0	99	0.03	1.33	1.16	0.76	[3]
Asenapine Maleate	146.2	35			95	0.59	1	1	1	[1]
Atomoxetine Hcl	26.04	63		3	98	0.20	1	1	1	[1]
Axitinib	38	58		0	99	0.28	1	1	1	[1]
Bortezomib			23		83	0.23	1	1	1	[1]
Caspofungin Acetate			0.72	1.4	96	0.01	1	1	1	[1]
Cefditoren		14	5	100	88	0.00		3.32	4.24	[1]
Cinacalcet	273	27.7	75.6		95	0.76	1	1	1	[1]
Ciprofloxacin Hcl	55.5	70		30	30	0.25	1.01	1.78	1.73	[4]
Conivaptan		44	15	1	99	0.15	1.12	1.8		[5]
Didanosine		42	21	18	2.5	0.17	1.38	2.11	3.44	[1]
Dronedarone		15	140	0	98	1.00	1	1	1	[1]
Eletriptan Hydrobromide		50	28	10	85	0.25	1	1	1	[1]
Entacapone	118.3	36	43.26	0.2	98	0.43	1	1	1	[1]
Entecavir	28.2	100	28.2	100	13	0.00	1.84	2.49	5.22	[1]
Epirubicin Hydrochloride Injection			65	6	77	0.61	1	1	1	[1]
Eplerenone Tablets	10	69		5	50	0.09			1.38	[1]
Eribulin Mesylate			3.22	9	57	0.03		1.5	1.5	[1]
Escitalopram Oxalate	36	80		8	55	0.24	1	1		[1]
Eszopiclone	15.5	77.5		10	55	0.12	1	1	1	[1]
Ezogabine		60	35	36	80	0.22	1.3	2	2	[1]
Famciclovir		77			10	0.23	1.07	3.18	8.66	[6]
Fingolimod		93	6.3	0	99	0.06			1.43	[1]
Fluvastatin Sodium		25	67.9	0	99	0.75		1.2	1.2	[1]
Hydromorphone Hydrochloride Extended Release	484	24		7	27	0.77		2	3	[1]
Icatibant			17.5	5	44	0.17	1	1	1	[1]
Lacosamide		100	2.80	40	15	0.02	1.25	1.25	1.6	[1]
Lamivudine	30.3	85	20.79	75	36	0.05		2.75	5.12	[7]
Lamotrigine Chewable Dispersible Tablets	2.2	98		78	60	0.00			1.08	[8]
Lansoprazole	16.8	85		0	97	0.14	2.07	1.24	1.04	[9]
Letrozole	2.21	100		3.6	60	0.02	1	1	1	[1]

Meropenem			15.4	73.7012987	2	0.04	2.49	4.33	10.91	[10]
Miglitol		59	7.21	100	4	0.00			2	[1]
Montelukast Sodium		64	2.73	0	99	0.03	1	1	1	[1]
Moxifloxacin Hydrochloride	14.9	89	13.261	22.8489555 8	48	0.10	1	1.13	1.13	[1]
Olmesartan Medoxomil		26	1.31	13	99.7	0.01		1.39	1.82	[1]
Paliperidone	272	28	27	60	74	0.11	1.5	2.6	4.8	[1]
Palonosetron Hydrochloride			11.2	40	62	0.07	1	1	1.28	[1]
Pantoprazole Sodium Delayed Release Tablets		77	7	0	98	0.07	1	1	1	[1]
Paricalcitol		0.79	2.7	5.7	99.8	0.03	1	1	1	[1]
Perindopril Erbumine		0.80	31.4	9.24	60	0.29	2	2		[1]
Quetiapine Fumarate		9	79.8	20	83	0.64	1	1	1.33	[1]
Ribavirin		51.8	25.04	27.7	0	0.18	1	2	3	[1]
Riluzole		64	47.64	0	96	0.48				
Risperidone		66	43	1.2	90	0.42	1.53	2.8	2.07	[11]
Rivaroxaban	10	90		30	94	0.06	1.44	1.52	1.64	[12]
Roflumilast	9.6	80		0	95	0.09			0.79	[1]
Romidepsin			15.30		93	0.15	1	1	1	[1]
Rosuvastatin Calcium		20	44.1		88	0.44	1	1	3	[1]
Saxagliptin	73.08	67		24	0	0.32	1.16	1.41	2.01	[13]
Sildenafil Citrate		41		2	96	0.60	1	1	2	[1]
Solifenacin Succinate		88	10	6.7	98	0.09			2.1	[1]
Tapentadol		32	91.86	3	20	0.70	1	1	1	[1]
Telavancin			0.917	68.4	90	0.01	1.13	1.29	2.18	[1]
Telbivudine	20.8		18.1	42	3	0.10	1.14	1.26	1.14	[1]
Telithromycin	64	57	58.80	7.410	65	0.54	1	1	1.9	[1]
Temozolomide		100	11.76		15	0.12	1	1		[1]
Teriflunomide		100	0.0304	0	99	0.00	1	1	1	[1]
Tolcapone		65	7	0	99.9	0.15	1	1		[1]
Triptorelin Pamoate			12.6	40	0	0.08		1.94	2.44	[1]
Trovafloxacin		88	5.978	10	76	0.05	1	1	1	[1]
Valproic Acid		100	0.462	3	90	0.00	1	1	1	[1]
Valsartan		25	2.00	30	95	0.01	1	1		[1]
Vardenafil		15	56	4	95	0.54	1	1.2	1.3	[1]
Vilazodone Hydrochloride	34	72		1	98	0.25	1	1	1	[1]
Voriconazole		96	15.96	2	58	0.16	1	1	1	[1]
Zaleplon	266	30	70	0	60	0.70	1	1	1	[1]
Zolmitriptan	141.24294	40		8	25	0.54	1	1	1.33	[1]
Zolpidem Tartrate		70	18.2	0	92	0.18	1	1	1	[1]

5.6. **References**

Abdi H. Partial least squares regression and projection on latent structure regression (PLS Regression). Wiley Interdisciplinary Reviews: Computational Statistics. 2010, 2:97-106.

Bastien P, Tenenhaus M. PLS regression and Multiple Imputations. In Proceedings of the PLS03 international Symposium, Vilares M. et al. editors. CISIA, Paris, pages 497-498, 2003.

Boike SC, Pue MA, Freed MI, Audet PR, Fairless A, Ilson BE, Zariffa N, Jorkasky DK. Pharmacokinetics of famciclovir in subjects with varying degrees of renal impairment. Clinical Pharmacology & Therapeutics. 1994, 55:418-26.

Boulton D, Li L, Frevert EU, Tang A, Castaneda L, Vachharajani NN, Kornhauser DM, Patel CG. Influence of renal or hepatic impairment on the pharmacokinetics of saxagliptin. Clinical pharmacokin 2011, 50: 253-265.

Clark P, Niblett T. The CN2 Induction Algorithm. J Machine Learning 1989, 3:261-283.

Christensson BA, Nilsson-Ehle I, Hutchison M, Haworth SJ, Oqvist B, Norrby SR. Pharmacokinetics of meropenem in subjects with various degrees of renal impairment. Antimicrobial agents and chemotherapy. 1992, 36:1532-7.

Coresh J, Selvin E, Stevens LA, et al.; Prevalence of chronic kidney disease in the United States. JAMA 2007, 298:2038–2047.

Delhotal-Landes B, Flouvat B, Duchier J, Molinie P, Dellatolas F, Lemaire M. Pharmacokinetics of lansoprazole in patients with renal or liver disease of varying severity. European journal of clinical pharmacology. 1993, 45:367-71.

Demsar J, Curk T, Erjavec A, Gorup et al. Orange: Data Mining Toolbox in Python. Journal of Machine Learning Research 2013, 14:2349-2353.

Demsar J, Curk T, Erjavec A, Gorup C, Hocevar T, Milutinovic M, Mozina M, Polajnar M, Toplak M, Staric A, Stajdohar M, Umek L, Zagar L, Zbontar J, Zitnik M, Zupan B. Orange: Data Mining Toolbox in Python. J Mach Learn Res. 2013;14:2349-2353.

Drusano GL, Weir M, Forrest A, Plaisance K, Emm T, Standiford HC. Pharmacokinetics of intravenously administered ciprofloxacin in patients with various degrees of renal function. Antimicrob Agents Chemother 1987, 31: 860-864.

Dowell JA, Stogniew M, Krause D, Damle B. Anidulafungin does not require dosage adjustment in subjects with varying degrees of hepatic or renal impairment. J Clin Pharmacol 2007, 47: 461-470.

Fung G. A Comprehensive Overview of Basic Clustering Algorithms, 2001. http://web.iiit.ac.in/~abhinav/PR/clustering.pdf , accessed Aug 1 2016.

Gaston Sanchez (2012). plsdepot: Partial Least Squares (PLS) Data Analysis Methods. R package version 0.1.17. http://CRAN.R-project.org/package=plsdepot.

Germani, M., Crivori, P., Rocchetti, M., Burton, P.S., Wilson, A.G.E., Smith, M.E., Poggesi, I., 2007. Evaluation of a basic physiologically based pharmacokinetic model for simulating the first-time-in-animal study. Eur. J. Pharm. Sci. 31, 190–201.

Jain AK, Murty MN, Flynn PJ. Data Clustering: A Review. ACM Computing Surveys (CSUR) Surveys 1999, 31: 264-323.

Johnson MA, Verpooten GA, Daniel MJ, Plumb R, Moss J, Van Caesbroeck D, De Broe ME. Single dose pharmacokinetics of lamivudine in subjects with impaired renal function and the effect of haemodialysis. British journal of clinical pharmacology. 1998, 46:21-7.

Joy MS, Frye RF, Nolin TD, Roberts BV, La MK, Wang J, Brouwer KL, Dooley MA, Falk RJ. In vivo alterations in drug metabolism and transport pathways in patients with chronic kidney diseases. Pharmacotherapy: The Journal of Human Pharmacology and Drug Therapy. 2014, 34:114-22.

Kliger AS, Foley RN, Goldfarb DS, Goldstein SL, Johansen K, Singh A, Szczech L. KDOQI US commentary on the 2012 KDIGO clinical practice guideline for anemia in CKD. American Journal of Kidney Diseases. 2013 62:849-59.

Kubitza D, Becka M, Mueck W, Halabi A, Maatouk H, Klause N, Lufft V, Wand DD, Philipp T, Bruck H. Effects of renal impairment on the pharmacokinetics, pharmacodynamics and safety of rivaroxaban, an oral, direct Factor Xa inhibitor. British journal of clinical pharmacology 2010, 70: 703-712.

Levey AS, Eckardt KU, Tsukamoto Y, Levin A, Coresh J, Rossert J, Zeeuw DD, Hostetter TH, Lameire N, Eknoyan G. Definition and classification of chronic kidney disease: a position statement from Kidney Disease: Improving Global Outcomes (KDIGO). Kidney international 2005, 67:2089-100.

Mallikaarjun S, Shoaf SE, Boulton DW, Bramer SL. Effects of hepatic or renal impairment on the pharmacokinetics of aripiprazole. Clin Pharmacokinet 2008, 47: 533-542.

Mueller BA, Scarim SK, Macias WL. Comparison of imipenem pharmacokinetics in patients with acute or chronic renal failure treated with continuous hemofiltration. Am J Kidney Diseases. 1993, 21:172-9.

Nu Phyu T. Survey of classification techniques in data mining. In Proceedings of the International MultiConference of Engineers and Computer Scientists. 2009, 1:18 – 20.

Preda C, Saporta G, Hedi M, Mbarek BH. The NIPALS algorithm for missing functional data, Rev Roumaine Math Pures Appl 2010,55:315-26.

R Core Team. R: A language and environment for statistical computing. R Foundation for Statistical Computing, Vienna, Austria. 2014. URL http://www.R-project.org/.

Roy MJ, Erdman KA, Abeyratne AT, Plumb LC, Lasseter K, Riff DS, Keirns JJ. Pharmacokinetics of intravenous conivaptan in subjects with hepatic or renal impairment. Clinical pharmacokinetics. 2013, 52: 385-95.

Snoeck E, Van Peer A, Mannens G, Woestenborghs R, Heykants J, Sack M, Horton M, Meibach R. Influence of age, renal and liver impairment on the pharmacokinetics of risperidone in man. Psychopharmacology. 1995, 122:223-9.

Velenosi TJ, Urquhart BL. Pharmacokinetic considerations in chronic kidney disease and patients requiring dialysis. Expert opinion on drug metabolism & toxicology. 2014, 10:1131-43.

Verbeeck RK, Musuamba FT. Pharmacokinetics and dosage adjustment in patients with renal dysfunctionEur J Clin Pharmacol 2009, 65:757–773

Wootton R, Soul-Lawton J, Rolan PE, Sheung CT, Cooper JD, Posner J. Comparison of the pharmacokinetics of lamotrigine in patients with chronic renal failure and healthy volunteers. British journal of clinical pharmacology. 1997, 43:23-7.

Yeo KR, Aarabi M, Jamei M, Rostami-Hodjegan A. Modeling and predicting drug pharmacokinetics in patients with renal impairment. Expert Rev Clin Pharmacol. 2014, 4:261–274.

Yeung CK, Yoshida K, Kusama M, Zhang H, Ragueneau-Majlessi I, Argon S, Li L, Chang P, Le CD, Zhao P, Zhang L. Organ impairment—drug–drug interaction database: a tool for evaluating the impact of renal or hepatic impairment and pharmacologic inhibition on the systemic exposure of drugs. CPT: Pharmacometrics & Systems Pharmacology. 2015, 4:489-94.

Yoshida K, Sun B, Zhang L, Zhao P, Abernethy DR, Nolin TD, Rostami-Hodjegan A, Zineh I, Huang SM. Systematic and quantitative assessment of the effect of chronic kidney disease on CYP2D6 and CYP3A4/5. Clinical Pharmacology & Therapeutics. 2016 Mar 1.

Chapter 6

Modelling DDI Combining Top-down/Bottom-up Approaches[5]

As indicated in the previous sections, the predictions of DDIs is one of the most striking successes of the PBPK modeling approaches. In this Chapter it is shown how, including a minimal physiological interpretation of the PK parameters obtained from an empirical compartmental model, good predictions can be obtained, even in absence of a full PBPK modeling approach.

6.1. Abstract

Physiology-based pharmacokinetic (PBPK) models are nowadays popular modeling approaches to provide verbiage in the label related to potential dose modifications to be adopted when drugs are given with other medications based on simulations, in absence of actual clinical studies. PBPK can predict the systemic exposure in subjects receiving the drug with the concomitant medications compared to that typically observed in the patient population in the absence of comedications, thereby providing suggestions of the dose level that, in these conditions, normalize the effect of drug-drug interactions (DDI). A drug can be victim of DDI if a coadministered medication is inhibiting or inducing the elimination of the first drug. Inhibition will cause an increased exposure of the drug, which can

[5] This chapter is essentially based on the poster communication: Rossenu S, Del Bene F, Vermeulen A, Poggesi I. Modelling potential drug-drug interaction risks with a combined top-down/bottom-up approach. PAGE 24 (2015) Abstr 3560 [www.page-meeting.org/?abstract=3560].

lead to safety issues. *Vice versa*, induction will cause a decreased exposure to the drug, which can lead to lack of efficacy.

This report implements an approach, that, mixing physiological concepts (bottom-up) with data-driven population pharmacokinetic modeling (top-down) can be used to predict the extent of the DDI caused by the effect of known cytochrome P450 inhibitors or inducers on the pharmacokinetics of a new molecular entity. The physiology-based inhibition concept, is essentially based on the knowledge of the fraction of the dose eliminated via a particular metabolic pathway (that can be established *via* in vitro assessments or based on a clinical study) and on the inhibitory/inducing (time-averaged) potency of a known DDI perpetrator, that is reported in the literature. This approach is applied here to the interaction between bedaquiline, a drug with very long half-life that is eliminated via Cytochrome P450 3A (CYP3A) metabolism, and a variety of CYP3A inhibitors and inducers.

The combination of the physiology-based approach with the population model available to describe the PK of bedaquiline allows to simulate the full extent of DDI, even in this case, in which the PK characteristics of the substrate make difficult or impossible to assess it experimentally in a clinical trial.

6.2. **Introduction**

It is often logistically difficult to design an appropriate DDI study to define a clinically meaningful extent of pharmacokinetic interaction. In these instances, we can resort to modeling [Nucci et al., 2008]. Bottom-up approaches such as physiologically-based pharmacokinetic models (PBPK) is currently used, in many cases, to provide verbiage in the labels of new drugs for describing the effects of DDI perpetrators on new molecular entities and suggesting modifications of the dose levels to be adopted in case they are associated with known metabolism inhibitors or inducers (see for instance the ibrutinib label https://www.janssenmd.com/pdf/imbruvica/PI-Imbruvica.pdf, accessed August 1, 2016).

In this respect, a number of approaches, based on the *in vitro* inhibition constants of DDI perpetrators have been proposed [Brown et al., 2006, Fahmi et al, 2009, Houston and Galetin, 2008]. The method recently proposed by a Japanese group [Ohno et al., 2007; Ohno et al., 2008] was instead based on the CYP3A inhibitory and induction potency that DDI perpetrators demonstrated in *in vivo* studies. Based on some basic physiologically-based pharmacokinetic considerations involving metabolic clearance, it is possible to derive that the ratio of the inhibited to uninhibited area under the plasma concentration-time curve of a CYP3A substrate can be derived using two parameters: the fractional CYP3A metabolic clearance (fCYP3A) and the in vivo potency of the inhibitor (IRCYP3A), integrated over time for the given dose of inhibitor. Ohno and coworkers examined the outcome of numerous DDI studies involving different substrates and inhibitors of different

potency, so that they were able to build up Tables for standard CYP3A substrates and inhibitors. Therefore, the method can be extended to new substrates (for which a fCYP3A can be measured or assumed), so that the extent of DDI can be predicted for all the inhibitors for which IRCYP3A is available. Viceversa, based on the outcome of a first DDI study for a compound behaving as CYP3A inhibitor, the effect of the same inhibitor can be predicted for all relevant substrates. The method demonstrated very good accuracy in the prediction of DDI for CYP3A substrates given both orally and intravenously with CYP3A inhibitors. An analogous approach was proposed in case of CYP3A inducers [Ohno et al., 2008].

Bedaquiline (TMC207) is a diarylquinoline antimycobacterial drug indicated as part of combination therapy against multi-drug resistant tuberculosis [Mahajan, 2013; see also the package insert: http://www.accessdata.fda.gov/drugsatfda_docs/label/2012/204384s000lbl.pdf, accessed Aug 1, 2016]. The compound, substrate of CYP3A, is characterized by a very long terminal half-life (6-9 months) [Lehay, 2013], which makes it very difficult to test the long-term extent of DDI.

The aim of this work is to predict the expected changes of exposure of bedaquiline when it is coadministered with inhbitors or inducers of different potency as long term therapy.

6.3. **Materials and Methods**

To anticipate the magnitude of DDI that can be observed on bedaquiline PK following long term co-administration with DDI perpetrators, simulations were performed based on the available NONMEM model developed for bedaquiline [Lehay, 2013]. The approaches and the parameters for CYP3A DDI perpetrators published in the papers of Ohno et al. [Ohno et al., 2007; Ohno et al., 2008] were used.

Using this approach, the inhibited oral clearance of bedaquiline is expressed as:

$$CLinh = CL \cdot (1 - fCYP3A \cdot IRCYP3),$$

where CL is the bedaquiline oral clearance in absence of the DDI perpetrator (2.78 L/h [Lehay, 2013]), fCYP3A is the fractional clearance of bedaquiline due to CYP3A4 involvement and IRCYP3A is the in vivo inhibition ratio reported by Ohno [Ohno et al., 2007] for the investigated inhibitors. Values of fCYP3A4 of 0.75, 0.90, 0.95 were considered for bedaquiline, compatible with CYP3A4 being responsible for most of its clearance [Liu et al., 2014]. An analogous approach was used for inducers [Ohno et al., 2008].

$$CLind = CL \cdot (1 + fCYP3A \cdot ICCYP3A),$$

where CLind is is the induced oral clearance of bedaquiline, ICCYP3A is the in vivo induction potency of the investigated inducers [Ohno et al., 2008] and the other parameters are as previously defined.

Similar relationships can be used for calculating the AUC of bedaquiline in the normal (without comedications) and in the altered status due to the coadministration of inhibitors and inducers of CYP3A metabolism

6.4. **Results**

6.4.1. Qualification of the approach

The conditions used in already available short-term clinical DDI studies (Table 6.1.) were initially simulated to validate the approach

Table 6.1. Observed levels of AUC ratio (inhibited to uninhibited) in the available DDI studies and predictions based on the proposed approach.

Perpetrator	Hypothesized f_{CYP3A4}		TMC207, AUC ratio comed/alone
Ketoconazole		**Observed**[5] *bedaquiline 400 mg qdx14; ketoconazole 400 mg qd on D12-14* AUC_{24h}, *D14 vs D11*	1.22 90% CI 1.12-1.32
	0.75	**Predicted**	1.23
	0.90		1.27
	0.95		1.28
Rifampicin		**Observed**[5] *bedaquiline 300 mg on D1 and D21; rifampicin 600 mg qd on D14-28;* AUC_{336h}, *D1 vs D21*	0.48 90% CI 0.43-0.54
	0.75	**Predicted**	0.57
	0.90		0.51
	0.95		0.49
Efavirenz		**Observed** *Bedaquiline 400 mg on D1 and D21; efavirenz 600 mg qd on D14-16* AUC_{336h}, *D1 vs D21*	0.82 90% CI 0.75-0.89
	0.75	**Predicted**	0.95
	0.90		0.91
	0.95		0.89

* Observations based on Dooley et al., 2012; Svensson et al., 2013

The predictions appeared in good agreement with the observation, so that the hypothesized fCYP3A appear well suited to start a simulation campaign to establish the extent of DDI in untested conditions; in particular, the method can be used for extrapolating the results to longer term bedaquiline treatments.

6.4.2. Simulations of the full DDI extent

In the Table 6.2 the predictions of the weekly AUC ratio (with/without consistent coadministration of DDI perpetrators) are reported at the end of a two weeks 400 mg qd + 22 weeks 200 mg thrice weekly bedaquiline regimen.

Table 6.2. Predicted levels of AUC ratio (inhibited to uninhibited) at the end of a two weeks 400 mg qd + 22 weeks 200 mg thrice weekly bedaquiline regimen.

Perpetrator	Hypothesized f_{CYP3A4}	TMC207, AUC_{168h} ratio comed/alone
Ketoconazole (IR_{CYP3A4} =1 for 200-400 mg daily[3])	0.75	1.80
	0.90	2.09
	0.95	2.21
Erythromycin (IR_{CYP3A4} =0.82 for 1000-2000 mg daily[3])	0.75	1.59
	0.90	1.78
	0.95	1.85
Cimetidine (IR_{CYP3A4} =0.44 for 800-1200 mg daily[3])	0.75	1.26
	0.90	1.32
	0.95	1.34
Rifampicin (IC_{CYP3A4} = 7.77 for 400-600 mg daily[4])	0.75	0.20
	0.90	0.17
	0.95	0.16
Efavirenz (IC_{CYP3A4} =1.4 for 600 mg daily[4])	0.75	0.59
	0.90	0.54
	0.95	0.53

Plasma concentration-time profiles of bedaquiline are shown in Fig. 6.1-6.3 for some simulated scenarios, with or without DDI; the simulations were obtained from the available population PK model, to provide a representation of the effect of inter-subject variability. In this particular plots, the 5th and 95th percentile of the non-inhibited bedaquiline profile are reported, together with the medians.

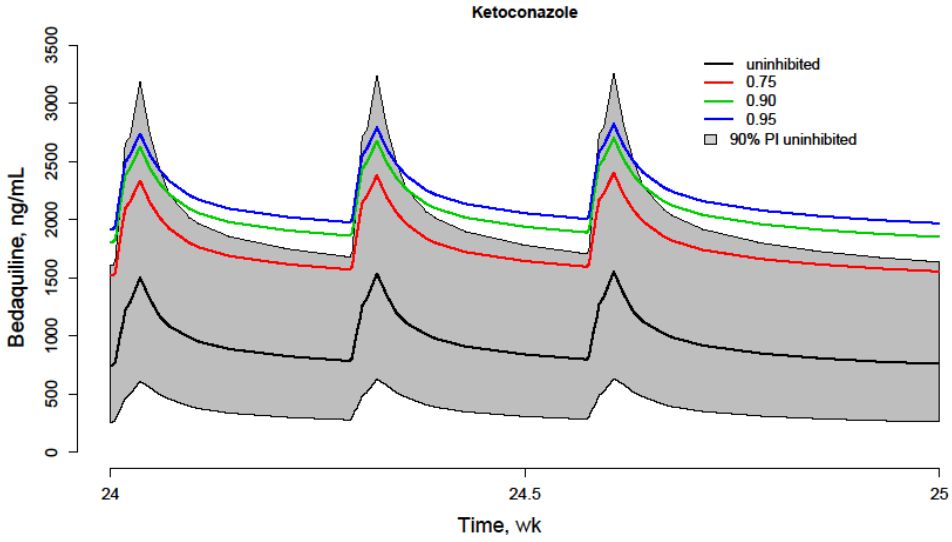

Figure 6.1. Predicted effect of ketoconazole (IRCYP3A4 =1 for 200-400 mg daily[2]) on bedaquiline PK (therapeutic regimen); in all plots, the legends report the fCYP3A4 scenarios used in the simulations.

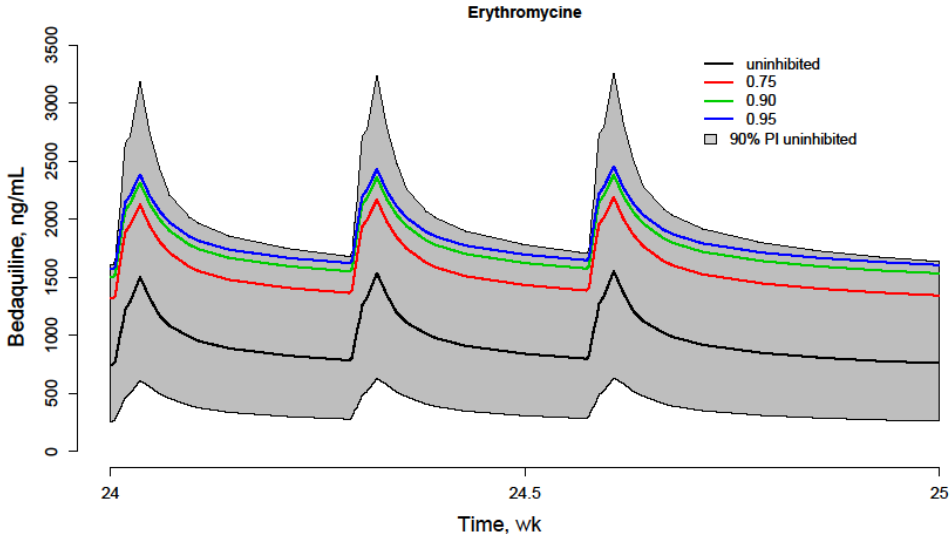

Figure 6.2. Predicted effect of erythromycin (IRCYP3A4 =0.82 for 1000-2000 mg daily[2]) on bedaquiline PK (therapeutic regimen).

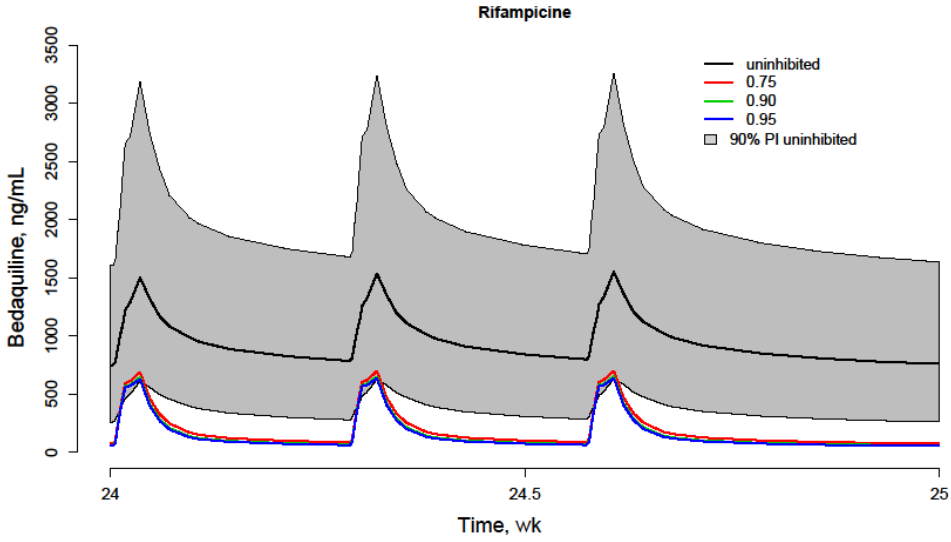

Figure 6.3. Predicted effect of rifampicin (ICCYP3A4 =7.7 for 400-600 mg daily[3]) on bedaquiline PK (therapeutic regimen)

6.5. **Conclusions**

Simulations based on the described approach indicated that the exposure of bedaquiline after long term co-administration of a strong CYP3A4 inhibitor provided an AUC increase of 1.80-2.21 fold. In contrast, DDI of moderate inhibitors was of minimal clinical relevance, considering the inter-subject variability. The extent of predicted DDI for efavirenz was similar to that predicted at steady state using a top-down NONMEM approach [Svensson et al., 2013].

The combination of top-down and bottom-up approaches provides useful information regarding the appropriate use of drugs when actual clinical data cannot be generated.

6.6. **References**

Brown HS, Galetin A, Hallifax D, Houston JB. Prediction of in vivo drug-drug interactions from in vitro data. Clinical pharmacokinetics. 2006, 45:1035-50.

Fahmi OA, Hurst S, Plowchalk D, Cook J, Guo F, Youdim K, Dickins M, Phipps A, Darekar A, Hyland R, Obach RS. Comparison of different algorithms for predicting clinical drug-drug interactions, based on the use of CYP3A4 in vitro data: predictions of compounds as precipitants of interaction. Drug Metabolism and Disposition. 2009, 37:1658-66.

Houston JB, Galetin A. Methods for predicting in vivo pharmacokinetics using data from in vitro assays. Current drug metabolism. 2008, 9:940-51.

Nucci G, Poggesi I, Gomeni R. Modelling and Simulation of Ketoconazole inhibition when co-administration time is not sufficient: role of CYP3A function recovery. PAGE 17 (2008) Abstr 1384.
Ohno Y, Hisaka A, Suzuki H. General framework for the quantitative prediction of CYP3A4-mediated oral drug interactions based on the AUC increase by coadministration of standard drugs. Clinical pharmacokinetics. 2007, 46:681-96.
Ohno Y, Hisaka A, Ueno M, Suzuki H. General framework for the prediction of oral drug interactions caused by CYP3A4 induction from in vivo information. Clinical pharmacokinetics. 2008, 47:669-80.
Mahajan R. Bedaquiline: First FDA-approved tuberculosis drug in 40 years. International Journal of Applied and Basic Medical Research. 2013, 1;3(1):1.
McLeay SC, Vis P, van Heeswijk RP, Green B. Population pharmacokinetics of bedaquiline (TMC207), a novel antituberculosis drug. Antimicrobial agents and chemotherapy. 2014, 58:5315-24.
Liu K, Li F, Lu J, Liu S, Dorko K, Xie W, Ma X. Bedaquiline metabolism: enzymes and novel metabolites. Drug Metabolism and Disposition. 2014; 42(5):863-6.
Dooley KE, Park JG, Swindells S, Allen R, Haas DW, Cramer Y, Aweeka F, Wiggins I, Gupta A, Lizak P, Qasba S. Safety, tolerability, and pharmacokinetic interactions of the antituberculous agent TMC207 (bedaquiline) with efavirenz in healthy volunteers: AIDS Clinical Trials Group Study A5267. Journal of acquired immune deficiency syndromes. 2012, 59:455–62.
Svensson EM, Aweeka F, Park JG, Marzan F, Dooley KE, Karlsson MO. Model-based estimates of the effects of efavirenz on bedaquiline pharmacokinetics and suggested dose adjustments for patients coinfected with HIV and tuberculosis. Antimicrobial agents and chemotherapy. 2013, 57:2780-7.

Chapter 7

Conclusions

The aim of this thesis was to demonstrate that numerous physiology-based approaches are available to facilitate the characterization and the utilization (and, in broad sense, the development) of new drugs.

These approaches can be based on full whole-body physiology based pharmacokinetic models, as the one described in Chapter 3 for the prediction of the pharmacokinetics in the "first in animal" and "first in human" studies. Alternatively, the adoption of simpler physiology-based elements can be adopted in these approaches. For instance, physiology-based description of principal pharmacokinetic parameters such as CL can be used for driving the predictions of AUC or AUC ratios in different conditions – e.g., in subjects with hepatic or renal impairment (Chapter 4 and 5), or following the coadministration of comedication known to alter the metabolism of drugs (Chapter 6).

Another interesting observation from this thesis is that these physiology-based methodologies can be used in applications that spans the full range of the development of new drugs: from the pre-clinical lead identification/optimization to the late development/post-marketing phases.

This thesis also illustrates the point that PBPK approaches can be efficiently combined with other modeling approaches. For instance, PCA and sensitivity analysis was applied in Chapter 3 to provide a better understanding of the conditions in which the predictive approaches are likely to fail. PCA and continuous regression analysis (NIPALS) were used in the same way in Chapter 4 and 5. In addition, in Chapter 5, other categorical approaches were used to provide a pragmatic identification of the cases in which a clinically relevant change of drug exposure, potentially leading to dosage change recommendations, may be expected in subjects with renal impairment. In Chapter 6, a physiology-based treatment is used in combination with the typical "top-down" approach of compartmental models implemented in the non-linear mixed-effects model setting.

The examples reported here show how these combined "Quantitative Sciences" approaches can provide a more efficient handle to problems, increasing the

understanding on how new drugs can be used and allowing to provide answers to a wide range of practical problems encountered during the drug research and development of new drugs. The use of this combination of diverse modeling approaches together with PBPK can also provide additional stimuli for a more detailed mechanistic understanding at the basis of the translational aspects (discovery-preclinical-clinical interface; normal population-population with organ impairment-population with comedications) of the pharmacokinetics of new drugs.

Finally, all the chapters of this thesis also shows that a wider knowledge-base, better experiments – controlling as possible all the potentially involved experimental variables – and a more profound scientific understanding are still needed to improve the predictive assessments of PK in these translational settings.